UNIVERSITY OF CALGARY

Genetics and biochemistry of cobalamin disorders

by

Darren Sean Froese

A THESIS

SUBMITTED TO THE FACULTY OF GRADUATE STUDIES

IN PARTIAL FULFILMENT OF THE REQUIREMENTS FOR THE

DEGREE OF DOCTOR OF PHILOSOPHY

DEPARTMENT OF BIOCHEMISTRY AND MOLECULAR BIOLOGY

CALGARY, ALBERTA

September 2009

UNIVERSITY OF
CALGARY

Abstract

Vitamin B_{12} (cobalamin, Cbl) is an essential nutrient in humans and functions as the cofactor for methylmalonyl-CoA mutase (Mut) and methionine synthase (MS). Genetic disorders linked to intracellular processing of cobalamin to methylcobalamin (MeCbl) and adenosylcobalamin (AdoCbl), the cofactor forms required for MS and Mut, respectively, have been defined through complementation analysis. Currently, all eight complementation groups, designated *cblA*-*G* and *mut*, have had their corresponding genes identified. Therefore, the challenge is now to understand the metabolic function of each of the corresponding proteins in intracellular cobalamin processing.

Accordingly, I first investigated the intracellular localization of MSR, a protein known to be involved in the cytosolic reduction of cobalamin but suggested to also function in the mitochondrion. Evidence of a possible mitochondrial function consisted of a putative mitochondrial leader on an alternate splice isoform of MSR as well as *in vitro* evidence that MSR could physically interact with MMAB, a mitochondrial protein, to produce AdoCbl. I demonstrated that, while there indeed was a second splice isoform of MSR, this isoform lacked a functional mitochondrial leader sequence. Additionally, while I confirmed the ability of MSR to interact with MMAB *in vitro*, I detected MSR in the cytosol but not the mitochondria by both Western blot analysis and immunofluorescence, thus demonstrating a restricted role for this protein as a cytoplasmic reductase only.

Secondly, I investigated the well documented but enigmatic differential response of *cblC* fibroblasts and patients to OHCbl compared to CNCbl. For this investigation I used

recombinant *cblC* (MMACHC) protein, including wild-type protein as well as forms with the G147D early-onset cobalamin unresponsive and R161Q late-onset cobalamin responsive *cblC* mutations. I demonstrated that wild-type MMACHC was able to bind OHCbl and CNCbl with the same tight affinity (K_d = 5.7 μM), that MMACHC-G147D did not bind either form and that MMACHC-R161Q bound OHCbl with wild-type affinity but was deficient in its ability to bind and decyanate CNCbl. Additionally, by mutating MMACHC-H122, the histidine suggested to be integral to the B_{12}-binding motif, I found that binding to OHCbl and CNCbl was reduced but not ablated, suggesting this histidine is not absolutely required for binding. These data pointed to the inability to bind cobalamin as the basis for functional deficiency in early-onset (G147D) *cblC* and differential binding of OHCbl and CNCbl as the basis for the better response to OHCbl with late-onset (R161Q) *cblC*. However, since MMACHC-R161Q was able to bind OHCbl with wild-type affinity, the nature of the defect in *cblC* patients with this allele remained unclear. To explore this further, I investigated the thermostability of MMACHC-R161Q in comparison to wild-type MMACHC. I found that MMACHC-wt and MMACHC-R161Q were both very thermolabile proteins, with melting temperatures (T_m) of 39.3 ± 1.0°C and 37.1 ± 0.7°C, respectively. However, with the addition of low concentrations of HOCbl, MMACHC-wt became significantly stabilized (T_m= 44.5°C and 47.0°C for 1 μM and 10 μM HOCbl, respectively) while MMACHC-R161Q only moderately stabilized (T_m= 38.5°C and 40.4°C for 1 μM and 10 μM HOCbl). Additionally, I surveyed the effect on stability upon binding to different forms of cobalamin and found that, at 10 μM cofactor concentration, both MMACHC-wt and MMACHC-R161Q were stabilized in the order AdoCbl > MeCbl > HOCbl > CNCbl.

Significantly, as for HOCbl, MMACHC-R161Q was stabilized less than MMACHC-wt after binding each of these forms of cobalamin. However, after binding to cobinamide, a cobalamin precursor form that lacks the lower dimethylbenzymidazole (DMB) base, MMACHC-wt and MMACHC-R161Q were stabilized equally. Together, these results suggested that MMACHC is an unstable protein that is normally stabilized in the cell by Cbl binding and the R161Q mutation doubly destabilizes this protein by decreasing its stability in the apo- form and decreasing the stability gain it achieves when bound to cobalamin. The fact that MMACHC-R161Q showed inhibited stability with all cobalamins tested but not with cobinamide suggested that the R161Q mutation may disrupt interaction with the DMB arm of cobalamin.

Finally, I investigated the possible interaction between MMAA, a cobalamin processing protein of unknown function, and Mut, the enzyme responsible for AdoCbl utilization, using *E. coli* as well as human cells. I found that YgfD and Sbm, the *E. coli* versions of MMAA and Mut, respectively, were endogenously expressed and that YgfD had GTPase activity. I showed that YgfD and Sbm can be co-immunoprecipitated from *E. coli* extracts using antibody to either protein, demonstrating *in vivo* interaction, a result confirmed using a strain deleted for *ygfD*. I showed further that, *in vitro*, purified His-tagged YgfD and Sbm behaved as a monomer and dimer, respectively, and that they formed a multi-subunit complex that is dependent on pre-incubation of YgfD with non-hydrolysable GTP, an outcome that was not affected by the state of Sbm, as holo- or apoenzyme. Using recombinant human MMAA and Mut, I found that while MMAA retained the ability to bind GTP and GDP and confirmed that our recombinant Mut binds

AdoCbl, these proteins did not form a complex *in vitro* as judged by native gel electrophoresis or size-exclusion chromatography under any conditions tested, including the addition of non-hydrolyzable GTP. However, following over-expression and pull-down of MMAA, Mut could be detected by Western blot analysis, indicating that these proteins do interact *in vivo*. These results suggested that human Mut and MMAA interact *in vivo* but the conditions for this interaction are not easily duplicated *in vitro*.

Overall, these studies have helped to define the function and interactions of the proteins responsible for the intracellular metabolism of cobalamin. Together, these studies give us a better understanding of how cobalamin goes from an ingested vitamin to a functional cofactor.

Preface

The material presented in this thesis has been previously published in:

1. Froese DS, Wu X, Zhang J, Dumas R, Schoel WM, Amrein M, Gravel RA. Restricted role for methionine synthase reductase defined by subcellular localization. Mol Genet Metab 2008;94:68-77
2. Froese DS, Dobson CM, White AP, Wu X, Padovani D, Banerjee R, Haller T, Gerlt JA, Surette MG, Gravel RA. Sleeping beauty mutase (*sbm*) is expressed and interacts with *ygfd* in *Escherichia coli*. Micro Res 2009;164:1-8
3. Froese DS, Zhang J, Healy S, Gravel RA. Mechanism of vitamin-B12 responsiveness in cblC methylmalonic aciduria with homocysteinuria. Mol Genet Metab *in press*.

Each person (supervisor's initials) and their contributions to each section are listed below:

Chapter 2: Xuchu Wu (RG) Westerns and intellectual, Jun Zhang (RG) MSR-MMAB interaction, Rick Dumas (RG) MSR antibodies, Michael Schoel (MA) immunofluorescence intellectual, Matthias Amrein immunofluorescence intellectual.

Chapter 3: Jun Zhang (RG) decyanase assay and intellectual for ligand binding, Shannon Healy (RG) mass spectrometry

Chapter 4: Shannon Healy (RG) DSF intellectual, Megan McDonald (RG) DSF intellectual, Grazyna Kochan (UO) protein expression and purification intellectual, Frank Niesen (UO) DSF intellectual, Udo Oppermann hosting laboratory

Chapter 5: Melissa Dobson (RG) *in vivo* pull-downs and Western, Aaron White (MS) knockout vector and intellectual, Xuchu Wu (RG) extensive intellectual, Dominique Padovani (RB) protein purification and *in vitro* interaction intellectual, Toomas Haller (JG) vectors

Chapter 6: Xuchu Wu (RG) protein purification and Westerns, Grazyna Kochan (UO) subcloning and intellectual for protein purification, Udo Oppermann hosting laboratory and intellectual

Collaborators/Contributing Principle Investigators:
RG= Roy Gravel, MA = Matthias Amrein, UO = Udo Oppermann, MS = Michael Surette, RB = Ruma Banerjee, JG = John Gerlt,

Acknowledgements

This thesis would not have been possible without the following people:

I thank Dr. Roy Gravel, who after his many incredible years in science, still gets excited when data is brought to his office door. His ability to skip lunch for chats about a particularly uncooperative result, his late night editing and propensity to suggest the most ridiculous hypotheses, many of which come true, will stay with me the rest of my career.

I am grateful to those who worked in Dr. Gravel's lab, including Melissa Dobson, Shannon Healy, Jun Zhang, Wendy Jia, Megan McDonald, Marko Vujanovic and particularly Xuchu Wu. They gave me much good advice, some of which pertained to science, and generally made the lab a fun place to spend the day.

I am grateful to Dr. Udo Oppermann for the opportunity to visit his lab and learn science Oxford style, as well as Grazyna Kochan and Wyatt Yue for their assistance while I was there.

I am grateful to my friends who occasionally were able to drag me out of the lab to keep me sane.

Finally, I am thankful to my parents who had to spend more than one Christmas without me because Science had taken over. Their unwavering support throughout the entire process kept me going. This is for them.

Generous financial support was provided by the Canadian Institute of Health Research through the Institute of Child and Maternal Health.

Table of Contents

Approval Page ii
Abstract iii
Preface vii
Acknowledgements viii
Table of Contents ix
List of Tables xii
List of Figures and Illustrations xiii
List of Symbols, Abbreviations and Nomenclature xv

CHAPTER 1: INTRODUCTION 1
General Introduction 1
B_{12} Structure 2
Vitamin B_{12} Origins 5
Human vitamin B_{12} ingestion and absorption 8
Human intracellular processing of B_{12} 11
Complementation Groups affecting both MS and MCM 13
Complementation groups affecting only MS 15
Complementation groups affecting only MCM 18
The Purpose of the Thesis 22

CHAPTER 2: RESTRICTED ROLE FOR METHIONINE SYNTHASE REDUCTASE DEFINED BY SUBCELLULAR LOCALIZATION 23
Introduction 23
Methods and Materials 26
RT-PCR 26
Plasmid Construction 26
Antibody Generation 28
Cell Culture and Protein Preparation 29
Cellular fractionation 29
Western Blots 30
Nucleofection and Immunofluorescence 31
Protein expression and purification 32
ATP:Cob(I)alamin Adenosyltransferase Assays 33
Results 33
Alternative splicing of MSR 33
Interaction of MSR with MMAB 34
MSR does not have a functional leader sequence 36
MSR protein is found in the cytoplasm but not in the mitochondria 38
Discussion 41

CHAPTER 3: MECHANISM OF VITAMIN B12-REPONSIVENESS IN CBLC METHYLMALONIC ACIDURIA WITH HOMOCYSTEINURIA 47
Introduction 47
Materials and Methods 51
Plasmid Generation and Site Directed Mutagenesis. 51

Protein Expression and Purification 52
Intrinsic Fluorescence Spectroscopy 53
UV-Visible Absorption Spectra 54
Decyanase Assay 54
Results 55
MMACHC purification and binding to cobalamin 55
MMACHC mutants distinguish OHCbl and CNCbl 58
MMACHC binds CNCbl base-off 59
MMACHC-R161Q has reduced decyanase activity 61
Discussion 63

CHAPTER 4: THERMOLABILITY OF THE MMACHC R161Q MUTANT IN VITAMIN B_{12}-RESPONSIVE *CBLC* DISORDER 67
Introduction 67
Materials and Methods 70
Materials 70
Plasmid Generation and Site Directed Mutagenesis 70
Protein Expression and Purification 71
Differential Scanning Fluorimetry 71
Statistics 72
Results 72
MMACHC-R161Q is a thermolabile mutant 72
Stability of MMACHC depends upon which form of cobalamin is bound 76
Discussion 78

CHAPTER 5: SLEEPING BEAUTY MUTASE (*SBM*) IS EXPRESSED AND INTERACTS WITH *YGFD* IN *ESCHERICHIA COLI* 82
Introduction 82
Materials and Methods 86
Materials 86
ygfD knockout 86
Purification of expressed proteins 87
Antibody production 87
Immunoprecipitation 88
Immunobloting procedures 89
Size exclusion chromatography 89
PAGE analysis of complex formation 90
GTPase Assay 90
Results 90
YgfD and Sbm characterization 91
YgfD and Sbm physically interact in vivo 93
Interaction of YgfD and Sbm in vitro 95
Discussion 98

CHAPTER 6: *IN VIVO* BUT NOT *IN VITRO* INTERACTION OF MMAA AND MUT 101
Introduction 101

Materials and Methods....104
Materials....104
Plasmid Generation....105
Protein Expression and Purification....106
Differential Scanning Fluorimetry....107
Cell culture and nucleofection....107
Immunoprecipitation procedures....108
Immunoblotting procedures....109
Size-exclusion chromatography....109
Native PAGE analysis of pure proteins....109
Results....110
Purification and ligand binding of MMAA and Mut....110
Ligand effect in native gel investigations of MMAA and Mut....113
Molar ratio and analysis by two dimensional electrophoresis....115
MMAA and Mut physically interact in vivo....119
Discussion....121

SUMMARY, CONJECTURE AND FUTURE DIRECTIONS: THE B_{12} CHAPERONE HYPOTHESIS....126

REFERENCES....134

List of Tables

Table 1.1. Distribution of B_{12}-dependent enzymes in eukaryotes whose genomes have been sequenced. 7

Table 2.1. Primers used to make GFP mitochondrial leader constructs. 27

Table 2.2. Subcellular localization predictions of MSR variant 2, as determined by various subcellular prediction programs. 44

Table 3.1. Apparent Kd Values of Wild-type and Mutant MMACHC Proteins 59

List of Figures and Illustrations

Figure 1.1. B_{12} Structure. 4

Figure 1.2. B_{12} synthesis and utilization across phyla. 6

Figure 1.3. Human B_{12}uptake. 10

Figure 1.4. Intracellular processing of B_{12}. 12

Figure 1.5. The Methionine Synthase Cycle 16

Figure 1.6. Metabolic pathways dependent on MCM 21

Figure 2.1. Splice variants of MSR and the predicted mitochondrial leader. 25

Figure 2.2. MSR acts with MMAB to produce AdoCbl. 35

Figure 2.3. Assay of functional N-terminal leader sequences. 37

Figure 2.4. Subcellular localization of MSR. 40

Figure 2.5. Multiple sequence alignment of the N-terminal amino acids of MSR from selected mammalian species. 42

Figure 3.1. SDS-PAGE of purified GST-MMACHC. 56

Figure 3.2. GST-MMACHC binding to OHCbl (A) and CNCbl (B). 57

Figure 3.3. MMACHC-GST binds CNCbl base-off. 60

Figure 3.4. Reductive decyanation of CNCbl by normal or mutant MMACHC. 62

Figure 4.1. Chemical structure of vitamin B_{12}. 68

Figure 4.2. Purification and Thermostability of MMACHC-wt and MMACHC-R161Q. 73

Figure 4.3. MMACHC-wt and MMACHC-R161Q stabilization by OHCbl 75

Figure 4.4. Stabilization of MMACHC-wt and MMACHC-R161Q by binding different forms of cobalamin and cobinamide. 77

Figure 5.1. A. Pathway for the AdoCbl-dependent conversion of succinate to propionate in *E. coli* by Sbm, YgfG and YgfH. B. Conserved domains in the G3E family of GTPases including members of the YgfD, CobW, HypB and UreG protein families. 85

Figure 5.2. Sbm and YgfD protein expression and GTPase activity of YgfD..... 92

Figure 5.3. Interaction of YgfD and Sbm *in vivo*. 94

Figure 5.4. Interaction of YgfD and Sbm *in vitro*..... 97

Figure 6.1. Purification and ligand binding test of MMAA and Mut. 112

Figure 6.2. Native 4-20% PAGE of Mut and MMAA..... 114

Figure 6.3. Increasing molar ratio of MMAA to MutA and 2nd dimension SDS-PAGE analysis of bands. 116

Figure 6.4. Gel filtration of Mut and MMAA..... 118

Figure 6.5. *In vivo* interaction of MMAA and Mut in human HepG2 cells. 120

List of Symbols, Abbreviations and Nomenclature

Symbol	Definition
AdoCbl	adenosylcobalamin
AdoMet	adenosylmethionine
Amp	Ampicillin
ATP	Adenosine triphosphate
BSA	bovine serum albumin
Cbl	cobalamin
cblA	complementation group A of the cobalamin metabolic disorders
cblB	complementation group B of the cobalamin metabolic disorders
cblC	complementation group C of the cobalamin metabolic disorders
cblD	complementation group D of the cobalamin metabolic disorders
cblE	complementation group E of the cobalamin metabolic disorders
cblF	complementation group F of the cobalamin metabolic disorders
cblG	complementation group G of the cobalamin metabolic disorders
CNCbl	cyanocobalamin
Co	cobalt
cubam	cubilin-amnionless
DMB	dimethylbenzimidazole
DNA	deoxyribonucleic acid
E. coli	*Escherichia coli*
FAD	flavin adenine dinucleotide
FPLC	fast performance liquid chromatography

GFP	green fluorescent protein
GMPPNP	non-hydrolyzable guanosine triphosphate
GST	glutathione S-transferase
GTP	guanosine triphospate
HC	haptocorrin
IF	intrinsic factor
IPTG	iosproylthiogalactoside
LB	Luria Bertani broth
LMBRD1	LMBR1 domain containing 1, *cblF* protein
Kan	Kanamycin
M. extorquens	*Methylbacterium extorquens*
MCM/Mut	methylmalonyl-CoA mutase
MeCbl	methylcobalamin
MMAA	methylmalonic aciduria (cobalamin deficiency) cblA type, protein
MMAB	methylmalonic aciduria (cobalamin deficiency) *cblB* type, protein
MMACHC	methylmalonic aciduria (cobalamin deficiency) *cblC* type with homocysteinuria, protein
MMADHC	methylmalonic aciduria (cobalamin deficiency) *cblD* type with homocysteinuria, protein
MS	methionine synthase
MSR	methionine synthase reducatse
NADPH	nicotinamide adenine dinucleotide phosphate
OHCbl	hydroxocobalamin

PAGE	polyacrylamide gel electrophoresis
PCR	polymerase chain reaction
Sbm	sleeping beauty mutase
SDS	sodium dodecylsulfate
TC	transcobalamin

CHAPTER 1: INTRODUCTION

General Introduction

Vitamin B_{12}, also known as cobalamin (Cbl), is a micronutrient synthesized only by microorganisms, yet is essential to human health. Cobalamin was first isolated by Smith (1) and Rickes (2), after Minot and Murphy (3) showed that pernicious anemia can be treated by oral liver extract. Later, vitamin B_{12} deficiency from genetic diseases became known in spite of adequate vitamin intake (4). Some patients responded successfully to high doses of B_{12}, suggesting blocks in vitamin processing. These patients had homocysteinuria and/or methylmalonic aciduria, implicating dysfunctional methionine synthase (MS) and/or methylmalonyl-CoA mutase (MCM). Now we know that cobalamin is required as methylcobalamin (MeCbl) for MS and as adenosylcobalamin (AdoCbl) for MCM, and that blocks in the intracellular processing of Cbl into these cofactor forms or in the utilization of Cbl by MS or MCM result in inborn errors. These genetic blocks may be devastating in the newborn period or early childhood. Additionally, mild mutations or polymorphisms in some of these steps (most notably steps affecting MS) may be associated with cardiovascular disease and neural tube defects. Therefore, understanding the genes, gene products and subcellular trafficking of B_{12} is important for minimizing disease burden from these disorders.

This introduction will outline the present knowledge of Cbl metabolism with a focus on steps related to the human pathway. Further detailed information defining each project will be introduced in subsequent chapters.

B_{12} Structure

The structure of cobalamin was first solved by Hodgkin (5) using x-ray crystallography. It is a large organometallic molecule, ~ 1300-1500 Da in size, and is the most chemically complex vitamin known. The focal point of B_{12} is the central cobalt atom, which has up to 6 ligands bound to it. Four of the ligands are the nitrogen atoms of the planar corrin ring that surround the cobalt atom (Fig. 1.1A). Another ligand, designated the α-axial ligand, extends below the cobalt atom. It is a nitrogen of a 5,6-dimethylbenzimidazole (DMB) phosphoribosyl moiety that also attaches back to the corrin ring through the side chain of ring D (Fig 1.1A). The final ligand, designated the upper or β-axial ligand, varies depending on the modification state of cobalamin (R-group in Fig 1.1B). Functional β-axial ligands are methyl (MeCbl) or 5'-deoxyadenosyl (AdoCbl) and correspond to the cofactors of methionine synthase and methylmalonyl-CoA mutase, respectively. Additionally, a hydroxyl group (OHCbl) or a cyano group (CNCbl) can be bound as physiologically relevant β-axial ligands.

There are three important and interrelated factors that contribute to cobalamin reactivity and function, including: the oxidation state of the cobalt, whether the DMB is

coordinated as the α-axial ligand and the identity of the R-group bound as the β-axial ligand. Cobalamin bound cobalt may exist in the +3 (cob(III)alamin), +2 (cob(II)alamin) or +1 (cob(I)alamin) oxidation state. These oxidation states influence how many axial ligands are bound to the cobalt. In general, cob(III)alamin has two axial ligands bound, cob(II)alamin has one axial ligand and cob(I)alamin has zero (6). Therefore, AdoCbl, MeCbl, CNCbl and OHCbl, which all exist as cob(III)alamins, prefer to adopt a configuration where the DMB is bound to the cobalt (base-on), giving two axial ligands (Fig. 1.1C). Some enzymes, however, are able to shift these cob(III)alamins to the base-off form (Fig. 1.1C). Interestingly, both MS and MCM, which bind MeCbl and AdoCbl, respectively, are able to bind in a different conformation such that the DMB is replaced by a histidine of the enzyme. This type of binding is considered to be base-off/his-on. Cob(II)alamin generally has no R-group bound, binding only the DMB as an axial ligand to make its preferred 5-coordinate state. However, in the presence of ATP, MMAB, the human adenosyltransferase enzyme, is able to bind cob(II)alamin in a novel four coordinate state, where neither axial position is occupied (7). Cob(I)alamin usually has no axial ligand, but does act as a strong nucleophile and is oxidized very easily back to cob(II)alamin (8). The identity of the axial ligands also affects the ease with which the central cobalt is reduced. Strongly coordinating ligands stabilize the cobalt against reduction, while weakly coordinating ligands allow the cobalt to be reduced more easily (6). Base-on Cbl falls into the former category, protecting the cobalt from reduction because the DMB has greater electron-donating character than the H_2O molecule that binds in its absence (9).

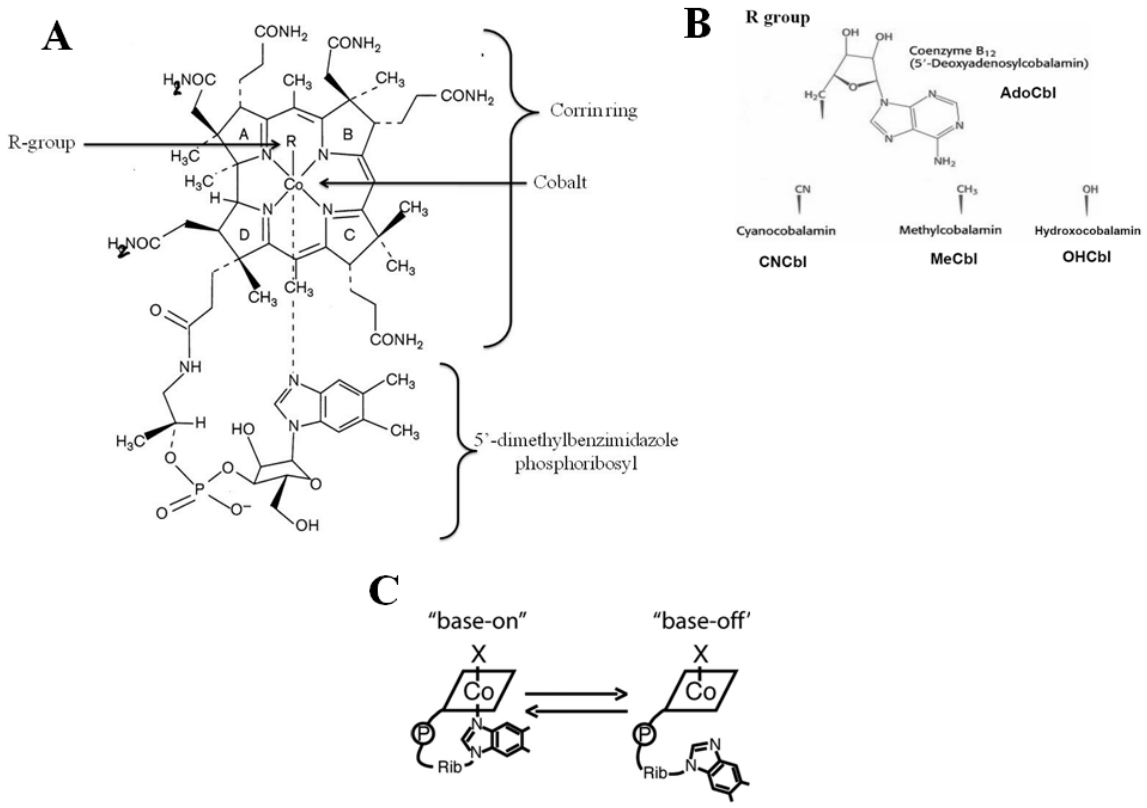

Figure 1.1. B_{12} Structure.

A. Overall structure of B_{12}. After (10). **B.** Possible R-groups bound to the cobalt. **C.** Depiction of base-on or base-off B_{12}.

Vitamin B_{12} Origins

B_{12} is an extremely old molecule in evolution. It has even been suggested B_{12} was synthesized prebiotically (11). Accordingly, B_{12} utilization is spread throughout evolution, occurring in both Eukaryota and Prokaryota, perhaps having been passed on from the "breakthrough organism", the last organism to use RNA as the sole genetically encoded catalyst (12). Interestingly, while B_{12} utilization is distributed vastly among phyla, B_{12} synthesis seems limited to only a select few *Archaea* and *Eubacteria* (Fig 1.2). Perhaps this is because synthesis of Cbl is so complex - involving in excess of 25 steps, which can proceed either aerobically (*cob* genes) or anaerobically (*cbi* genes) (13). Therefore, while mammals and other higher organisms require B_{12} for life, they ostensibly acquire it from their prokaryotic counterparts. Another interesting attribute of B_{12} evolution is that B_{12} users seem more scattered than spread out through evolution, with whole phyla sometimes gaining or losing this attribute. This is readily apparent in eukaryotes, where plants, fungi, and insects have lost all B_{12}-dependent proteins, while some green algae and slime molds have seemed to gain them (Table 1.I.). Additionally, while mammals and other higher eukaryotes are restricted to two cobalamin-dependent enzymes, MS and MCM, prokaryotes employ a plethora of enzymes requiring this cofactor, including 3 classes of AdoCbl dependent-mutases, the isomerases (e.g. MCM, ribonucleotide reductase, glutamate mutase), the eliminases (e.g. diol dehydratase) and the aminomutases (e.g. D-Lysine-5,6-aimnomutase), as well as the MeCbl-dependent methyltransferases (e.g. MS) and the B_{12}-dependent reductive dehalogenases (e.g. 3-

chloro-4-hydroxybenzoate dehlogenase) (14, 15). Therefore, since higher eukaryotes share common B_{12} ancestry with prokaryotes, but have apparently limited use and no synthesis in comparison, prokaryotes in general and a few specific bacteria in specific, have proved very useful models to understand B_{12} metabolism.

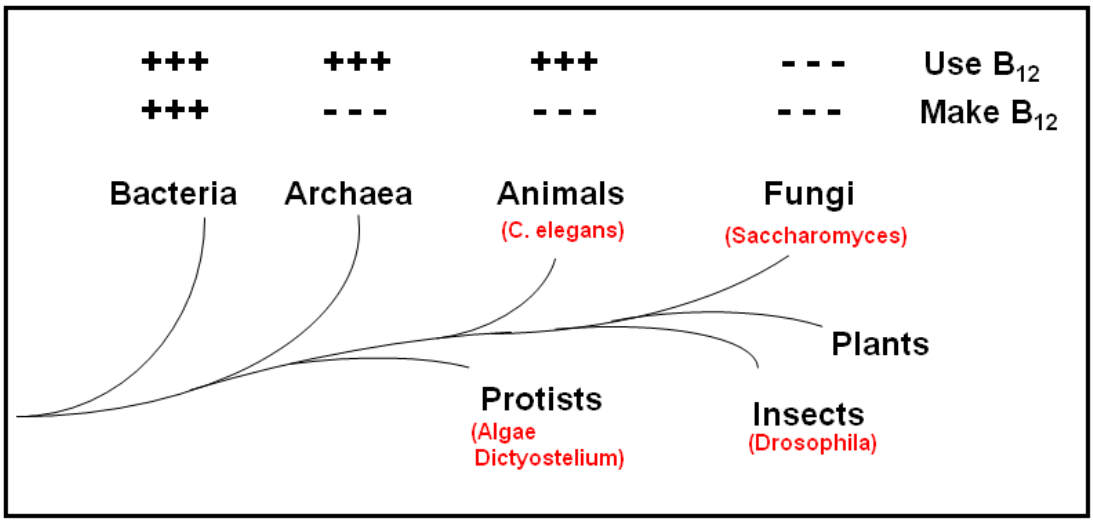

Figure 1.2. B_{12} synthesis and utilization across phyla.
Adapted from (13).

Table 1.1. Distribution of B_{12}-dependent enzymes in eukaryotes whose genomes have been sequenced.

Adapted from (16).

Phylum	Num. of organisms	B_{12}-utilizing organisms	MetH	MCM	RNR II
Cryptophyta	1	-	-	-	-
Diplomonadida	1	-	-	-	-
Parabasalidea	1	-	-	-	-
Kinetoplastida	5	3	3	3	-
Stramenopiles	4	4	4	4	3
Alveolata/Perkinsea	1	1	1	-	-
Alveolata/Apicomplexa	13	-	-	-	-
Alveolata/Ciliophora	2	-	-	-	-
Rhodophyta	1	-	-	-	-
Viridiplantae/Chlorophyta	3	3	3	-	-
Viridiplantae/Streptophyta	3	-	-	-	-
Dictyosteliida	1	1	1	1	1
Entamoebidae	3	-	-	-	-
Fungi/Ascomycota/Pezizomycotina	29	-	-	-	-
Fungi/Ascomycota/Saccharomycotina	24	-	-	-	-
Fungi/Ascomycota/Schizosaccharomycetes	2	-	-	-	-
Fungi/Basidiomycota	8	-	-	-	-
Fungi/Microsporidia	1	-	-	-	-
Fungi/Zygomycota	1	-	-	-	-
Metazoa/Pseudocoelomata/Nematoda	3	3	3	3	-
Metazoa/Coelomata/Others	2	2	2	2	-
Metazoa/Coelomata/Arthropoda (Insects)	19	-	-	-	-
Metazoa/Coelomata/Chordata/Others	10	10	10	10	-
Metazoa/Coelomata/Chordata/Mammals	22	22	22	22	-
Total	**160**	**49**	**49**	**45**	**4**

Human vitamin B_{12} ingestion and absorption

Since B_{12} is made only by select microorganisms, it is therefore acquired through dietary uptake in animals. Human dietary sources include milk, eggs, fish and meat in quantities in excess of a few micrograms a day (17). Accordingly, B_{12} intake increases with increasing consumption of animal-source foods, so that, in one study, B_{12} intake of vegans averaged 0.4 µg/day, of lactoovovegetarians 2.6 µg/day, of lactoovovegetarians who also consumed fish 5.0 µg/day, and people who consumed meat averaged 7.2 µg/day (18). Additionally, prevalence of deficiency increases throughout adulthood. The American National Health and Nutrition Examination Surveys in 1999 and 2002 reported that $\leq$ 3% of 20-39 year olds were B_{12} deficient, ~4% of 40-59 year olds were B_{12} deficient and ~6% of persons $\geq$70 years old were B_{12} deficient (19, 20). While the main cause of vitamin B_{12} deficiency in the young is due to inadequate intake, in the elderly it is malabsorption from food (21). Marginal depletion of vitamin B_{12}, caused by low dietary intake or malabsorption, does not usually result in megaloblastic anaemia (22), the hallmark of B_{12} deficiency, but can result in an increase in methylmalonic acid and homocysteine in the blood (21) which have been associated with cardiovascular disease (23) and cancer (24, 25) among other diseases.

In humans, the absorption, transport and cellular uptake of cobalamin is complex (Fig. 1.3). Food bound cobalamin is released in the stomach with the help of peptic activity, where it is subsequently bound by haptocorrins (HC) (26). In the small intestine, cobalamin is re-released from HC by pancreatic protease digestion and this time bound

by intrinsic factor (IF), to form an IF-Cbl complex. Importantly, IF is very specific for cobalamin, i.e. forms which have the lower DMB intact, which acts as an early screening mechanism to prevent degraded cobalamins from intracellular access (27). The IF-Cbl complex passes through the small intestine where it is bound by a heterodimer of amnionless and cubilin, called cubam, which aids in the endocytosis of IF-Cbl into ileal epithelial cells (28, 29). Failure of IF to bind cobalamin or failure of uptake of the IF-Cbl complex into epithelial cells results in the malabsorption of Cbl (30). Once transported across the ileal receptor cell, cobalamin is taken up into the bloodstream and binds to either haptocorrin (HC) or transcobalamin (TC) (31). While HC binds the bulk of plasma cobalamin (75-90%), it is not involved in cellular cobalamin uptake apart from uptake in hepatocytes (31, 32). Therefore, individuals who have deficient or absent HC have serum Cbl values in the deficient range, but show no signs of Cbl deficiency (17). While TC binds only a minor fraction of circulating cobalamins (10-25%), it is the protein responsible for facilitating uptake of cobalamin by cells (33, 34). In opposition to HC, mutations in TC result in severe tissue Cbl insufficiency, megaloblastic anaemia, failure to thrive and often neurological complications, in spite of normal plasma Cbl concentrations (30, 35). Additionally, TC acts a final screening mechanism because, like IF, TC is very specific for cobalamin forms with the lower DMB intact (36, 37). Treatment of TC deficiency requires very high serum Cbl levels, ranging from 1000-10,000 pg/ml, achieved by oral ingestion 0.5-1.0 mg of CNCbl or HOCbl once or twice weekly (17). There is some evidence that at sufficiently high concentrations at least some tissues are capable of taking up unbound Cbl (17). Presumably this is how treatment works.

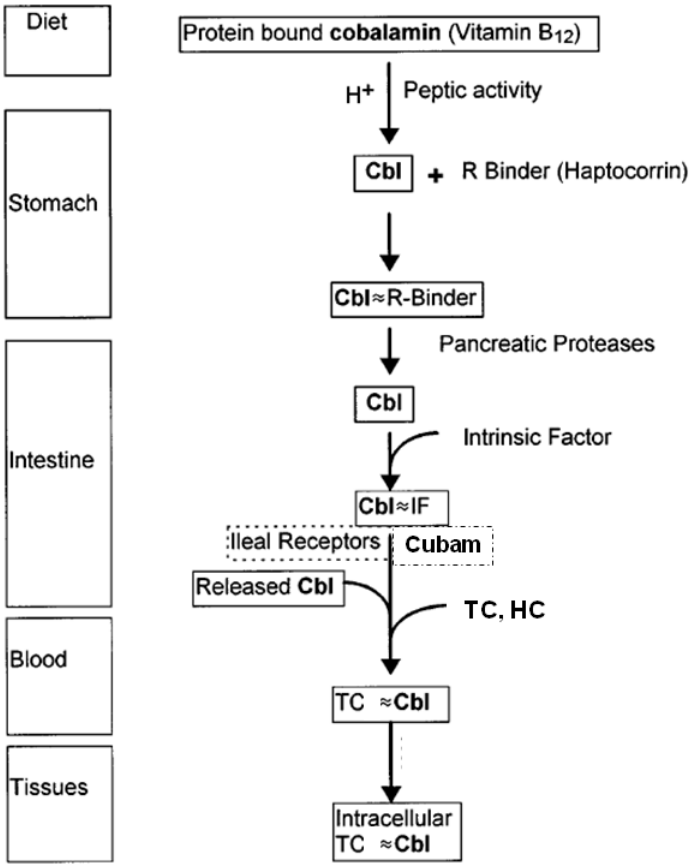

Figure 1.3. Human B_{12}uptake.

Adapted from (26). Abbreviations are as follows: Cbl, cobalamin; IF, intrinsic factor; Cubam, Cublilin/Amnionless; TC, transcobalamin; and HC, haptocorrin.

Human intracellular processing of B_{12}

From the bloodstream, Cbl is taken up into cells via receptor mediated endocytosis as a complex of cobalamin-TC bound to the TC-receptor (TCblR) (38-40). In the lysosome, the Cbl-TC complex is digested to create free cobalamin, which is subsequently transported into the cytosol in the cob(III)alamin oxidation state. Once in the cytosol, cobalamin is processed by many enzymes, some known - others unknown, to produce the cofactors methylcobalamin (MeCbl) and adenosylcobalamin (AdoCbl). MeCbl is the functional cofactor form of methionine synthase (MS), a cytosolic enzyme responsible for the conversion of homocysteine to methionine, while AdoCbl is the cofactor of methylmalonyl-CoA mutase (MCM), a mitochondrial enzyme that rearranges methylmalonyl-CoA to succinyl-CoA. Failure to produce these cofactors results in lack of functional enzymes and causes a block of methionine production with resultant homocystinuria, homocysteinemia and hypomethioninemia for MS, or a block in the catabolism of branched chain amino acids, odd-numbered chain fatty acids and cholesterol for MCM, resulting in methylmalonic aciduria.

Genetic disorders that have blocks in the cellular metabolism of cobalamin have been defined by complementation analysis of patient cell lines (41). So far, eight complementation groups, *cblA-G* and *mut*, have been described that have blocks in the production or utilization of MeCbl, AdoCbl, or both. While all of the genes corresponding to these disorders have now been described, many of their functions remain unclear. Figure 1.4 illustrates the known or predicted location of function for

these genes. Three complementation groups - *cblF*, *cblC* and *cblD* - correspond to blocks in steps that are common to the synthesis of both cofactors and deficient MS and MCM. Three groups, *cblD* variant 1, *cblE* and *cblG*, have blocks in the cytosolic pathway leading to MeCbl synthesis, and result in deficient MS only. The final groups, *cblD* variant 2, *cblA*, *cblB* and *mut*, affect steps occurring in the mitochondrion and result in deficient MCM only.

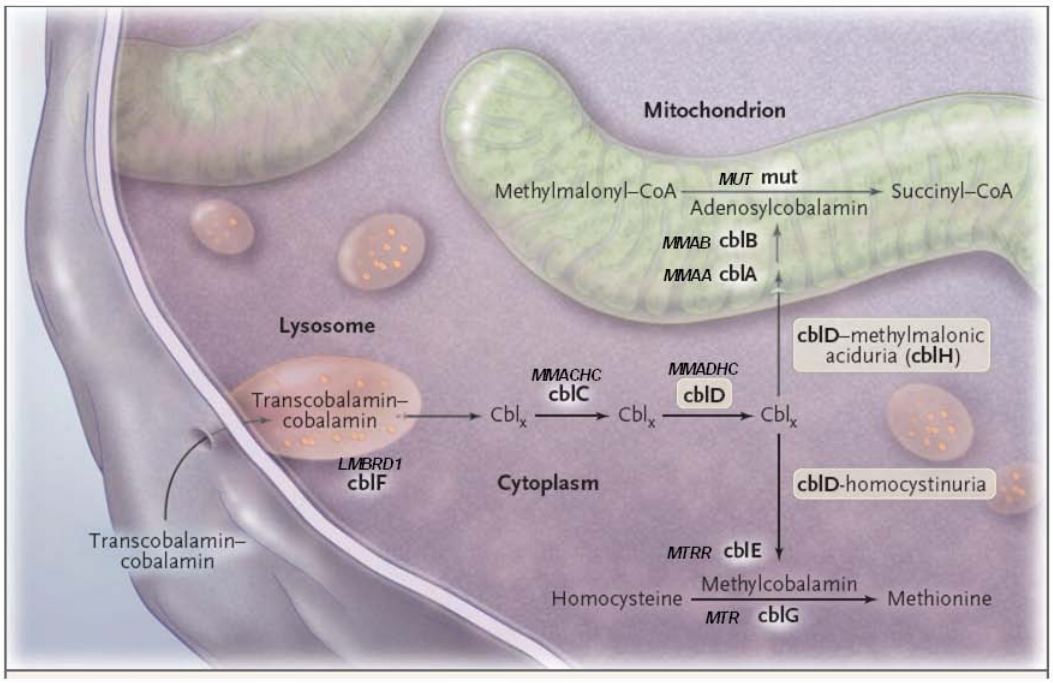

Figure 1.4. Intracellular processing of B_{12}.
Adapted from (42).

Complementation Groups affecting both MS and MCM

cblF. Only 12 patients have been described with *cblF* (43). These patients have presented with variable clinical manifestations, but most of them responded positively to HOCbl therapy (43). Due to early work demonstrating that defects in this gene results in accumulation of B_{12} in the lysosome (44), *cblF* has long been predicted to be responsible for transport of Cbl out of the lysosome into the cytosol. The gene responsible for *cblF* was very recently cloned by homozygosity mapping and found to correspond to *LMBRD1*, which encodes a lysosomal membrane protein (43). This protein is consistent with a role for exporting Cbl from the lysosome.

cblC. Approximately 400 patients have been described with *cblC*, making it by far the most common disorder of intracellular B_{12} metabolism (45). *cblC* also has variable presentation, but often includes haemotological abnormalities, neurological problems and ophthalmological symptoms (46). Two distinct phenotypes, correlating with age of onset, can be seen. Early onset patients present within the first year of life with severe disease and rarely respond clinically to treatment, while late-onset patients present in childhood to adulthood, are more likely to have less severe symptoms, and usually respond better to treatment (46). The gene responsible for the *cblC* group, called *MMACHC*, was described in 2006 (47). The protein has been predicted to have a B_{12} binding site and a TonB like domain (47) and has been shown to bind and decyanate CNCbl (48) as well as to dealkylate cobalamins containing C2-C6 alkanes, CN-, Ado-, or Me- as the upper axial ligand (49). The deficiency in *cblC* was initially predicted to be a

block in the cytosolic cob(III)alamin reductase (50). However, based on the protein structure and recent Cbl binding data, MMACHC is now predicted to be responsible for intracellular Cbl transport and processing, perhaps interacting with the *cblF* protein for export of Cbl out of the lysosome and then passing Cbl on to the *cblD* protein for distribution to the rest of the pathway (27, 45). Further background information and clues as to the possible function of MMACHC will be given in chapters 3 and 4.

cblD. The *cblD* complementation group was first described in two siblings who had combined deficiency of MCM and MS (51). For over 25 years these two remained the only *cblD* patients described, and biochemical analysis revealed only that this complementation group seemed to act in a similar manner as *cblC* but with less severe defects (50). However, in 2004, Suormala *et al.* (52) described three new cases of *cblD*, two of which had only MS deficiency (called *cblD* variant 1) and one of which had only MCM deficiency (*cblD* variant 2). These results suggested that the *cblD* protein might be responsible for the branching of the Cbl metabolism pathways to the cytosolic or mitochondrial compartments. The same group cloned the *cblD* gene 4 years later (42), named it *MMADHC*, and with an additional 4 patients, showed a clear genotype-phenotype relationship where truncation mutations in the 5' region resulted in only methylmalonic aciduria (MCM deficiency), truncation mutations in the middle and 3' regions resulted in combined methylmalonic aciduria and homocysteinuria (MCM and MS deficiency), and missense mutations in the 3' region resulted in only homocysteinuria (MS deficiency). Additionally, they demonstrated that the *cblH* complementation group, which had been previously described as one patient with unidentified methymalonic

aciduria (53), actually belonged to *cblD* variant 2. The MMADHC protein has a predicted mitochondrial leader sequence, a putative B_{12} binding sequence and shows homology to a bacterial ABC transporter (42). While no functional or biochemical data is yet available for MMADHC, it is currently speculated to interact with MMACHC as part of a chaperone role to present Cbl to the cytosolic and mitochondrial proteins (27, 42).

Complementation groups affecting only MS

The gene responsible for *cblG* was shown to be *MTR*, which encodes methionine synthase (MS) itself (54-56). MS, or 5-methyltretrahydrofolate:homocysteine methyltransferase, catalyzes the methylation of homocysteine to form methionine using 5-methyltetrahydrofolate as a methyl group donor and requires the presence of enzyme bound MeCbl for activity (57, 58) (Fig. 1.5). The reaction proceeds by methyl group transfer from 5-methyltetrahydrofolate to cob(I)alamin bound by MS to form MeCbl, followed by transfer of the methyl group from MeCbl to homocysteine to form methionine and a return to cob(I)alamin (59, 60). MS activity is important for maintaining adequate levels of cellular methionine and for the methylation cycle, which maintains the cellular level of the methionine derivative S-adenosylmethionine, a methyl donor in a number of cellular processes including DNA and RNA methylation and neurotransmitter synthesis (61). Additionally, MS is the only mammalian enzyme to use 5-methyltetrahydrofolate, meaning it is part of the folate cycle as well (61). MS deficiency results in hyperhomocysteinemia, homocystinuria and hypomethioniemia (62,

63) as well as trapping cellular folate as 5-methyltetrahydrofolate, blocking purine and pyrimidine biosynthesis and other single-carbon-transfer reactions (61). Patients with *cblG* usually present with megaloblastic aneamia and developmental delay, typically in the first 2 years of life, although patients who presented as adults have been reported (17). Mammalian MS and *E. coli* MS (called MetH) are 55% identical (64), and on the basis of crystallized *E. coli* MetH functional domains of MS have been identified. For MetH, residues 2-353 make up the homocysteine binding and activation domain, residues 354-649 are responsible for 5-methyltetrahydrofolate binding (65), residues 650-896 constitute the cobalamin-binding domain (66) and residues 897-1227 are responsible for the activation domain and binding site for S-adenosylmethionine, required for reductive methylation of enzyme-bound cobalamin (67).

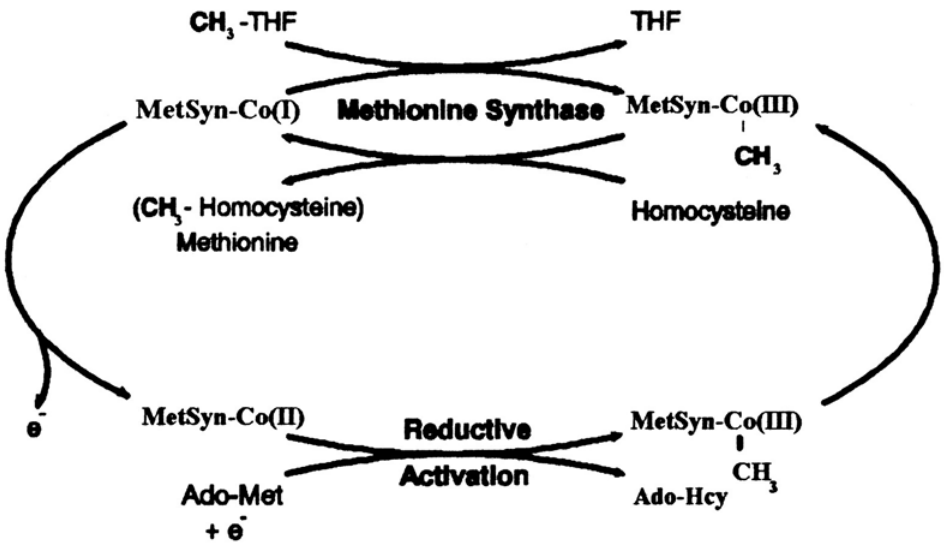

Figure 1.5. The Methionine Synthase Cycle.
From (68).

cblE. *cblE* corresponds to defects in methionine synthase reductase (MSR), encoded by *MTRR* (68). Since the reaction catalyzed by MS involves cob(I)alamin, a supernucleophile very sensitive to oxidation, the cofactor is oxidized to cob(II)alamin about once every 2000 turnovers, which inactivates MS (69). To recover catalytic function, MS needs to have the cob(II)alamin returned to MeCbl. This happens via reductive activation, involving AdoMet and an electron donor (70, 71) in a reaction catalyzed by MSR, a dual flavoprotein containing FMN and FAD (72) (Fig. 1.5). Mammalian MSR has been shown to be the reductive partner of MS (68, 72), as well as a molecular chaperone for MS, having the ability, *in vitro*, to enhance the formation of holoMS by stabilizing apoMS (73). Additionally, MSR can catalyze the reduction of aquacob(III)alamin to cob(II)alamin (73), making it an aquacobalamin reductase and possibly functioning as such in the cytosolic pathway. The mitochondrial pathway, by contrast, has no protein yet identified to fulfill this function. However, given the potential mitochondrial leader sequence found by alternative splicing in the *MTRR* gene, as well as *in vitro* results demonstrating production of cob(I)alamin via physical interaction with a mitochondrial pathway protein (MMAB), it was hypothesized that MSR might also function as the reductase responsible for the production of cob(I)alamin in the mitochondria (68, 74). This question will be addressed in chapter 4. Clinical presentation of *cblE* patients is similar to *cblG*, and it is usually impossible to separate the two groups clinically (62). However, one *cblE* patient presented with methylmalonic aciduria, possibly indicating a block in MCM as well MS, although the authors suspected it might be due to a defect outside of cobalamin metabolism since propionate fixation did not respond to an addition of OHCbl to patient fibroblasts(62).

Complementation groups affecting only MCM

cblA. *cblA* causes methylmalonic aciduria, but is very often responsive to vitamin B_{12} therapy (17, 75). In a study of 20 *cblA* patients in 3 cohorts, all patients were clinically responsive to B_{12} and only 1 out of the 20 died during the study, giving *cblA* patients the best outcome of the methylmalonic aciduria patients studied (76). The defect in *cblA* is due to mutations in the *MMAA* gene (77). Originally, the block in *cblA* had been postulated to correspond to a defect in mitochondrial cob(II)alamin reductase because, while *cblA* patients have low AdoCbl levels, cell free extracts from these patients were able to synthesize AdoCbl normally when incubated with OH-[^{57}Co]-Cbl, ATP and a reducing system (78). Upon cloning of *MMAA*, however, it was recognized that the protein did not have any NAD(P)H-binding sites suggestive of a reductase, but rather belonged to the G3E family of P-loop GTPases (77). The authors speculated that MMAA might instead be involved in the translocation of cobalamin into mitochondria (77). Our current understanding of the function of MMAA comes from work done on bacterial homologs of MMAA. This work suggests that MMAA physically interacts with MCM in a GTP modulated fashion and this interaction stimulates GTPase activity of MMAA, as well as protect cobalamin bound by MCM from oxidation (79-82). This work will be further explained and expanded on in chapters 5 and 6.

cblB. The *cblB* group is also deficient in AdoCbl synthesis (46). Biochemically, this group has long been expected to correspond to a defect in the ATP:cob(I)alamin

adenosyltransferase (ATR) enzyme, ever since *cblB* cell free extracts incubated with OH-[^{57}Co]-Cbl, ATP and a reducing system were unable to generate AdoCbl (78). The gene responsible for *cblB* has since been identified, named *MMAB*, and indeed it does correspond to ATR (83, 84). Most of the mutations in this gene cluster in exon 7, which encodes the active site of the enzyme (85, 86). Characterization of the most common mutants, R186W, R190H, R191W and E193K, revealed anomalously, that all but R191W result in no expressed protein *in vivo* (87). Further, R191W is also the only protein of these mutants that is enzymatically active, although it has a much increased K_m for both ATP and cob(I)alamin (87). Human MMAB has been crystallized (86). It was found to exist as a trimer with 3 active sites, 2 of which bound ATP. Interestingly, 20 residues at the enzyme's N-terminus become ordered upon ATP binding, forming a novel ATP-binding site and a cleft for binding cobalamin. Additionally, human MMAB has been found to bind with similar K_d to multiple forms of cobalamin (AdoCbl, HOCbl, MeCbl and CNCbl) as well their DMB-deficient analogs (AdoCbi and CNCbi). Surprisingly, in the presence of ATP, MMAB has also been found to bind cob(II)alamin in an unusual base-off four-coordinate state, most likely in order to facilitate the reduction to cob(I)alamin (7). Additional understanding of MMAB function comes from work on bacterial homologs. Unlike humans, who only have one type of ATR, bacteria have up to 3 different kinds, CobA-type, EutT-type and PduO-type, the last representing the closest homolog to human (88, 89). In *Salmonella enterica*, deletion of the *pduO* gene resulted in only partial replacement of function by CobA, even though both enzymes catalyze the same reaction, suggesting that there may be a specific interaction between the ATR and its concomitant AdoCbl utilizing enzyme (90). Further, Padovani *et al.* (91)

demonstrated that, *in vitro*, the PduO-type ATR MeaD catalyzes the direct transfer of generated AdoCbl to MCM without diffusion into the surrounding milieu. Additionally, they showed that binding of ATP to MeaD drives release of AdoCbl to MCM in a rotary mechanism where only two active sites are used at once, and binding of ATP to the third site drives release of AdoCbl out of the first site to the awaiting MCM (92).

mut. Finally, the *mut* complementation group is representative of mutations in the *MUT* (MCM) gene. MCM is important for the metabolism of branched chain amino acids, odd-chain fatty acids and cholesterol (17) and catalyzes the reversible isomerization of $_{L}$-methylmalonyl-CoA to $_{L}$-succinyl-CoA, which is key to the breakdown of propionate as well as for replenishing the TCA cycle (Fig. 1.6). Nearly 200 disease causing mutations have been found in the *MUT* gene (93). Common mutations of *MUT* include c. 655A>T (p. N219Y), c. 1106G>A (p. R369H), c. 2080C>T (p.R694W), c. 322C>T (p.R108C) (Hispanic patients) and c.2150G>T (p.G717V) (Black patients) (94). Two distinct defects of *mut* have been described. Mutations described as *mut*$^{-}$ when there is still residual activity of the MCM enzyme or if there is detectable [^{14}C]-propionate metabolism and mutations described as *mut*° in the absence of either of those two (95). Unsurprisingly, patients can be clinically split into these two groups as well. *mut*° patients have a higher frequency of morbidity, mortality and neurologic complications than *mut*$^{-}$, and *mut*$^{-}$ are more responsive to cobalamin therapy (76). Mutase from *P. shermanii* has been crystallized, giving evidence for the structure of human MCM, since the α-subunit is 60% identical (75% similar) to the human enzyme (96). Each *P. shermanii* MCM subunit contains an N-terminal $(\beta\alpha)_8$ TIM barrel (residues

88-422) housing the substrate binding site, a C-terminal $(\beta\alpha)_5$ AdoCbl binding domain (residues 578-750) with a groove for binding the DMB side chain and residues to stabilize the lower face of the corrin ring and a linker region (residues 423-577) between them that houses the upper face of the corrin ring and the 5'-deoxyadenosyl group (97-99). Human MUT exists as a homodimer in the mitochondrial matrix with 1 mole of AdoCbl bound per subunit (100, 101). Bacterial evidence, as previously described, suggests that MCM does not exist alone, but functions as a complex with other proteins, notably MMAA and MMAB.

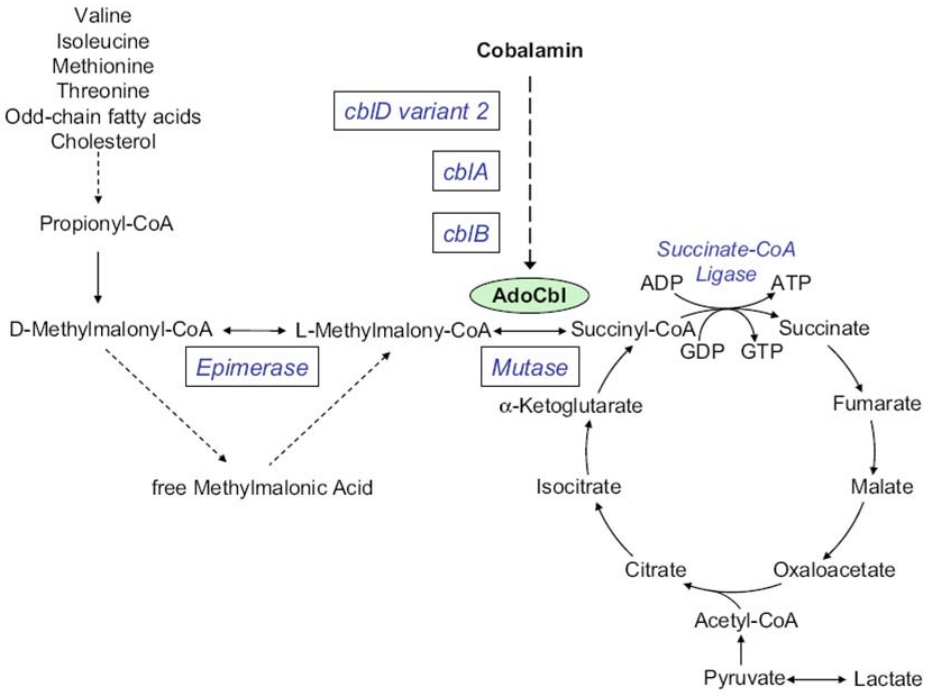

Figure 1.6. Metabolic pathways dependent on MCM.
From (94).

The Purpose of the Thesis

As a lab we are interested in defining the human intracellular metabolic pathway of Cbl. While my project fell under this broader heading, it specifically focused on three separate branches of this pathway. First, I investigated whether MSR, a protein known to catalyze the reductive activation of Cbl in the cytosol, also performed this as yet unidentified function in the mitochondria (Chapter 2). Next, I tested the binding of early-onset and late-onset MMACHC mutant proteins to CNCbl and HOCbl to solve the old conundrum of why they are more responsive to the latter (Chapter 3), as well as determining why late-onset patients have disease in the first place (Chapter 4). Finally, I probed the interaction of MMAA and MCM using an *E. coli* model (Chapter 5) as well as the human proteins (Chapter 6). These projects have helped to define the function and interactions of the proteins responsible for the chaperoning and modification of Cbl and its interaction with the proteins that utilize the cofactor. Together, these studies give us a better understanding of how cobalamin goes from an ingested vitamin to a functional cofactor.

CHAPTER 2: RESTRICTED ROLE FOR METHIONINE SYNTHASE REDUCTASE DEFINED BY SUBCELLULAR LOCALIZATION

Introduction

Thus far, the enzyme responsible for the mitochondrial reduction of cob(II)alamin to cob(I)alamin, a step required for the synthesis of AdoCbl, has yet to be described. MSR, the protein responsible for this same reaction in the cytosolic pathway, might be a candidate for this role for two reasons. 1) When the *MTRR* gene was originally cloned, it was found to produce two mRNA splice variants with different 5' ends (68) (Fig. 2.1AB). While the first variant produced a protein whose predicted cellular location was consistent with being cytosolic, the second and larger variant had a 58 bp 5' extension that was predicted to produce an extra 27 N-terminal amino acids, generating a peptide sequence predicted by the mitochondrial prediction program TRANSPEP to constitute a mitochondrial leader sequence (102) (Fig. 2.1C). These data suggested that a version of MSR might be normally present in the mitochondria. 2) An investigation by Leal *et al.* demonstrated that *in vitro* MSR and MMAB (ATR in their nomenclature) were able to convert cob(II)alamin to AdoCbl at a level that might be sufficient to meet physiological needs (74). In this way MSR may participate in the reduction of cobalamin for MMAB in the same way it reduces cobalamin for MS (Fig. 2.1D). With these studies in mind, we set out to determine if MSR does localize to the mitochondria *in vivo* and therefore has the possibility of filling the role of the missing AdoCbl synthesizing reductase.

Here we report that both isoforms of MSR mRNA are detectable by RT-PCR, as previously reported. We also confirm that MSR and MMAB can indeed function together *in vitro* to produce AdoCbl. However, we show that, unlike other mitochondrial proteins involved in the AdoCbl pathway, variant 2 MSR does not produce a functional mitochondrial leading sequence. We also show that MSR protein is localized to the cytoplasm but not to the mitochondria, in both Western blot and immunofluorescent studies. These data confirm that MSR is restricted to the cytosol and therefore does not function as the missing mitochondrial reductase.

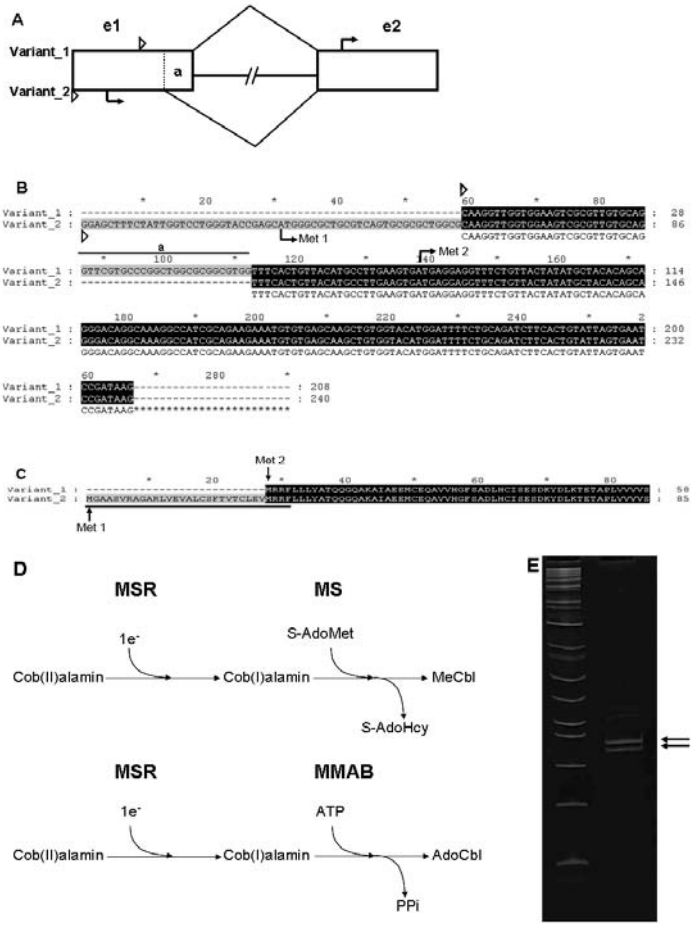

Figure 2.1. Splice variants of MSR and the predicted mitochondrial leader.

A. A schematic of the two splice variants of MSR mRNA. Represented here are the first two exons (rectangles, e1 and e2), the first intron (lines connecting rectangles), the beginning of the 5' untranslated region (small triangles) for each splice variant, the start site (arrow) of each, and the 26 bp region at the end of exon 1 that is found as 5'UTR in variant 1, but spliced out in variant 2 ("a") of MSR. **B.** Alignment of the mRNA transcribed from the first 2 exons in both splice variant 1 and 2. The red "Met" shows the position of the initiation codon of each variant splice form. The rest of the markings are the same as in A. **C.** The predicted protein translation of the N-terminus of the two splice variants. Variant 2 is predicted to have an extra N-terminal 27 amino acids, which was originally predicted to make up the bulk of the putative mitochondrial leader sequence (underlined) (102). **D.** Schematic of the reduction of cob(II)alamin to cob(I)alamin by MSR for the generation of MeCbl by MS or AdoCbl for MMAB. E. RT-PCR of MSR mRNA from exon 1-2 run on an 8% acrylamide gel demonstrating the two different bands which correspond to the 26 base-pair difference between the two splice variants. Upper arrow: Variant 1. Lower arrow: Variant 2.

Methods and Materials

RT-PCR

RNA isolation, reverse-transcription and PCR reactions were performed as described (55).

Plasmid Construction

The plasmid pAcGFP1-Mito was purchased from Clontech (Mountain View, CA). This vector contains the mitochondrial targeting sequence from subunit VIII of human cytochrome C oxidase consisting of the first 29 residues of that protein, followed by the green fluorescent protein (GFP) variant AcGFP1. Flanking the mitochondrial leader sequence are the unique restriction enzyme sites NheI (5') and BamHI (3'). For construction of the GFP plasmid without the mitochondrial leader sequence, we cut pAcGFP1-Mito with NheI and BamHI, filled in the ends with Klenow enzyme and blunt-end ligated the vector to itself using T4 DNA Ligase (all from New England Biolabs; Mississauga, ON). For construction of mmabLeader-GFP, mutLeader-GFP and msrLeader-GFP we used the PCR product from the amplification of the N-terminal regions of each cDNA as specified by the primers shown in Table 2.1, and ligated them into pAcGFP1 using NheI and BamHI.

Table 2.1. Primers used to make GFP mitochondrial leader constructs.

Gene	Primers	Sequence	Product Length	Amino acids covered
MMAA	cblA 5'	GGGCTAGCATGCCCATGCTGCTACCACAT	180 bp	60 aa
	cblA 3'	G*GGATCC*CCATCTGACAGCAGCATCCAC		
MMAB	cblB 5'	GGGCTAGCATGGCTGTGTGCGGCCTGG	261 bp	87 aa
	cblB 3'	G*GGATCC*CCCACGGCTTCAAACACTT		
MUT	MUT 5'	GGGCTAGCATGTTAAGAGCTAAGAA	183 bp	61 aa
	MUT 3'	G*GGATCC*CATATTAGGTCTTCTGGGT		
MSR	MSR 5'	GCTAGCGGAGCTTTCTATTGGTCCTGGGTACCGAGC ATGGGCGCTGCGTCAGTGC	173 bp	47 aa
	MSR 3'	G*GGATCC*TCTTCTGCGATGGCCTTT		

Antibody Generation

Antibodies against MSR were produced at the Sheldon Biotechnology Centre (Montreal, Canada) by immunizing rabbits with either i) a synthetic peptide encompassing amino acids 37-56 of MSR (MSR-FMN-domain) (Sheldon Biotechnology Centre; Montreal, Canada) or ii) a protein fragment of amino acids 155-306 of MSR plus a 6x His-tag expressed from the plasmid pQE-30 (Qiagen; Mississauga, ON) (MSR-linker-domain). To ensure antigenic specificity before use in Western blot and immunofluorescence, both antibodies were affinity purified to expressed and purified full-length MSR protein using HiTrap NHS-activated HP columns, following manufacturer's protocols (Amersham/GE Healthcare; Baie d'Urfe, QC). Antibodies against MUT were generated at the SACRI Hybridoma Facility (University of Calgary) by immunizing mice against a protein fragment encompassing amino acids 1-371 of MUT with a C-terminal 6x His-tag expressed from pET28a (Novagen; Madison, WI) . The primary antibody, anti-p38MapK, was purchased from BD Biosciences (Mississauga, ON). The secondary antibodies used for Western blotting: Goat anti-Rabbit IgG HRP and Goat anti-Mouse IgG HRP were purchased from Biorad (Mississauga, ON) and the secondary antibodies used for immunofluorescence: Cy3-conjugated donkey anti-rabbit IgG and Cy3-conjugated donkey anti-mouse IgG were purchased from Jackson Immunoresearch (West Grove, PA).

Cell Culture and Protein Preparation

Huh-1 (human hepatoma) [18], MCH65 (normal human fibroblasts) and WG1296 (*cblE* patient fibroblasts) cells were cultured in DMEM (Invitrogen; Burlington, ON) supplemented with 10% serum (5% fetal bovine serum, 5% bovine calf serum) and antibiotics-antimycotics. MCH65 and WG1296 were from the Cell Repository, Montreal Children's Hospital. Confluent cells were harvested by trypsinization, washed in PBS, resuspended in 2x cell pellet volume of NETN buffer (150 mM NaCl, 1 mM EDTA, 50 mM Tris-HCl, pH8.0, 0.01% NP-40) plus protease inhibitors and disrupted using an Ultrasonic Processor XL (Mandel Scientific; Guelph, ON). The cell lysate was then centrifuged at 10,000 x *g* for 10 minutes at 4°C, and the supernatant containing total soluble cell protein was recovered and protein concentration determined using the Bradford Assay (BioRad).

Cellular fractionation

Cells were fractionated according to methods described by Isaya *et al.* [19] with a few exceptions. Briefly, cells were grown in a monolayer on a 10 cm plate, washed with PBS, then incubated with 1.5 ml of digitonin release buffer (250 mM sucrose; 17 mM MOPS, pH 7.5; 2.5 mM EDTA; 0.8 mg of digitonin per ml) for exactly 2 minutes. Treatment was stopped by diluting with 3 ml of buffer without digitonin. The solution was aspirated and transferred to two 2 ml microcentrifuge tubes and centrifuged at 7,500 x *g* at 4°C for 5 minutes. The supernatant (containing the cytosolic fraction) was moved to a new tube and held at 4°C. The "perforated" cell monolayer remaining on the plate was scraped from the plate after addition of 0.5 ml release buffer (without digitonin) and

homogenized by 20 passages of a tight-fitting Teflon pestle in a 1 ml tapered glass tissue grinder (Wilmad-Labglass; Buena, NJ) at 4°C. One volume of release buffer without digitonin was added to the homogenate, followed by centrifugation at 1500 x *g* for 15 minutes at 4°C, resulting in a low speed pellet (unbroken cells, cell debris and nuclei) and a low speed supernatant. The supernatant was centrifuged at 15,000 x *g* for 15 minutes at 4°C, resulting in a pellet (the mitochondrial enriched fraction) and a high-speed supernatant. The cytosolic and mitochondrial enriched fractions were then used for subsequent experiments. Purity of the fractions was tested by the detection of anti-MUT as a mitochondrial marker and by the detection of anti-p38 as a cytoplasmic/nuclear marker for each fraction.

Western Blots

Cell lysates or immunoprecipitations were resolved by SDS-PAGE and transferred to nitrocellulose membranes by capillary action. The membranes were blocked with 5% skim milk in PBS for 1 hour at room temperature with shaking and then incubated with primary antibody (anti-MSR-FMN-domain at 1:100; anti-MSR-linker-domain at 1:100; anti-MUT at 1:2000; anti-p38 at 1:2000) overnight at 4°C. Membranes were then washed 3 x with TBST and incubated with secondary antibody (1:5000 Goat anti-Rabbit IgG HRP; 1:5000 Goat anti-Mouse HRP IgG) for 45 minutes at room temperature. Membranes were washed 3 x with TBST and immune complexes were detected using ECL Reagent (Amersham/GE Healthcare) according to manufacturer's recommendations and exposed to Hyperfilm (Amersham/GE Healthcare).

Nucleofection and Immunofluorescence

Plasmids noLeader-GFP, mitoLeader-GFP (pAcGFP1-mito), msrLeader-GFP, mutLeader-GFP and mmabLeader-GFP were introduced into cells by nucleofection as per manufacturer's protocol (Amaxa Biosystems; Gaithersburg, MD). Immunofluorescence was performed according to Narang *et al.* (103) with a few exceptions. Cells were grown on coverslips and fixed with fresh 4% paraformaldehyde in PBS for 20 minutes at 37°C. Cells transfected with GFP constructs were stained with DAPI (Sigma-Aldrich; Oakville, ON) (1:5000 in PBS) for 30 seconds and visualized. Cells to be probed with antibody were washed 1 x with PBS, and permeabolized by 0.1% Triton X-100 (Sigma-Aldrich) in PBS for 15 minutes at room temperature. Cells were washed 3 x PBS and blocked in 10% BSA in PBS with slow rocking for 1 hour at room temperature, washed 3 x PBS and incubated with anti-MSR-linker-domain or anti-MUT (1:250) for 1 hour at 37°C, washed 3 x PBS, and incubated with secondary antisera (Cy3-conjugated donkey anti-rabbit, 1:250 or donkey anti-mouse IgG, 1:250) for 1 hour at 37°C. Cells were then counterstained with DAPI (1:5000 in PBS) for 30 seconds. Cells were mounted and visualized using a Leica DMR microscope with Metamorph 6.1 (Universal Imaging). Images involving cellular localization of GFP were not processed further; however, images involving the colocalization of MSR or MUT and mitochondria were deconvolved using a nearest-neighbors algorithm to reduce background haze and improve image contrast with Autodeblur 7.0 (AutoQuant) software.

Protein expression and purification

A human MMAB clone in a pET3a vector (Novagen) was kindly provided by H.L. Schubert and C.P. Hill, University of Utah. MMAB protein was expressed and purified as previously described (86). A human MSR clone was generated by RT-PCR of mRNA from MCH65 cells using the oligonucleotides 5'GGATCCATGAGGAGGTTTCTGTTACTA-3' and 5'AAGCTTTTATGACCAAATATCCTGAAG-3', where underlined base-pairs represent addition of restriction endonuclease sites. After restriction with BamHI and HindIII, the MSR product was cloned into the pQE-30 vector (Qiagen) in the 5'-BamHI and 3'-HindIII restriction sites. The recombinant MSR was overexpressed in BL21 (DE3) cells in LB with induction by 1 mM IPTG. Cell pellets were lysed by passing through a French Pressure Cell (SLM Instruments Inc) x 2 at 12,000 psi in lysis buffer (50 mM NaH_2PO_4, 300 mM NaCl, 10 mM Imidazole; pH 8.0) and centrifuged at 15,000 rpm for 30 minutes. The soluble fraction was incubated with a 5 mL slurry of Ni-NTA beads (Qiagen), rinsed in lysis buffer and allowed to mix by end-over-end rotation overnight at 4°C. Once washed in wash buffer (50 mM NaH_2PO_4, 300 mM NaCl, 20 mM Imidazole; pH 8.0), the purified protein was eluted in elution buffer (50 mM NaH_2PO_4, 300 mM NaCl, 250 mM Imidazole; pH 8.0). Protein was further purified using an FPLC Superose 6 HR 10/30 prepacked column (Pharmacia/GE Healthcare). The protein solution was applied to the column which had been pre-equilibrated with 100 mM potassium phosphate, pH 7.4. Elution was then carried out at 8°C with 100 mM potassium phosphate, pH 7.4, at a flow rate of 0.5 ml/min with protein detection at 280 nm. Protein purity was monitored by SDS-PAGE.

ATP:Cob(I)alamin Adenosyltransferase Assays

Adenosyltransferase assays were performed inside an anaerobic chamber (Coy Laboratories; Ann Arbor, MI) as previously described (74) with a few exceptions. Reaction mixtures contained a final concentration of 200 mM Tris (pH 8.0), 1.6 mM KH_2PO_4, 2.8 mM $MgCl_2$, 100 mM KCl, 0.1 mM HOCbl, 0.4 mM ATP, 1 mM DTT, 1 mM NADPH and 10 uM MMAB. Reactions were initiated by the addition of purified recombinant MSR and AdoCbl formation was measured by following the increase in absorbance at 525 nm ($\Delta\varepsilon_{525}$ = 4.8 cm^{-1} mM^{-1}).

Results

Alternative splicing of MSR

We first re-examined the splice isoforms generated by alternative splicing in exon 1. These two forms contain the distinct translation initiation codons corresponding to putative cytosolic (variant 1) and mitochondrial (variant 2) coding sequences. We performed RT-PCR using the primers AB191: 5' CAAGTTGGTGGAAGTCGCGTTG and 1803E: 5' AACCCATACCGCAGGTGAGCAAA, as originally described (68, 104). Under similar PCR conditions, we were able to identify the same two bands, corresponding to the two different isoforms of MSR mRNA (Fig 2.1E), as seen previously (104). The identity of these bands was confirmed by sequencing (data not shown). Therefore, MSR has 2 distinct splice isoforms, variant 2 of which Leclerc *et al.*

(102), using the cellular localization prediction program TRANSPEP, predicted to have mitochondrial localization signal.

Interaction of MSR with MMAB

The other rationale for predicting mitochondrial expression is the finding by Leal e*t al.* (74) that MSR can provide the reducing activity for the MMAB-catalyzed production of AdoCbl from cob(II)alamin. We set out to confirm this result by incubating MMAB with MSR and assessing the production of AdoCbl. We found no significant production of AdoCbl when MMAB was incubated in OHCbl, ATP, $MgCl_2$, DTT and NADPH (Fig. 2.2). However, upon addition of MSR there was immediate production of AdoCbl, and the rate of product formation increased with increasing concentration of MSR (Fig. 2.2). Thus, MSR and MMAB can combine to produce AdoCbl from cob(II)alamin *in vitro*. If MSR is targeted to mitochondria along with MMAB *in vivo*, it may act as the elusive mitochondrial reductase.

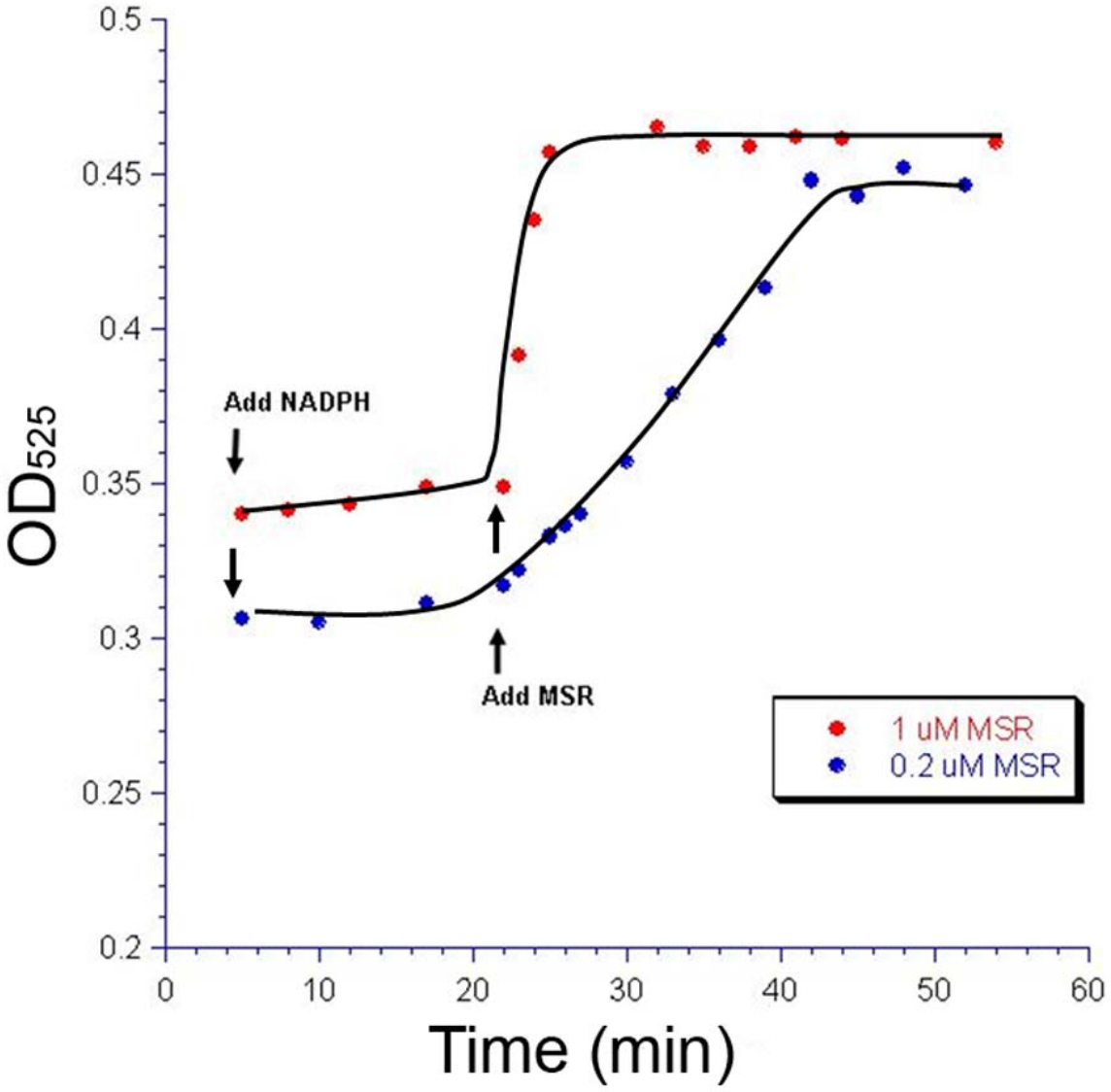

Figure 2.2. MSR acts with MMAB to produce AdoCbl.

MMAB protein (10 µM) was incubated in the presence of DTT, $MgCl_2$, ATP, OHCbl and NADPH with no significant production of AdoCbl as monitored by absorption at 525 nm. Upon addition of MSR (0.2 µM or 1 µM), AdoCbl was produced. Adding an increased concentration of MSR produced a corresponding increase in the rate of AdoCbl production (Red vs. Blue). Therefore, as was shown previously by Leal *et al.* (74), MSR can act with MMAB to make AdoCbl.

MSR does not have a functional leader sequence

To assess the functionality of the putative MSR mitochondrial leader sequence, we created different plasmids that have known or candidate mitochondrial leader sequences attached to the N-terminus of GFP from the plasmid pAcGFP1-mito (Fig. 2.3A) and assessed by immunofluorescence whether they direct GFP into the mitochondria. When we transiently transfected the plasmid pAcGFP1-mito, with the mitochondrial targeting sequence of subunit VIII of cytochrome c oxidase, into the human fibroblast cell line MCH65, the expressed GFP was distributed in the typical punctate or worm-like pattern of mitochondrial proteins (Fig. 2.3B, Panel 1). However, when we excised the mitochondrial leader sequence of pAcGFP1-mito, expressed GFP was found to be distributed throughout the cytoplasm (Fig. 2.3B, Panel 2). When we replaced the cytochrome c oxidase targeting sequence with the coding sequence of the first 47 amino acids of MSR variant 2, we found that the GFP was again distributed diffusely throughout the cytoplasm, mimicking the pattern of the control plasmid with its mitochondrial targeting sequence removed (Fig. 2.3B, Panel 3). It is important to note that this protein could only be expressed if we included the 30 bp 5' UTR in front of the MSR coding sequence. In contrast, when the coding sequences of the N-terminal regions of MUT and MMAB were spliced upstream of the GFP sequence, GFP was again directed to the mitochondria (Fig. 2.3B, Panels 4 & 5, respectively). These results demonstrate that, unlike MMAB and MUT, two cobalamin metabolism proteins known to target to mitochondria, MSR does not possess a functional mitochondrial leader sequence, at least as evaluated by attachment to GFP.

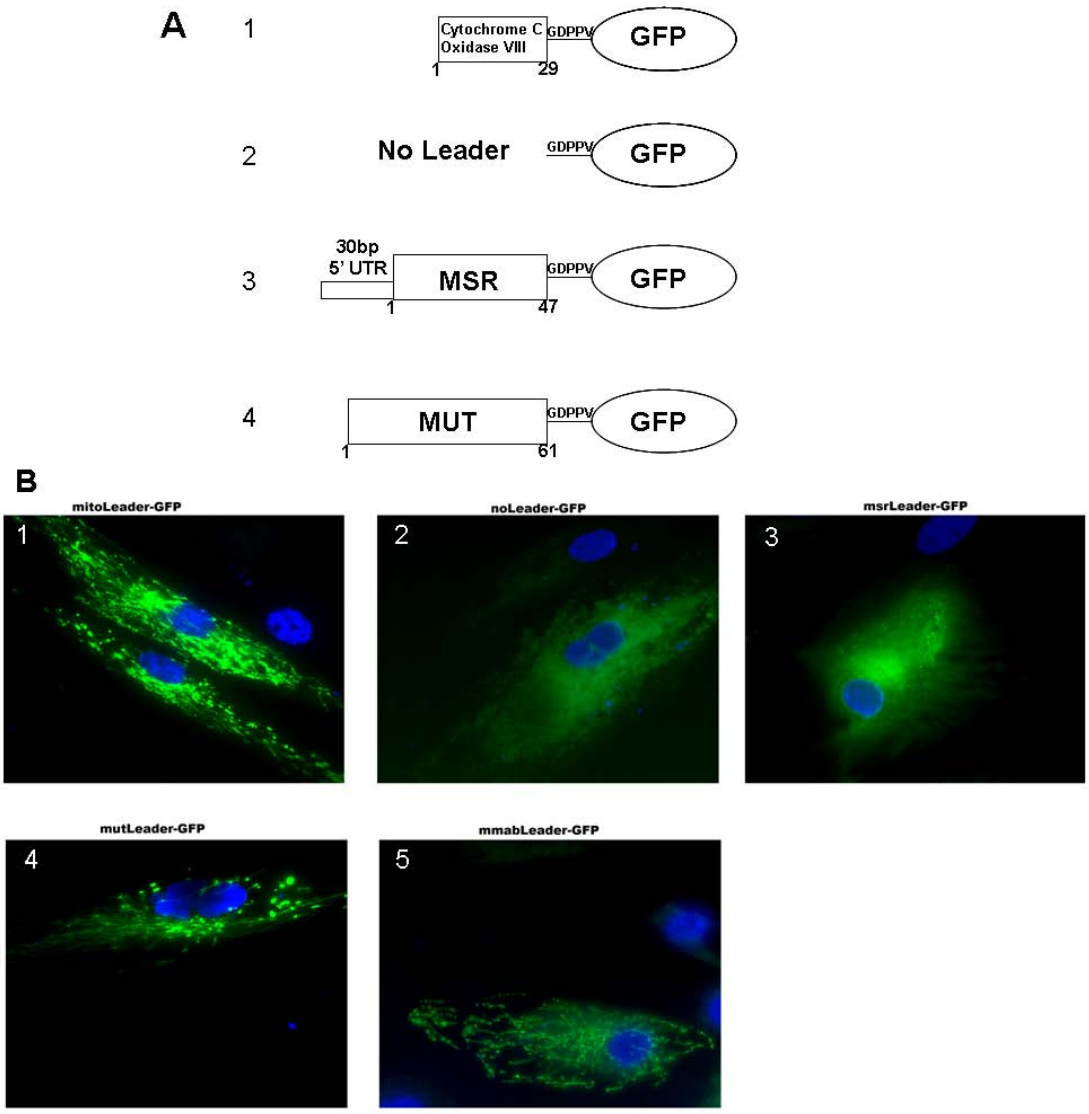

Figure 2.3. Assay of functional N-terminal leader sequences.

A. Schematic of the different mitochondrial leader constructs made from the pAcGFP1-mito vector. 1. Original pAcGFP1-vector with cytochrome C oxidase subunit VIII leader sequence (positive control). 2. Cytochrome C oxidase subunit VIII leader sequence is cut out, leaving the vector with expression of GFP but no mitochondrial leader (negative control). 3. pAcGFP with the 30bp 5'UTR and first 173 base pairs (47 amino acids) of MSR variant 2 attached to the N-terminus of GFP. 4. The first coding 183 base pairs (61 amino acids) of MUT attached to the N-terminus of GFP. 5. The first coding 261 base pairs (87 amino acids) of MMAB attached to the N-terminus of GFP. **B.** Brightfield fluorescent images of the constructs described and numbered as above, after transfection into MCH65 fibroblasts. Note the punctate pattern of GFP expression in panels 2, 4 and 5 and diffuse expression in panels 1 and 3.

MSR protein is found in the cytoplasm but not in the mitochondria

To inspect MSR localization directly, we examined the distribution of MSR protein by Western blot of cytosol and mitochondrial extracts and by immunofluorescence analysis of Huh-1 cells and human fibroblasts. The Western blot was accomplished using antibodies independently generated against two different sites in MSR, the FMN-domain at the N-terminus and the central linker-domain. In both cell lines and for both antibodies, MSR was detected in the cytosol but not the mitochondrial extracts (Fig. 2.4A,B). Note that only one band corresponding to MSR was detected, likely due to the small size difference between the two predicted isofroms, 2.7 kDa, so that if there were two bands they would appear in the same location in this experiment. Antibody specificity was demonstrated by the absence of the MSR band in the MSR deficient cell line WG1296. Successful separation of mitochondria and cytosol was demonstrated by the detection of MUT in the mitochondrial fraction but not cytosolic fractions, and by the presence of the cytoplasmic/nuclear marker p38 in the cytosol and near absence in the mitochondrial fraction (Fig. 2.4C).

To evaluate the subcellular distribution of MSR in cells *in situ*, we probed MCH65 fibroblasts for MSR and compared it with the distribution of GFP (AcGFP1) containing the N-terminal mitochondrial targeting sequence from subunit VIII of human cytochrome C oxidase expressed following nucleofection with the pAcGFP1 plasmid. MSR, detected by immunofluorescence using the MSR linker-domain antibody, was observed to be distributed throughout the cytoplasm and did not colocalize with the GFP mitochondrial

marker (Fig. 2.4D). In contrast, the mitochondrial protein MUT did show colocalization with mitochondrial GFP (Fig. 2.4E). These experiments demonstrate that MSR protein is not found in the mitochondria of cells and that it is instead restricted to the cytosol.

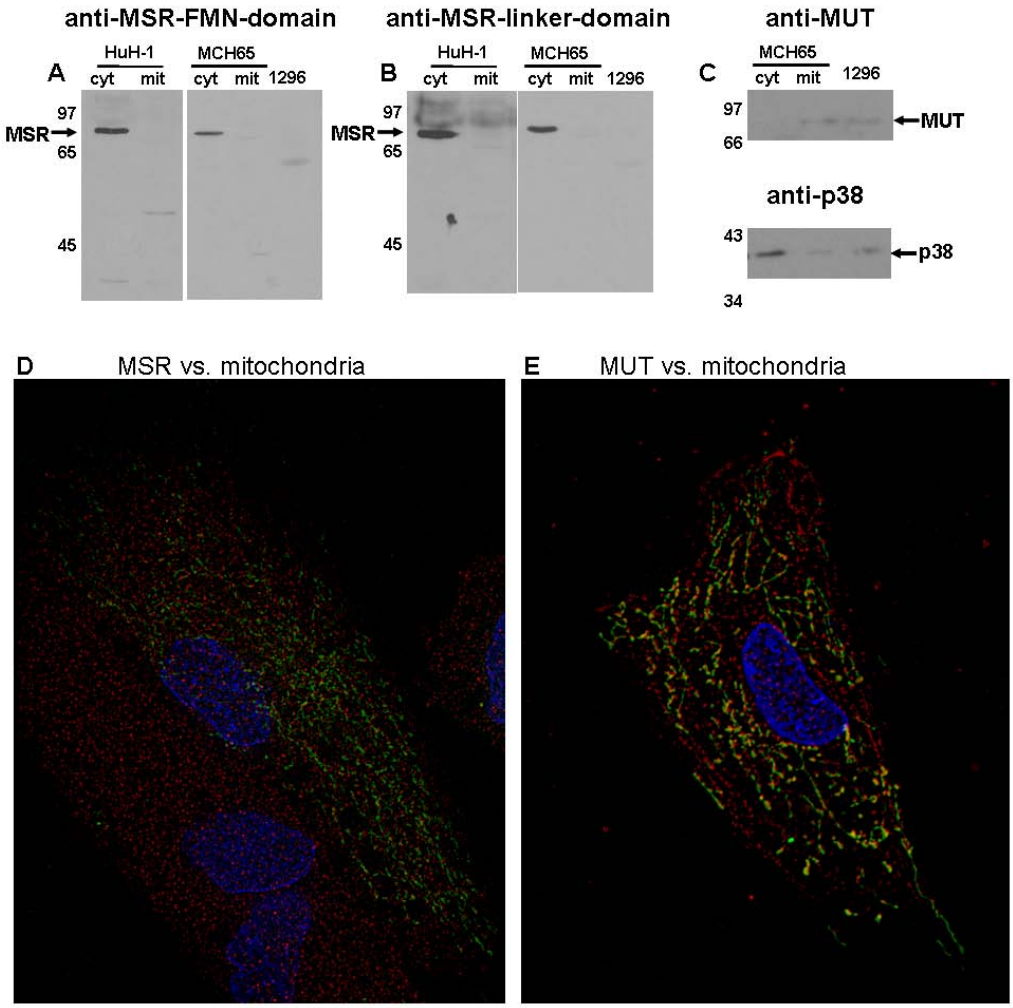

Figure 2.4. Subcellular localization of MSR.

Panels **A** & **B**. Western blot of cytosolic (cyt) and mitochondrial (mit) fractions of Huh-1 and MCH65 cells and total cell protein of WG1296 (1296) probed with anti-MSR-FMN-domain (panel **A**) or anti-MSR-linker-domain (panel **B**). Panel **C**. Control to test purity of mitochondrial and cytoplasmic fractions. Upper panel shows anti-MUT (mitochondrial protein); lower panel shows anti-p38 (cytosolic and nuclear protein). There appears to be a small amount of cytosolic contamination of the mitochondrial fraction (band in 'mit' of p38), but almost no mitochondrial contamination of cytoslic fraction (band 'c' in MUT). Lanes are the same as indicated for Panel **A** and **B**. Panel **D** & E. Immunofluorescent localization of MSR. MCH65 cells were transfected with pAcGFP1-mito (mitochondrial label, Green) and were immunostained for either MSR (anti-MSR-linker-domain) Panel **D** or methylmalonyl-CoA mutase (anti-MUT) Panel **E** (Red). Nuclei are stained with DAPI (Blue). After deconvolution, MUT was found to co-localize with mitochondria (yellow) but MSR was not.

Discussion

The role of MSR in the reductive activation of MS and recently as an aquacobalamin reductase, has been well documented (72, 73, 105). In contrast, the reductase responsible for the reduction of cob(II)alamin to cob(I)alamin prior to adenosylation by MMAB in the mitochondria has yet to be found. Given the ability of MSR to reduce cobalamin for the production of adenosylcobalmin by MMAB *in vitro* (74) and the presence of a putative mitochondrial leader sequence in one splice form at its N-terminus, it was tempting to evaluate MSR as the missing mitochondrial cobalamin reductase. However, our results show that MSR does not traverse the mitochondrial membrane. These studies showed MSR to be restricted to the cytoplasm in human Huh-1 hepatoma cells and in human fibroblasts. The results indicate that the two splice forms, which differ in utilizing different translation initiation codons separated by 27 amino acids, do not confer any special properties with respect to organelle targeting, leaving it unclear as to why this difference in N-terminal sequence exists. It could affect protein stability and even, potentially, net enzyme activity; however, such alternatives have not been considered in the past. Interestingly, the additional sequence borders the FMN binding domain although it does not show sequence homology with the FMN domain of other proteins. In this regard, it seems unlikely that the additional sequence has a functional role.

One clue to the origin of the additional variant sequence comes from the examination of the N-terminal sequence of MSR from different mammalian species. An alignment of MSR protein shows that the N-terminal extension found in human variant 2 is partially

conserved in primates (chimp, macaque, bushbaby) but very poorly conserved in lower mammals (Fig. 2.5). Moreover, two lower mammals that have an upstream Met-initiated in-frame sequence before Met2, opossum (5 amino acids) and guinea pig (21 amino acids), have much shorter N-terminal extensions (Fig. 2.5). These data point to the longer version of MSR being introduced as a late evolutionary addition which, due to the variation in sequence in lower mammals, is unlikely to have a functional role.

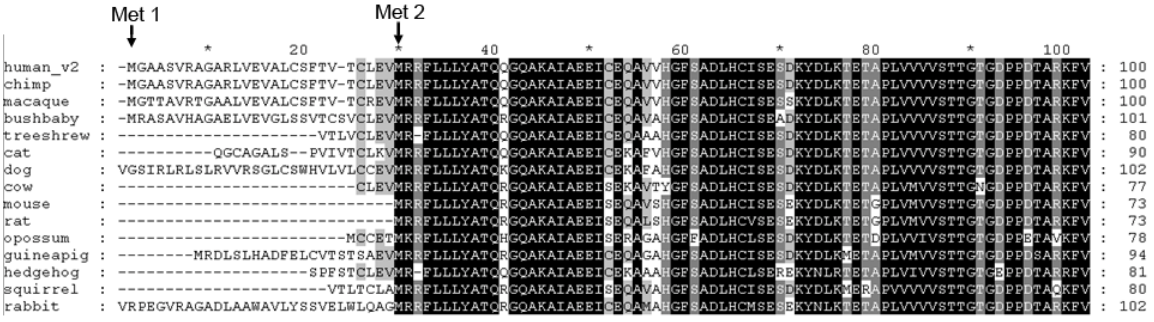

Figure 2.5. Multiple sequence alignment of the N-terminal amino acids of MSR from selected mammalian species.

MSR protein sequences of selected mammals (human, ENST00000264668; chimp, ENSPTRP00000028690; macaque, ENSMMUP00000024676; bushbaby, ENSOGAP00000000920; treeshrew, ENSTBEP00000011472; cat, ENSFCAP00000014011; dog, ENSCAFP00000014869; cow, ENSBTAP00000012372; mouse, ENSMUSP00000039810; rat, ENSRNOP00000024041; opossum, ENSMODP00000002568; guinea pig, ENSCPOP00000005952; hedgehog, ENSEEUP00000001324; squirrel, ENSSTOP00000004416; and rabbit, ENSOCUP00000003139) were aligned using Clustalw (106) and visualized using GeneDoc (107). For clarity, only the first 100 amino acids are shown.

MSR variant 2 was predicted to have a mitochondrial leader sequence by TRANSPEP in 1999, a program that was then part of the PCGENE package from Intelligenetics. It is interesting to assess whether current mitochondrial prediction programs would give the same subcellular location. Table 2.2 contains the subcellular localization predictions of MSR variant 2 from several targeting sequence prediction programs. Three of the four programs used predict that the variant 2 sequence “is possibly” or “is” mitochondrial. By comparison, two of the four programs predict mitochondrial localization for MSR variant 1, a protein known to be cytosolic, but all four predict MUT to be in the mitochondria (Table 2.2). It seems that even with the advanced prediction programs of today, there is still an uncertainty in predicting whether proteins like MSR with putative, if not strong, mitochondrial signals are targeted to this organelle.

Table 2.2. Subcellular localization predictions of MSR variant 2, as determined by various subcellular prediction programs.

	MitoProt II 1.0a4		Predotar v. 1.03		iPSORT		TargetP1.1 (mTP score)	
	Score	Prediction	Score	Prediction	Score	Prediction	Score	Prediction
MSR v2	0.5931	Mitochondria-probable	0.23	Mitochondria-possible	>0.083? no	Not Mitochondrial	0.404	Mitochondrial
MSR v1	0.3846	Mitochondria-probable	0.36	Mitochondria-possible	>0.083? no	Not Mitochondrial	0.268	Other
MUT	0.5959	Mitochondria-probable	0.71	Mitochondrial	>0.083? yes	Mitochondrial	0.768	Mitochondrial

While MSR does not target to mitochondria, the ability of MSR to take part in the adenosylation sequence suggests that a candidate in this role might be a homologous protein. Thus far, only four mammalian proteins are members of the family of dual flavin reductases: MSR, nitric oxide synthase (NOS), cytochrome P450 reductase (POR) and NADPH dependent diflavin oxidoreductase 1 (NDOR1). NOS has three major isoforms and one potential mitochondrial isoform, all of which have been well characterized as producers of NO and citrulline from l-arginine and oxygen (108). Cytochrome P450 reductase is an endoplasmic reticulum-associated protein that is important in the metabolism of drugs and in steroid biosynthesis (109). Interestingly, it has been shown, in combination with soluble cytochrome b5, to catalyze the reductive activation of MS *in vitro* (110). Less is known about NDOR1; however, it has been shown to be a cytoplasmic protein that is suggested to play a role in the bioreduction of anti-cancer drugs (111), possibly by a mechanism that is modulated by the histidine triad protein DCS-1 (112). It also can participate in the reductive methylation of MS *in vitro* (113). Given the redundancy of functions displayed by this family of proteins *in vitro*, the ability of MSR to act as the reducing enzyme in conjunction with the adenyltransferase *in vitro* may be a further reflection of the biochemical breadth of these proteins. In this light, it is possible that the real mitochondrial reductase may be an as yet undiscovered member of this family.

An early clue that MSR was unlikely to be the mitochondrial cobalamin reductase was the absence of methylmalonic acidemia in *cblE* patients with defects in MSR (62, 63). However, the absence of any patients at all with a block in the mitochondrial reduction of

cobalamin is unexpected given the occurrence of metabolic defects throughout this pathway including the several complementation groups associated with mitochondrial metabolism of cobalamin. It is conceivable that this is an essential step, incompatible with embryonic development, resulting in the absence of live-born infants with such a disorder. Alternatively, it is also possible that this vital step can be performed by multiple reductases so that a defect in one of them would be made up by the others. However, such enzymes would almost certainly have to interact closely with MMAB to prevent re-oxidation of the highly reactive cobalt centre on cobalamin. This is a property of MSR (74). Whether additional proteins with this capacity occur in human cells remains to be investigated.

CHAPTER 3: MECHANISM OF VITAMIN B12-REPONSIVENESS IN CBLC METHYLMALONIC ACIDURIA WITH HOMOCYSTEINURIA

Introduction

A striking aspect of genetic deficiencies involving vitamin B_{12} (cobalamin, Cbl) metabolism is the potential to treat patients with megadose vitamin therapy. For the most common deficiencies, such as dietary insufficiency or malabsorbtion, increasing the intake of cobalamin or providing the vitamin by injection is often sufficient to correct the problem. Genetic defects in the cellular processing of cobalamin, although rare, are more challenging but may respond to megadose vitamin therapy (up to 1000x RDA of 2.4 µg), usually in conjunction with other relevant metabolites. While not all patients respond to treatment, the fact that many do suggests that intracellularly mass action effects are sufficient to overwhelm or circumvent the offending block.

The most common disorder of cobalamin metabolism is represented by the complementation group, *cblC*, with nearly 400 patients described (45). Affected patients have combined homocystinuria and methylmalonic aciduria due to an early block in the synthesis of methylcobalamin (MeCbl) and adenosylcobalamin (AdoCbl), cofactors of methionine synthase and methylmalonyl-CoA mutase, respectively (114). Clinically, *cblC* patients comprise a heterogeneous group with early or late onset forms and highly variable symptoms (115). Patients with the severe, early onset form may present in the neonatal or early infantile period with failure to thrive, poor feeding/growth, seizures,

lethargy and neurological deterioration, often with hematologic or ophthalmologic abnormalities (116, 117). Others may present in childhood or adulthood (late-onset) with a more moderate clinical course that may include dementia, behavioural problems and myelopathy (46, 117). The early-onset form is more common and much more severe, with clinical outcome being generally poor despite metabolic management (46). Late-onset *cblC* patients, in contrast, have a less severe presentation and may have a more favourable outcome if treated (115).

The gene responsible for *cblC* has been identified and given the name *MMACHC* (85). The deduced protein is 282 amino acids in length and its C-terminus-residues 181-282, described as showing similarity with TonB, a bacterial protein involved in energy-coupled transport of vitamin B_{12}. It also contains a putative cobalamin binding site between amino acids 122-156 fitting the HXXG-$X_{\sim 30}$-GG motif found in methionine synthase and methymalonyl-CoA mutase. The most frequent mutation identified so far is c.271dupA accounting for 42% of mutant alleles (45). Over 50 additional mutations have been identified with many also causing a putative premature truncation of the protein while others caused missense mutations. The most common missense mutations are 440G→A (G147D), which was homoallelic in 5 *cblC* cases all presenting with an early onset severe disease, and 482G→A (R161Q), which is associated almost exclusively with late onset disease, as 9 out of 10 different patients have been described as late onset regardless of the nature of the second allele (45, 47, 117-119).

While natural vitamin B_{12} is the hydroxyl form (OHCbl), the generally available vitamin taken as a supplement is a cyano derivative (CNCbl). One of the most intriguing aspects of the *cblC* disorder is that patients are generally unresponsive to treatment with CNCbl but are more responsive to OHCbl. This phenomenon has been documented as far back as 1979 when Mellman *et al.* (50) found that fibroblasts from *cblC* patients took up and retained less CNCbl than OHCbl compared to controls and were uniquely unable to remove the cyanide ion from CNCbl. This *cblC*-specific block in CNCbl utilization was subsequently shown to be true *in vivo*, as Andersson and Shapira (120) reported that methylmalonic acid excretion and plasma homocysteine levels remained elevated with CNCbl treatment but decreased to normal on switching to OHCbl. Additionally, Rosenblatt *et al.* (46), in a review of 50 *cblC* patients, reported that CNCbl was used in 14 cases where it was found to be ineffective in improving biochemical parameters in some patients. Those patients were switched to OHCbl and some showed biochemical or clinical response.

Recently, Banerjee and colleagues (48) characterized MMACHC processing of CNCbl and showed that, in the presence of a reductase such as methionine synthase reductase or novel reductase 1, the MMACHC-bound CNCbl could be reduced to cob(II)alamin, suggesting a path for introducing this unnatural form of vitamin B_{12} into the cobalamin processing pathway. These results were extended to other alkylcobalamins with the demonstration that fibroblasts cultures are able to dealkylate cobalamins containing C2-C6 alkanes as the upper axial ligand in addition to CN-, adenosyl- or methylcobalamin

(49). In all cases, *cblC* fibroblast cultures from patients with severe, null type mutations were unable to utilize any of these molecules as cobalamin sources.

These results suggest that the difference in the ability of *cblC* patients to respond to OHCbl but not CNCbl might lie with the MMACHC protein directly. We set out to determine the molecular basis for the discrepancy in the response of *cblC* patients to the two vitamin forms by examining cobalamin binding by recombinant control and mutant MMACHC protein. We report here that wild-type MMACHC binds both OHCbl and CNCbl with similar, tight affinity. We also show that CNCbl binds MMACHC in the base-off form with the DMB base displaced from coordination with the cobalt atom of cobalamin. In this configuration, wild-type protein is able to perform reductive decyanation to cob(II)alamin in the absence of any associated reductase, requiring only the presence of NADPH and FAD. We report that MMACHC containing the early-onset G147D mutation does not bind either vitamin form, providing a simple explanation for absence of responsiveness with either vitamin. On the other hand, MMACHC with the late-onset R161Q mutation binds OHCbl with wild-type affinity but shows reduced binding to CNCbl and impaired decyanation. Finally, we found that H122A showed reduced but not ablated binding, making it unlikely that this residue is involved in binding the cobalt in a manner analogous to the coordinating histidine in methylmalonyl-CoA mutase and methionine synthase.

Materials and Methods

Plasmid Generation and Site Directed Mutagenesis.

The cDNA of MMACHC was obtained from OriGENE (Rockville, MD) cloned into the pCMV6-Entry vector. Using the primers GGATCCATGGAGCCGAAAGTCGCAGAGC and GGCTCGAGTCAAGGGCCAGGGGATGCAGG where the underlined sequences represent a created BamHI and XhoI site, respectively, the cDNA was then amplified using PCR and cloned into the vector pGEX-4T-1 (GE Healthcare; Baie d'Urfe, QC) by cleavage of the PCR product and vector by BamHI and XhoI, followed by ligation with T4 DNA Ligase (Invitrogen; Burlington, ON). For pNIC28-Bsa4 (GenBank accession EF198106), the primers were TACTTCCAATCCATGGAGCCGAAAGTCGCAGAGC and TATCCACCTTTACTGCTATCAAGGGCCAGGGGATGCAGG where the underlined sequences represent LIC sites. Mutants were generated by site-directed mutagenesis using the primers GGGGGAACCAGCGCATATCAG**AT**GTGTGCATACACCCCCGATT and AATCGGGGGTGTATGCACAC**AT**CTGATATGCGCTGGTTCCCCC for G147D, TTGGGGGCTGGTTTGCCATC**CA**AGGGGTAGTGCTGCTGCCAGG and CCTGGCAGCAGCACTACCCC**TTG**GATGGCAAACCAGCCCCCAA for R161Q, and CCTGGCCCAGACAGCAGCC**GC**TGTAGCTGGGGCTGCTTACTAC and GTAGTAAGCAGCCCCAGCTAC**AGC**GGCTGCTGTCTGGGCCAGG for H122A, where the underlined letters represent the codon to be changed and the letters in bold represent the mutated nucleotides. This was done following the manufacturer's

instructions (Stratagene; La Jolla, CA). All vectors were sequenced to verify the correct insert.

Protein Expression and Purification

MMACHC and mutants in pGEX-4T-1 (N-terminal GST-tag) were expressed and purified according to manufacturer's instructions (GE Healthcare; Baie d'Urfe, QC) with a few exceptions. Briefly, cultures were grown from single colonies in LB medium. MMACHC expression was induced with 0.5 mM IPTG with incubation at 30°C for 8 hours with shaking. Cells were pelleted by centrifugation at 6000 x *g* for 10 min and resuspended in PBS plus protease inhibitors (Roche; Laval, QC) and PMSF (Sigma-Aldrich; Oakville, ON) and lysed by passing through a French Pressure Cell (SLM Instruments; Urbana, IL) two times at 12,000 psi. The homogenate was centrifuged at 27,000 x *g* for 30 min and the soluble fraction was incubated with a 10 mL of a 1:1 slurry of glutathione-sepharose 4B (GE Healthcare) and PBS and incubated overnight at 4°C with rotation. Beads were washed 6x by addition of PBS, with pelleting and recovery of the beads between steps. Protein was eluted with 10 mM reduced glutathione (Sigma-Aldrich) in 50 mM Tris pH 8.0. Purified protein was concentrated using spin concentrators (Millipore; Billerica, MA) and stored at -20°C until use. For cleavage of the GST-tag, 1 µg of thrombin (Sigma-Aldrich) was added per mg protein and incubated with rotation at room temperature overnight. MMACHC and MMACHC-R161Q used for the decyanase assay were in pNIC26-Bsa4 (N-terminal His-tag) using the same cDNA as outlined above and was expressed and purified minus TEV-cleavage as described in Picaud *et al.* (121).

Intrinsic Fluorescence Spectroscopy

Protein intrinsic fluorescence measurements were carried out using a MOS-250 spectrophotometer and recorded using Bio-Kine 32 v4.20 software (BioLogic Science; Knoxville, TN), as previously described (122). The excitation wavelength was 280 nm (slit width, 10 nm) and emission spectra were recorded between 300 and 450 nm (slit width, 10 nm). To determine the dissociation constant (K_d), 2 ml of 10 µM wild-type or mutant MMACHC in buffer (100 mM Tris, pH 7.0) was titrated with 4-10 µl aliquots of CNCbl or OHCbl (0.5, 1, or 5 mM stocks) which were prepared in the same buffer. After each addition of ligand, the sample was mixed and incubated in the dark at room temperature for ~10 min to reach equilibrium after which the stable fluorescence spectrum was obtained. Fluorescence intensities and ligand concentrations were corrected for both dilution and inner filter effects using the equation $F_{corr} = F_{obs}(V_i/V_0)10^{0.5(Aex+Aem)}$, where F_{corr} is the corrected value of the fluorescence intensity, F_{obs} is the observed intensity, V_0 is the initial volume of the sample, V_i is the volume of the sample in the titration, and Aex and Aem are the absorbance of the sample at the excitation and emission wavelengths, respectively (123). Free CNCbl (100 µM) and OHCbl (100 µM) showed negligible fluorescence emission. The change in fluorescence intensity at 345 nm was plotted against different concentrations of ligand (CNCbl or OHCbl). To determine the dissociation constants (K_d), using KaleidaGraph 4.0 (Synergy Software, Reading, PA), the data were fitted to the equation $\Delta F = \Delta F_{max}[S]/(K_d + [S])$, where ΔF is the change in fluorescence intensity ($F_{protein} - F_{protein} + ligand$) at 345 nm upon ligand addition, [S] is the concentration of ligand, and ΔF_{max} is the maximal

change in the intrinsic fluorescence intensity at 345 nm at saturating ligand concentration (124). All values of K_d were determined in triplicate and the errors are standard deviations. Values of K_d calculated as $>10^8$ μM were recorded as "N.B.", no binding.

UV-Visible Absorption Spectra

To determine if MMACHC binds CNCbl base-on or base-off, 400 μl of 50 μM MMACHC protein in buffer (100 mM Tris, pH 7.0) was incubated in the dark with 5 μM CNCbl, prepared in the same buffer, for 5 min at room temperature. Absorption spectrum measurements of CNCbl were carried out using a MOS-250 spectrophotometer and recorded using Bio-Kine 32 v4.20 software.

Decyanase Assay

Decyanase activity of MMACHC was performed as described previously (48) except it was done in the absence of added reductase and other minor modifications. The total reaction volume was 1 ml. Anaerobic assay mixture (100 mM HEPES, pH 7.5; 0.5 M NaCl; 5% glycerol) containing 0.5 mM NADPH, 25 μM CNCbl and 25 μM MMACHC (wild-type or R161Q), were incubated at 37^{o}C for 5 min. The reactions were initiated by the addition of 25 μl FAD stock solution with 0.05 mM final concentration. Spectra were recorded using a MOS-250 spectrophotometer inside an anaerobic chamber (Coy Laboratory). The decyanation rate was monitored at 550 nm.

Results

MMACHC purification and binding to cobalamin

Wild-type and mutant (G147D, and R161Q) MMACHC were expressed as N-terminal GST fusion proteins with a detected molecular mass of 55-60 kDa (expected mass = 58 kDa) following SDS-PAGE electrophoresis (Fig. 3.1, lane 1, 3 and 4). Upon cleavage of GST-MMACHC with thrombin, two distinct proteins were resolved, corresponding to the expected sizes of MMACHC (32 kDa) and GST (26 kDa) (Fig. 3.1, lane 2). To measure binding of OHCbl to MMACHC, we took advantage of the intrinsic fluorescence of the protein obtained on excitation at 280 nm. By this method, GST-MMACHC was found to bind OHCbl with an apparent K_d of 5.7 ± 2.2 μM (Fig. 3.2A) and CNCbl with almost the exact same affinity, K_d = 5.5 ± 2.3 μM (Fig. 3.2B).

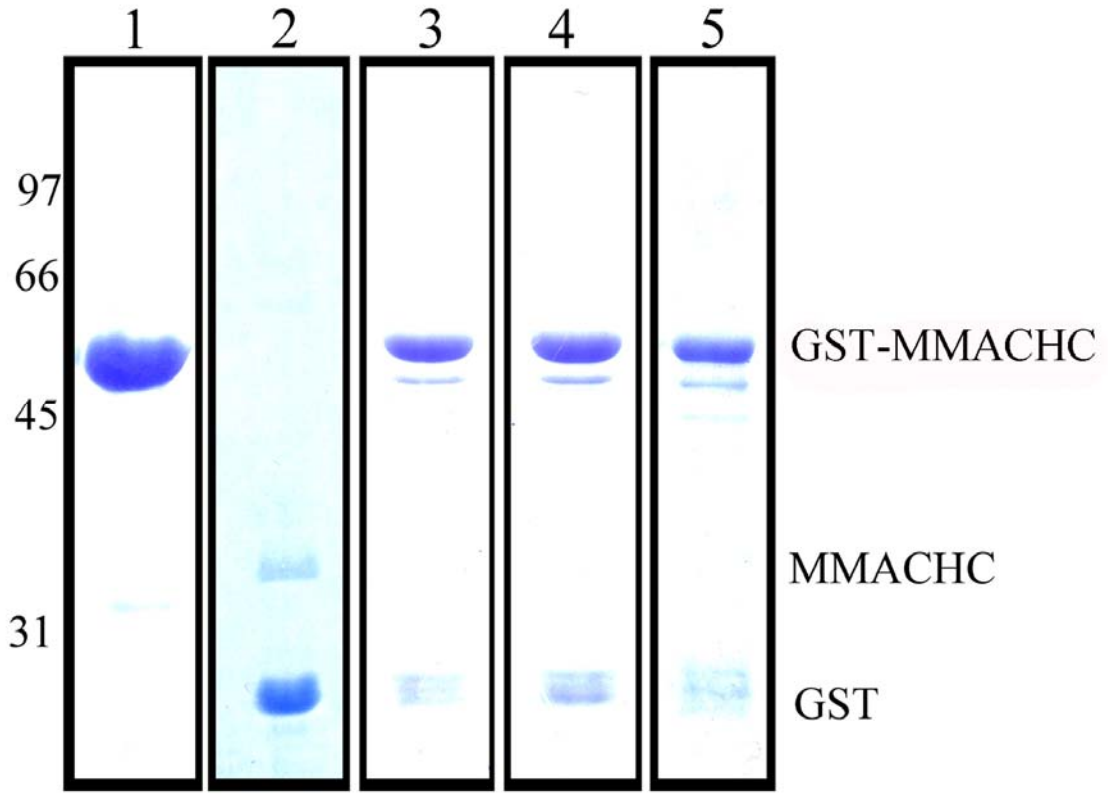

Figure 3.1. SDS-PAGE of purified GST-MMACHC.

Gel stained with Coomassie Brilliant Blue. Lane 1: GST-MMACHC-wt; Lane 2: MMACHC-wt and GST, cleaved by thrombin; Lane 3: GST-MMACHC-R161Q; Lane 4: GST-MMACHC-H122A; Lane 5: GST-MMACHC-G147D.

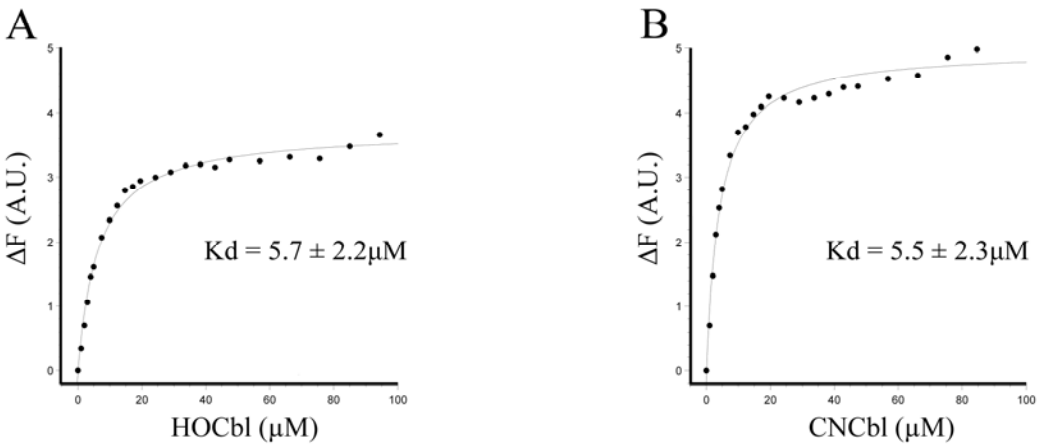

Figure 3.2. GST-MMACHC binding to OHCbl (A) and CNCbl (B).

Graphs are represented as the change in fluorescence (ΔF) upon addition of ligand (OHCbl or CNCbl). Representative graphs. K_d's are given in μM as the average of at least 3 experiments. The ΔF values are corrected for the inner filter effect (see Methods).

To determine if the N-terminally attached GST affected binding, we cleaved the GST-MMACHC fusion protein using thrombin. MMACHC, separated from GST, bound OHCbl with the same affinity as the attached version (K_d = 5.8 ± 2.8 μM; Table 3.1), indicating that the attached GST had no effect on ligand binding. GST and thrombin alone did not bind OHCbl (N.B.; Table 3.1). However, the yield of MMACHC following removal of the GST was very poor. Therefore, since GST had no effect on binding, it was left on for all subsequent experiments.

MMACHC mutants distinguish OHCbl and CNCbl

While wild-type MMACHC bound OHCbl and CNCbl with similar affinity, the mutant versions of MMACHC did not (Table 3.1). When MMACHC with the R161Q mutation was examined, it bound OHCbl with a K_d of 3.8 ± 2.0 μM, similar to the wild-type protein, but bound CNCbl with several-fold lower affinity, K_d = 19.6 ± 7.4 μM. By contrast, G147D, a mutation that causes early onset disease, did not bind either OHCbl or CNCbl. As well, H122A, a mutation that would be expected to ablate binding if the predicted vitamin B_{12} binding motif is functional, showed only a reduced affinity for OHCbl compared to wild-type (K_d = 18.6 ± 4.3 μM) but interestingly, like R161Q, had a several-fold reduced affinity for CNCbl (K_d = 84.2 ± 6.7 μM).

Table 3.1. Apparent Kd Values of Wild-type and Mutant MMACHC Proteins

	HOCbl (μM)	CNCbl (μM)
GST-MMACHC	5.7 ± 2.2	5.5 ± 2.3
MMACHC + GST + Thrombin	5.8 ± 2.8	
GST + Thrombin	N.B.	
GST-MMACHC (R161Q)	3.8 ± 2.0	19.6 ± 7.4
GST-MMACHC (H122A)	18.6 ± 4.3	84.2 ± 6.7
GST-MMACHC (G147D)	N.B.	N.B.

*N.B. = no binding

MMACHC binds CNCbl base-off

To understand why MMACHC may bind CNCbl and OHCbl with different affinities, we investigated the configuration in which CNCbl is bound. Previously, MMACHC was reported to bind CNCbl in the base-on form (48). However, using high concentration protein to drive binding, we observed CNCbl in the base-off configuration (Fig. 3.3). To achieve this outcome, the molar ratio of MMACHC to CNCbl was 10:1, since at lower ratios remaining, free cobalamin obscured the outcome.

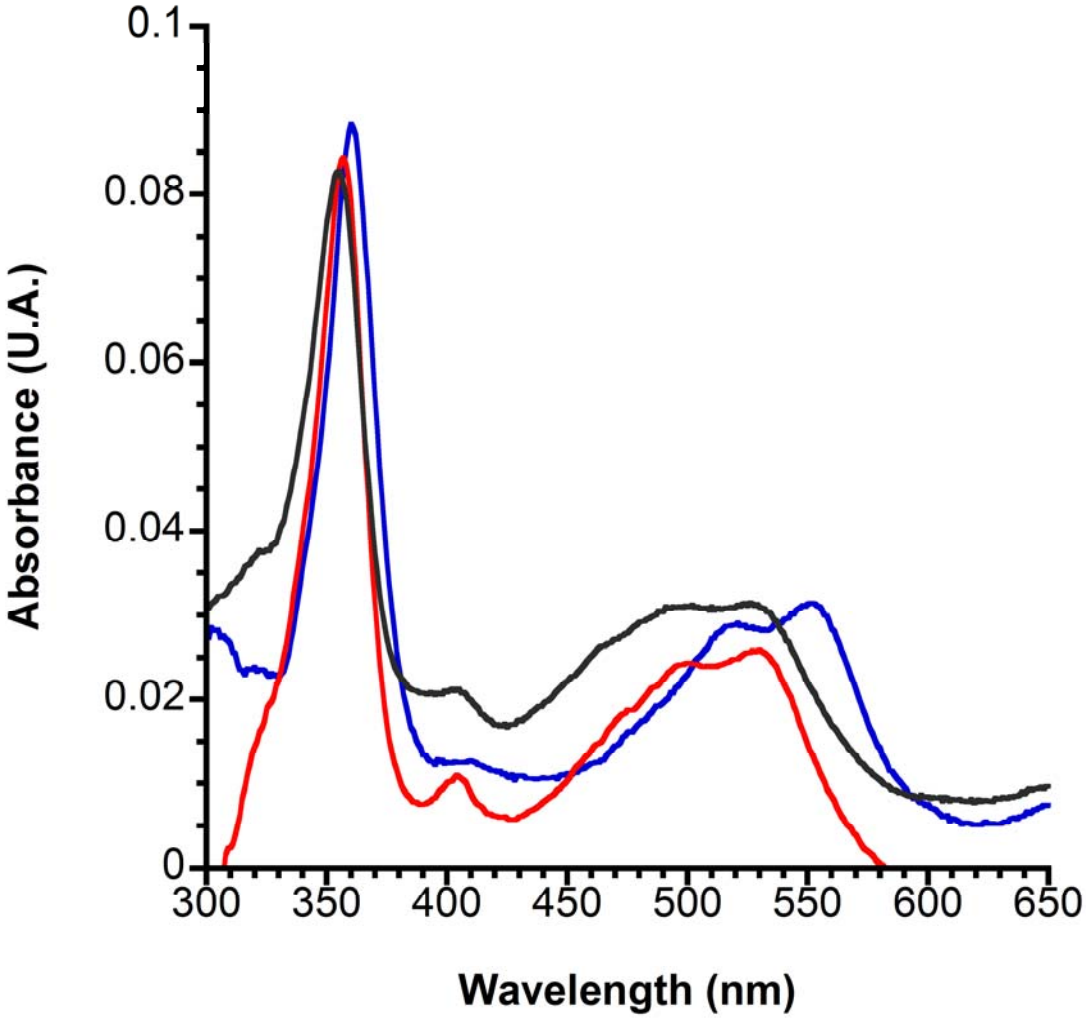

Figure 3.3. MMACHC-GST binds CNCbl base-off.

UV-Visible spectra of 5 µM free CNCbl in pH 7.0 (base-on; Blue), 5 µM free CNCbl in 6% $HClO_4$ (base-off; Grey) and bound to 50 µM MMACHC-GST (Red).

MMACHC-R161Q has reduced decyanase activity

We first assessed whether CNCbl could be reductively decyanated in the presence of MMACHC and natural reducing agents, NADPH and FAD. In the absence of protein, reduction of FAD was observed by the characteristic decrease in absorbance at 470 nm but no reduction of CNCbl was observed, monitored at 550 nm (Fig. 3.4A inset). However, on addition of MMACH, a decrease in absorbance at 550 nm and increase at 470 nm was observed, demonstrating the generation of cob(II)alamin (Fig. 3.4A). MMACHC-R161Q was also able to catalyze this reaction; however, it proceeded at a slower rate than with wild-type enzyme (Fig. 3.4B).

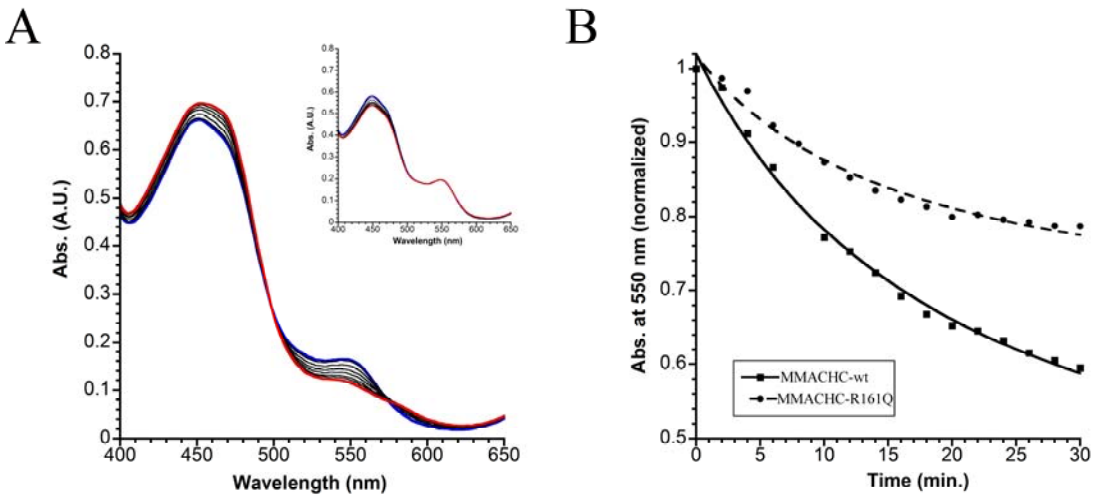

Figure 3.4. Reductive decyanation of CNCbl by normal or mutant MMACHC.

A. Decyanation of CNCbl catalyzed by MMACHC in the presence of 0.5 mM NADPH and 0.05 mM FAD. Note, as CNCbl (blue) turns to cob(II)alamin (Red), absorbance decreases at 550 nm and increases at 470 nm. Inset: No decyanation in the absence of MMACHC. Absorbance at 550 nm is unchanged and absorbance at 470 nm decreases as a result of reduction of FAD. Abs. (A.U.) is absorbance in arbitrary units. **B.** Decyanase activity is plotted as the change in absorbance at 550 nm versus time. Wild-type and mutant (R161Q) MMACHC are identified in the figure. Data were normalized so that baseline absorbance was equal to 1.

Discussion

The mechanism by which OHCbl is a better supplement than CNCbl for the treatment of the *cblC* disorder has been an enigma since first reported in cell culture experiments in 1979 (50). Our studies reveal an intrinsic difference in the ability of mutant MMACHC protein to bind CNCbl and OHCbl, indicating that this difference lies with the protein rather than in the pathways utilized for processing cobalamin.

Retrospective studies on *cblC* patients documented a better response to OHCbl compared to CNCbl (46, 120). Our results bear out this view. We showed five-fold weaker binding of CNCbl versus OHCbl by mutant MMACHC protein, in contrast to identical affinities obtained for wild type protein. Although the difference is not large when considered against the megadose vitamin B_{12} regimens given to affected patients, they are physiologically relevant. Circulating cobalamin ranges from 200 to 700 pmol/L in healthy individuals and was shown to rise to 7400 pmol/L on sustained cobalamin treatment of transcobalamin deficient patients (31, 114). Liver tissue cobalamin has been estimated at 0.6 μM, with other tissues as low as 0.03 μM (brain) (125). These results make it unlikely that MMACHC protein sees concentrations of cobalamin above micromolar even during high dose vitamin B_{12} treatment. Therefore, with a K_d of 5.7 ± 2.2 μM, the wild type protein is unlikely to be saturated regardless of the vitamin B_{12} regimen.

Interestingly, we also found that mutating the histidine residue in the putative vitamin B_{12} binding motif, HXXG-$X_{\sim 30}$-GG, affects but does not ablate cobalamin binding. In a comparable mutation with methylmalonyl-Coa mutase, an enzyme where the histidine has been shown to coordinate to the cobalt (97), mutating the corresponding histidine to alanine gave a > 1500-fold increase in K_d for AdoCbl (126). In our study, mutating the putative coordinating histidine to alanine gave only a 3-fold increase in K_d for OHCbl and a 15-fold increase for CNCbl (Table 3.1). This suggests that this sequence is involved but does not drive cobalamin binding. It is also noteworthy that a similar mutation, H122R, has been described in patients with late-onset OHCbl-responsive *cblC* disorder (117). From our binding results, we would expect this mutation to be more responsive to OHCbl than CNCbl.

The remarkable aspect of our finding is that a single point mutation in MMACHC can cause discrimination between OH- and CNCbl, when superficially the vitamins differ only in the structure of the upper axial ligand. This would seem perplexing since the difference in size between these two ligands is remarkably small in comparison to the large chemical structure of cobalamin. Instead, the answer may lie in the binding state of the lower ligand. At pH 7.0, CNCbl normally exists in the “base-on state”, with the DMB nitrogen coordinated to the cobalt in the lower axial position. However, upon binding to MMACHC we found that CNCbl shifts to the “base-off” state (Fig. 3.3). Therefore, rather than interact with the upper axial ligands, OH- or CN-, we suggest that R161 may affect the binding of the DMB moiety in the base-off state.

The proposed decyanase activity of MMACHC coupled to a reducing system confers the ability of MMACHC to reduce the bound CNCbl to cob(II)alamin (48). This activity is likely made possible by the rendered base-off configuration adopted by CNCbl on binding MMACHC. The redox potential of base-on CNCbl is very low, ~ -1000 mV versus the standard hydrogen electrode (SHE), and should not be easily reduced (9). In contrast, in base-off form with the DMB base displaced from the cobalt atom, the redox potential is increased to -350 mV (127). This is well within reach of the reducing environment of the cytosol (128). Decyanation by the R161Q mutant, like CNCbl binding, was found to be inhibited but not ablated and this reduced activity is likely to be a reflection of the reduced binding. With this result, a clearer picture of why these patients are less responsive to CNCbl emerges. Mutant R161Q has a decreased ability to bind incoming CNCbl, which results in a decreased ability to reductively decyanate the CNCbl to the cob(II)alamin form that is useful to the rest of the metabolic pathway. With OHCbl treatment, binding is normal and reduction to cob(II)alamin is not expected to be an issue. OHCbl has a redox potential of +200 mV versus the SHE and equilibrium should strongly favor the cob(II)alamin state, free or bound to MMACHC. Indeed, Yamada *et al.* (73) showed that methionine synthase reductase can reduce aquacobalamin to cob(II)alamin when free in solution. Therefore, OHCbl is easily reduced to cob(II)alamin and passed on to the rest of the pathway, most likely bound to MMACHC (27).

A major question raised by this work is that if late-onset patients have little or no disruption of binding to OHCbl, why do they get sick in the first place? Since OHCbl

reduction is not at issue and OHCbl binding by patients with the R161Q mutation is not impaired, two additional possibilities come to mind. First, MMACHC binding of cobalamin may be an essential feature of cobalamin processing in the cell. If the mutant protein is unstable *in vivo*, increased protein turnover could be the problem. We observed significant instability of the R161Q protein expressed *in vitro*, suggesting the possibility that net protein may be reduced in patient cells. Second, cobalamin is largely in the bound state in cells (32, 129) suggesting that the role of MMACHC may be to ferry the vitamin between its release at the lysosomal membrane to delivery to distant sites for further metabolism. If so, the R161Q protein may be compromised in its ability to interact with donor or acceptor proteins. Our results underscore the importance of faithfully treating *clbC* patients with OHCbl. They also indicate the futility of using CNCbl as an alternative vitamin source, even at exceptionally high dose.

CHAPTER 4: THERMOLABILITY OF THE MMACHC R161Q MUTANT IN VITAMIN B_{12}-RESPONSIVE *CBLC* DISORDER

Introduction

Vitamin B_{12} (cobalamin, Cbl) is a complex organometallic molecule whose structure was determined by Hodgkin (5) in 1956 after being first isolated by Smith (1) and Rickes (2). The cobalamin core consists of a cobalt atom caged in a corrin ring (Fig.4.1). Extending beneath the corrin ring is the 5,6-dimethylbenzimidazole (DMB) base which may be coordinated to the cobalt atom to form the lower or α-axial ligand. When attached, the structure is considered "base-on"; when unattached, "base-off". If the DMB moiety is not present, the structure is called cobinamide (Cbi). The upper or β-axial ligand varies depending on the modification state of cobalamin (R-group in Fig. 4.1). Cyanocobalamin (CNCbl) was the form initially crystallized and continues to be the most common commercially available form of cobalamin; however, it does not occur naturally in plants, micro-organisms or animal tissues (130). Hydroxocobalamin (HOCbl), methylcobalamin (MeCbl) and 5'-deoxyadenosylcobalamin (AdoCbl) are the three forms that have been frequently isolated from mammalian tissues (17) and, for humans, are considered to be the naturally occurring forms.

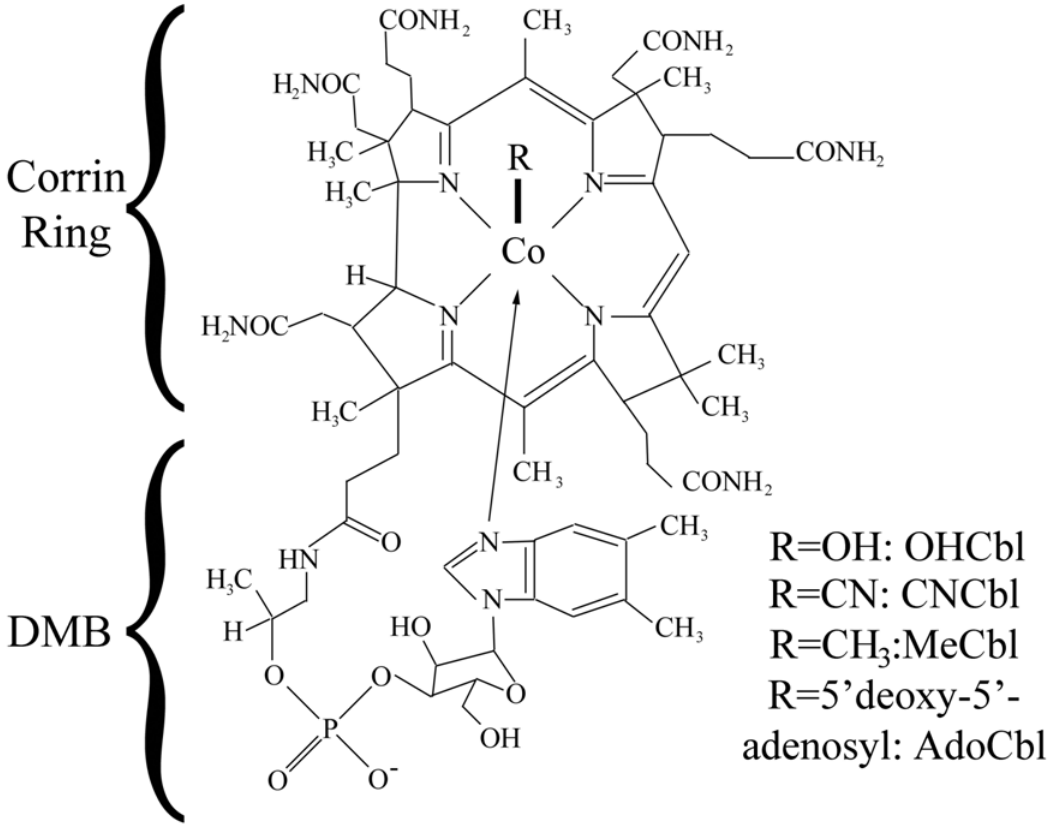

Figure 4.1. Chemical structure of vitamin B_{12}.

The arrow from the DMB group up to the cobalt represents the bond that may exist, making this structure base-on.

Recently, we used recombinant MMACHC to investigate cobalamin binding with a mutant protein model of early-onset (G147D) and late-onset (R161Q) *cblC*. We found that MMACHC-G147D was unable to bind HOCbl or CNCbl, while MMACHC-R161Q was able to bind HOCbl with wild-type affinity but was impaired in CNCbl binding with reduced decyanase activity (131). This work provided a rational explanation for the better response of *cblC* fibroblasts (50) and patients (46, 120) to HOCbl compared to CNCbl and demonstrated ablated binding to HOCbl as the basis for functional deficiency in early-onset (G147D) *cblC*. However, since MMACHC-R161Q exhibited normal HOCbl binding, this study failed to explain the disease mechanism in late-onset *cblC* patients with an R161Q allele. An intriguing possibility, however, was that this protein is unstable since we observed significant instability of the R161Q protein during recombinant expression (131).

In the work described here, we investigated the thermostability of the MMACHC-R161Q protein in comparison to wild-type (MMACHC-wt) in the presence or absence of cobalamin as a possible mechanism for dysfunction of the mutant protein. Using differential scanning fluorimetry, we demonstrate that MMACHC is exceedingly labile with a melting temperature near physiologic temperature, while MMACHC-R161Q is marginally more labile. We show that cobalamins significantly stabilize MMACHC, though less so for MMACHC-R161Q. However, we show that cobinamide equally stabilizes wild-type MMACHC and MMACHC-R161Q, suggesting inhibition of DMB binding with the R161Q mutation. These results point to increased lability and decreased

stabilization by cobalamin binding as contributors to disease mechanism in the *cblC* disorder.

Materials and Methods

Materials

HOCbl, CNCbl, AdoCbl, MeCbl and Cbi (as dicyanocobinamide) were purchased from Sigma-Aldrich (Oakville, ON). All other chemicals were reagent grade.

Plasmid Generation and Site Directed Mutagenesis

The cDNA of MMACHC was obtained from OriGENE (Rockville, MD) cloned into the pCMV6-Entry vector. To transfer the cDNA into pNIC28-Bsa4 (SGC expression vector, GenBank accession EF198106), the primers were TACTTCCAATCCATGGAGCCGAAAGTCGCAGAGC and TATCCACCTTTACTGCTATCAAGGGCCAGGGGATGCAGG where the underlined sequences represent LIC sites. LIC cloning was performed by first digesting the vector with BsaI (NEB; Ipswich, MA) for 2 hours at 50°C, followed by incubating the digested plasmid with insert, made by PCR using the primers above, as well as dGTP (Invitrogen: Burlington, ON), and T4 DNA polymerase (NEB) for 30 minutes at 22°C followed by 70°C for 20 minutes. Plasmid and insert were then ligated by mixing together for 10 minutes at room temperature and finally transformed into BL21 DE3 cells following the manufacturer's instructions. Mutant sequences were generated by site-directed mutagenesis of the wild type vector using the primers

TTGGGGGCTGGTTTGCCATCC**A**AGGGGTAGTGCTGCTGCCAGG and CCTGGCAGCAGCACTACCCC**TT**GGATGGCAAACCAGCCCCCAA for R161Q, where the underlined letters represent the codon to be changed and the letters in bold represent the mutated nucleotides. This was done following the manufacturer's instructions (Stratagene; La Jolla, CA). All vectors were sequenced to verify the correct insert.

Protein Expression and Purification

MMACHC and MMACHC-R161Q in pNIC26-Bsa4 (N-terminal His-tag) were expressed and purified as described by Picaud *et al.* (121). Purified protein before treatment with TEV had the N-terminal His-tag intact (His-MMACHC-wt and His-MMACHC-R161Q), while purified protein after TEV treatment had the His-tag removed (MMACHC-wt and MMACHC-R161Q).

Differential Scanning Fluorimetry

DSF was performed and analyzed as described in Niesen *et al.* (132), with minor modifications. Purified MMACHC proteins were diluted to 0.1mg/ml (3 µM) in buffer (10 mM HEPES pH 7.5, 0.5 M NaCl, 5% glycerol) with 1:1000 Sypro Orange (Sigma-Aldrich) and run in triplicate. The proteins were subjected to a ramp of 1°C/min in a thermocycler (Bio-rad C1000 Thermocycler, CFX96 Real-time system) at a temperature gradient of 5 to 75°C. All graphs were normalized so that minimum fluorescence was set to 0 and maximum fluorescence set to 1. This was done because all cobalamins showed fluorescence quenching at higher concentrations. However, quenching did not affect

T_m's as a control protein (GST) showed no T_m shift with any cobalamin used. Final graphs were generated using Kadeidagraph 4.0 software (Synergy Software, Reading, PA).

Statistics

All experiments were determined using at least n=3. Error bars shown are ± 1 S.D. All statistics were performed using a two-tailed Student's T-test, with significance determined at $p < 0.05$, unless otherwise indicated.

Results

MMACHC-R161Q is a thermolabile mutant

Wild-type (MMACHC-wt) and mutant (MMACHC-R161Q) MMACHC were expressed and purified to >95% purity, with His-tag removed, as judged by SDS-PAGE (Fig. 4.2A). In order investigate the thermostability of MMACHC we used differential scanning fluorimetry (DSF), a method that measures protein stability and ligand-induced changes in stability (133, 134). DSF uses an environmentally sensitive dye, such as Sypro orange, to monitor protein-unfolding caused by heat denaturation. As the protein unfolds, the dye, which has a higher fluorescent yield in nonpolar environments than in aqueous media, binds the hydrophobic regions of the protein and gives a large increase in fluorescence (135, 136). Protein stability is calculated as the melting point of the protein (T_m), the transition midpoint of the fluorescence curve, corresponding to the temperature at which half the protein is folded and half is unfolded (135). By this method, we found

that the melting temperatures for MMACHC-wt (T_m = 39.3 ± 1.0°C) and MMACHC-R161Q (T_m = 37.1 ± 0.7°C) were near physiological temperature (Fig. 4.2B). However, MMACHC-wt had a small but significantly higher T_m than MMACHC-R161Q ($p<0.01$) (Fig 4.2B).

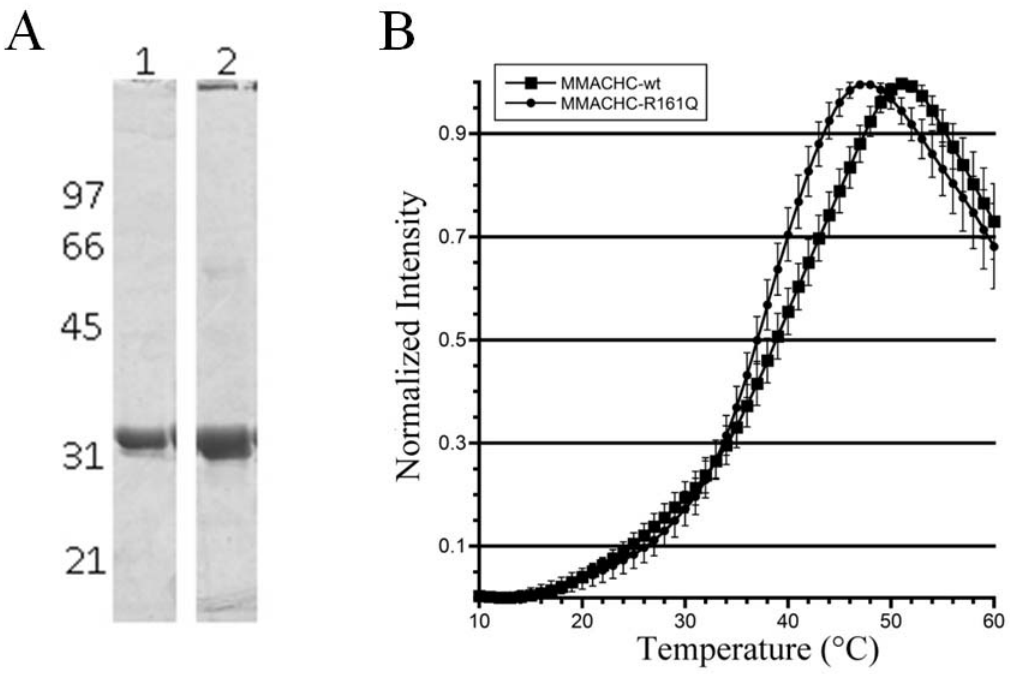

Figure 4.2. Purification and Thermostability of MMACHC-wt and MMACHC-R161Q.

A. Pure MMACHC-wt and MMACHC-R161Q. Protein was cut with TEV and analyzed by 10% SDS-PAGE with staining by Coomassie blue. **B.** Thermostability of MMACHC-wt and MMACHC-R161Q. Protein stability was determined by DSF as described in Materials and Methods. Curves are shown as an average (± S.D.) of an n= at least 9. At T_m (Normalized Intensity = 0.5) MMACHC-wt = 39.3 ± 1.0°C and MMACHC-R161Q = 37.1 ± 0.7°C, which is significantly different at $p<0.01$

To determine whether incubation with HOCbl would result in an increase in protein stability, we incubated MMACHC-wt and MMACHC-R161Q with increasing concentrations of HOCbl. Both proteins showed concentration dependent increases in T_m, indicating that they were stabilized on binding to HOCbl (Fig. 4.3A,B). For easier visualization of the gain in thermostability, we plotted the change in T_m against increasing HOCbl concentration (Fig. 4.3C). The graph shows that the stabilization gained by MMACHC-wt was much more pronounced than for MMACHC-R161Q. For MMACHC-wt, with the addition of only 1µM of HOCbl, the T_m was increased (ΔT_m) 5.2°C, and with 10µM HOCbl, was increased further to 7.7°C. In contrast, with 1 µM HOCbl, MMACHC-R161Q achieved a stabilization increase of only 1.4°C, and with 10 µM HOCbl the increase in ΔT_m was 3.3°C (Fig. 4.3C). Indeed, MMACHC-R161Q achieved a maximum increase in ΔT_m of only a 5.4°C at 50 µM OHCbl, roughly the same degree of stabilization as obtained with 1 µM HOCbl for MMACH-wt.

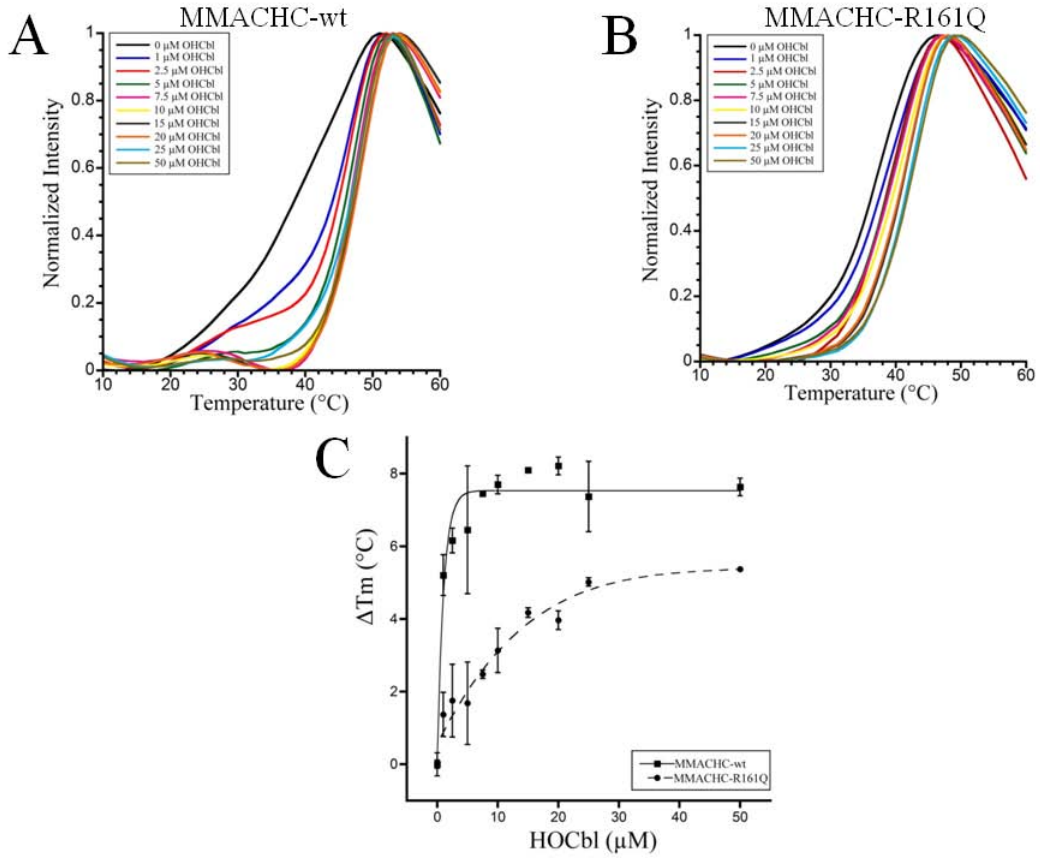

Figure 4.3. MMACHC-wt and MMACHC-R161Q stabilization by OHCbl.

MMACHC-wt (**A**) and MMACHC-R161Q (**B**) were incubated with 0 µM, 1 µM, 2.5 µM, 5 µM, 7.5 µM, 10 µM, 15 µM, 20 µM, 25 µM or 50 µM HOCbl and analyzed by DSF. Each curve is the average of n = 3. **C.** Plot of ΔTm vs. HOCbl concentration to easier visualize the stability gain by increasing levels of OHCbl. ΔTm is the difference between the Tm at each OHCbl concentration and the reference Tm (at 0 µM HOCbl).

Stability of MMACHC depends upon which form of cobalamin is bound

Since MMACHC has been shown to bind different forms of cobalamin (48), we determined which form might result in the greatest stabilization of MMACHC. We found that MMACHC-wt was stabilized most by the two cofactor forms of cobalamin, AdoCbl and MeCbl (Fig. 4.4A). It was stabilized to a lesser degree by HOCbl and cobinamide (Cbi) and least stabilized by CNCbl (Fig. 4.4A). MMACHC-R161Q was likewise most stabilized by AdoCbl and then MeCbl (Fig. 4.4B). However, it was stabilized by Cbi more than HOCbl, but like MMACHC-wt, was least stabilized by CNCbl (Fig. 4.4B). Importantly, for all forms of cobalamin but Cbi, the ΔT_m of MMACHC-wt was increased significantly more than for MMACHC-R161Q at both 10 μM and 50 μM (Fig. 4.4C).

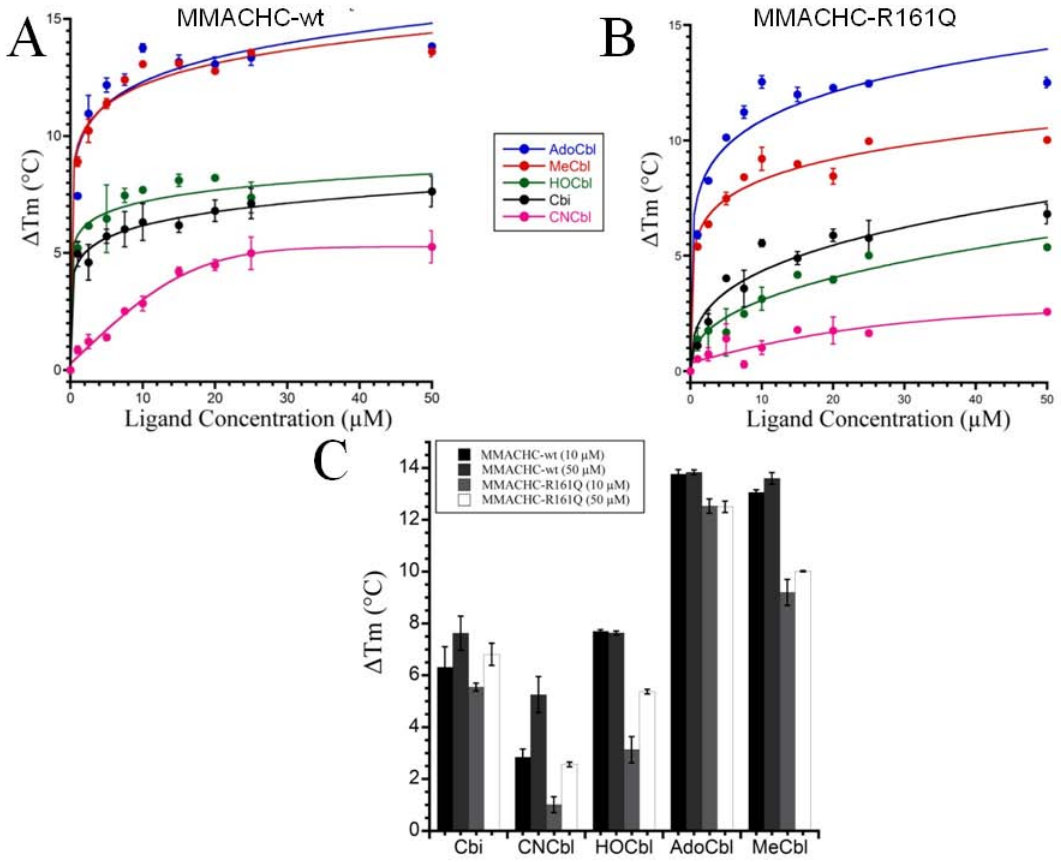

Figure 4.4. Stabilization of MMACHC-wt and MMACHC-R161Q by binding different forms of cobalamin and cobinamide.

MMACHC-wt (**A**) and MMACHC-R161Q (**B**) were incubated with 0 μM, 1 μM, 2.5 μM, 5 μM, 7.5 μM, 10 μM, 15 μM, 20 μM, 25 μM or 50 μM of AdoCbl, MeCbl, OHCbl Cbi and CNCbl and analyzed by DSF. Each data point was run in triplicate and represents the average ± 1 S.D.. **C.** Bar graph showing ΔT_m for each ligand at 10 μM and 50 μM to illustrate the higher ΔT_m for MMACHC-wt compared to MMACHC-R161Q for each ligand but Cbi. Differences between MMACHC-wt and MMACHC-R161Q for each concentration and ligand are significantly different at the $p < 0.05$ level except for Cbi (10 μM and 50 μM).

Discussion

The MMACHC protein appears to be a vitamin B_{12} carrier, likely functioning in cobalamin transport in the cytosol. Integral to this hypothesis are recent demonstrations of MMACHC's ability to bind many forms of cobalamin, including OHCbl, CNCbl, AdoCbl and MeCbl (48). We have previously demonstrated that an early-onset MMACHC mutation (G147D) resulted in protein unable to bind either CNCbl or OHCbl, providing a rational explanation for the defect resulting from this *cblC* mutation (131). However, MMACHC containing the late-onset mutation R161Q was able to bind OHCbl with wild-type affinity, leaving the basis for disease in patients with at least one R161Q mutation perplexing (131). Here we studied the thermostability of wild-type and R161Q mutant protein in the presence or absence of cobalamin to determine whether this substitution might confer significant instability.

To study MMACHC-wt and MMACHC-R161Q thermostability we used differential scanning fluorimetry, a method that monitors the heat-induced unfolding of proteins in the presence of a fluorescent dye (137, 138). Unexpectedly, we found that MMACHC-wt itself is a very thermolabile protein, with a T_m of 39.3 ± 1.0°C. This is a lower T_m than obtained for 39 out of 42 recombinant proteins (93%) investigated by Vedadi *et al.* (139) in a survey of proteins investigated by the screening method used here. The R161Q mutation further destabilizes MMACHC with a reduction in T_m to 37.1 ± 0.7°C. These data suggest that at the physiological temperature of 37°C, neither wild-type nor MMACHC-R161Q are particularly stable in their apo- form. However, the wild-type

protein is stabilized dramatically by HOCbl. The T_m was increased by 5.2°C with 1 μM HOCbl and by 7.7°C with 10 μM HOCbl. MMACHC-R161Q did not show as strong a stabilization effect with only a 1.4°C and 3.1°C shift in T_m, respectively. Our results suggest that with the low levels of HOCbl expected to exist intracellularly (125) wild-type MMACHC will be in a much more stable configuration than the R161Q mutant form. Therefore, it is possible that the mutant protein will have a more rapid turnover compared to wild-type MMACHC. It will be interesting to examine the protein in cells *in situ* or by Western blot analysis following growth in high versus absent vitamin $B_{12,}$ when MMAHCH-specific antibodies become available. Importantly, since patients with the R161Q mutation have been seen to respond to HOCbl therapy (see above; (140)), even a small increase in intracellular HOCbl obtained with mega-vitamin therapy may be enough to at least partially stabilize the mutant protein.

Since MMACHC is known to bind many different forms of cobalamin, we set out to discover which forms confer the greatest stabilization on the MMACHC protein. Interestingly, the T_m shifts were not similar for the different cobalamin forms. AdoCbl and MeCbl had the greatest impact on thermostability, conferring a 13-14°C increase in T_m with 10 μM of ligand, an exceedingly large effect. This may be related to the base-off character of the cobalamin cofactors which may be the favoured binding configuration (48). HOCbl had an intermediate effect (at 10 μM, ΔT_m, 7.7°C), similar to Cbi (6.3°C) while CNCbl stabilized the protein poorly (2.8°C). MMACHC containing the R161Q mutation showed a similar pattern of T_m profiles as wild type protein, but in all cases but Cbi, was somewhat less stabilized than wild type for each ligand. The weakest shifts,

compared to wild type, were for CNCbl (10 μM ΔT_m only 1.0°C) and OHCbl (3.1°C) which, strikingly, are formal substrates of MMACHC. That Cbi stabilized MMACHC-R161Q to the same extent as MMACHC-wt is interesting since Cbi was the only corrinoid form used here that did not have a DMB. This suggests that the R161Q mutation may interfere with the stabilization upon binding the DMB of cobalamin.

It is unclear the extent to which the thermostability data reported here can be extrapolated to the intracellular environment. The near physiologic T_m of the wild type protein was unexpected and intuitively would unlikely apply *in vivo*. The MMACHC protein is expected to act as an intracellular shuttle of cobalamin, possibly docking with the cobalamin efflux protein, LMBRD1 (43) for delivery of the vitamin to the cytosol, and with the MMADHC protein, proposed to be responsible for sorting cobalamin between the cytosol and mitochondrial compartments (42). While such interactions might stabilize the protein intracellularly, there is no basis for speculating at this time that in shuttling between such sites there might be other interacting proteins, such as conferring a chaperone role, or perhaps simply a more stabilizing environment. An example of a large difference in *in vitro* and *in vivo* thermostability is illustrated by firefly luciferase used as a reporter gene in cellular expression experiments. While its half-life is as little as 3 minutes at 37ºC *in vitro*, it increases to 49 minutes at 37ºC when expressed in mammalian cell culture (141). Thermostable mutant luciferase similarly showed an enhanced half-life when expressed in cells, suggesting that the cellular environment was responsible for the enhanced half-life *in vivo*. The authors speculated that the basis of intracellular protection was chaperone activity, since steady-state luciferase levels were

reduced by geldanamycin, an inhibitor of Hsp90. Therefore, while it would be premature to extrapolate the absolute melting temperatures to the intracellular environment, the relatively weaker stabilization of the mutant protein compared to wild type protein by cobalamin binding would likely carry over to the intracellular environment. Therefore, we see the impaired stabilization as a strong rationale for disease mechanism in patients with the R161Q mutation.

In summary, these results demonstrate the thermolability of MMACHC and illustrate the importance of this protein binding to cobalamin for stabilization. Additionally, they show that the R161Q mutation doubly destabilizes the protein by decreasing its stability in apo- form and, perhaps more importantly, decreases the stability gained by binding cobalamin. They also show that binding cobalamin in the base-off form is important for protein stability for the mutant as well as the wild-type protein. This work suggests instability as the basis of disease for R161Q *cblC* and highlights the importance of increasing cellular cobalamin levels as treatment for stabilizing mutant protein.

CHAPTER 5: SLEEPING BEAUTY MUTASE (*SBM*) IS EXPRESSED AND INTERACTS WITH *YGFD* IN *ESCHERICHIA COLI*

Introduction

E. coli has the ability to synthesize methionine from homocysteine using either a vitamin B_{12}-(cobalamin)-dependent (MetH) or a cobalamin-independent (MetE) methionine synthase (142-144). Therefore, *E. coli* are not obligate cobalamin users, but utilize it with availability. Not surprisingly, they do not have all the machinery required for cobalamin synthesis, but have retained all components required for its uptake and modification to active cofactor forms. Recently, a previously unrecognized cobalamin-dependent pathway was proposed for *E. coli* that catalyzes the conversion of succinate to propionate (145). The genes associated with this pathway are members of a four-gene operon: *sbm-ygfD-ygfG-ygfH*. Three of the encoded proteins were assigned functions based on enzymatic analysis of the expressed proteins *in vitro*: Sbm, shown to be methylmalonyl-CoA mutase, catalyzes the rearrangement of succinyl-CoA to L-methylmalonyl-CoA; YgfG, as methylmalonyl-CoA decarboxylase, catalyzes the decarboxylation of methylmalonyl-CoA to form propionyl-CoA; YgfH, as propionyl-CoA:succinate-CoA transferase, transfers the CoA of the propionyl-CoA product to an available succinate, thus priming another round of succinate to propionate decarboxylation (Fig. 5.1A) (145). The fourth protein, YgfD, however, could not be assigned a function, although the authors speculated that it might act as a possible

kinase/phosphatase that is involved in the regulation of the other enzymes (145). This operon, while shown to be functional *in vitro*, was not thought to function *in vivo* due to the lack of a functioning promoter, a notion reflected in the name of the first gene, "sleeping beauty mutase" (145, 146).

While the function of YgfD remains unknown, a few clues to its possible role exist. Homologs of YgfD are often found associated with MCM in bacterial operons (77, 147), suggesting a role in the production of AdoCbl, the cofactor required for MCM function, or a role in the protection or facilitation of MCM function. As well, structurally, YgfD belongs to the G3E family of P-loop GTPases, a family defined by the glutamate residue in the Walker B motif and an intact NKxD, members of which include: UreG, HypB, CobW, and MeaB (148) (Fig. 5.1B). Of these, MeaB is the closest homolog of YgfD, and MeaB from *Methylobacterium extorquens* has been shown to form a complex with *M. extorquens* MCM *in vitro* and that binding of MeaB to MCM was altered depending on the state of MCM, holo- vs. apoenzyme (79, 81). Based on these data, we were interested to discover whether YgfD had a similar role as its homolog MeaB, and whether the interaction with methylmalonyl-CoA mutase would occur *in vivo*, as well as *in vitro*.

In the work described here, we report that contrary to its name, Sbm is indeed endogenously expressed in *E. coli* cells and is therefore not "sleeping". We also demonstrate that YgfD and Sbm physically interact both *in vitro* and *in vivo*. Finally, we demonstrate that like its P-loop orthologs, YgfD binds and cleaves GTP, and this binding is integral to its interaction with Sbm. These studies reveal a functional role for YgfD, as

the fourth member of the *Sbm* operon, and extend earlier work by establishing the *in vivo* interaction of YgfD and Sbm.

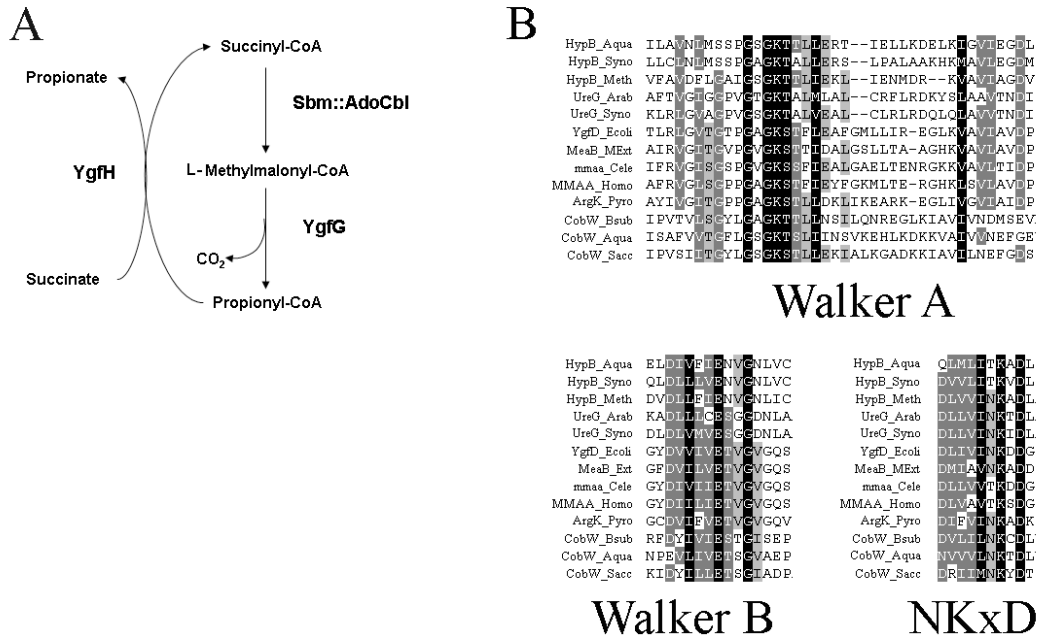

Figure 5.1. A. Pathway for the AdoCbl-dependent conversion of succinate to propionate in *E. coli* by Sbm, YgfG and YgfH. B. Conserved domains in the G3E family of GTPases including members of the YgfD, CobW, HypB and UreG protein families.

The alignment shows the three most highly conserved regions, the Walker A and the surrounding strands (block 1), the Walker B and surrounding area (block 2), and the area including the NKxD motif (block 3). Species names are abbreviated as follows: Aqua, *Aquifex aeolicus*; Arab, *Arabidopsis thaliana*; Bsub, *Bacillus subtilis*; Cele, *Caenorhabditis elegans*; Ecoli, *Escherichia coli*; Homo, *Homo sapians*; Meth, *Methanobacterium thermoautotrophicum*; MExt, *Methylobacterium extorquens;* Pyro, *Pyrococcus abyssi*; Sacc, *Saccharomyces cerevisiae*; and Syno, *Synechococcus PCC8801*. Based on studies by Leipe (148).

Materials and Methods

Materials

AdoCbl, OHCbl, GTP, guanosine 5′-[β,γ-imido]triphosphate (GMPPNP), GDP, ATP and methylmalonic acid were purchased from Sigma-Aldrich (Oakville, ON). All other chemicals were reagent grade. The plasmid vectors containing pET16-b:*sbm* and pET16-b:*ygfD*, each containing N-terminal His tags, have been previously described (145).

ygfD knockout

A mutant of *E. coli* deleted for *ygfD* was created using a method for allelic replacement by homologous recombination (149, 150). Briefly, PCR was used to clone 5' and 3' segments of the *ygfD* gene (overlapped into the adjacent genes), which were combined and subcloned into pHSG415 (Hashimoto-Gotoh et al., 1981) so as to effectively delete amino acid residues 8-283 of the 331 residue protein. The primers used were ygfD-A (GAATTCTGCGCAAAGCTATCATCAGTCTGAG [an *Eco*RI site is underlined]) and ygfD-B (CTGCAGCAGCGTGGCTTCATTAATCATGCTG [a *Pst*I site is underlined]) for the first fragment and ygfD-C (CTGCAGAAGAAGTACTGAATCACCTGTTCGC [a *Pst*I site is underlined]) and ygfD-D (AAGCTTACCTTCCACCATCGAAATGATCGGT [a *Hin*dIII site is underlined]) for the second fragment. The two resulting PCR fragments were digested with *Pst*I, ligated, cloned into pGEM and sequenced to verify the correct insert. The fragment was released using *Eco*RI and *Hin*dIII and ligated into pHSG415. Recombinant pHSG415::Δ*ygfd* was used to generate a Δ*ygfd* mutant strain following established procedures (149, 150). Presence of the chromosomal *ygfD* deletion was detected by PCR and DNA sequencing

using the primers ygfDKo1 (TGGTGCCAAGCCAGTGTGTT) and ygfDKo2 (CCGCCACTTTGTTGATAGTGAC).

Purification of expressed proteins

YgfD and Sbm His-tagged proteins were expressed in *E. coli* (BL21) transformed with pET16-b:*ygfD* or pET16-b:*sbm*, respectively, and purified as described by Haller *et al.* (145), with some exceptions. Cells were grown in LB and lysed by passing through a French Pressure Cell (SLM Instruments; Urbana IL) two times at 12,000 psi and centrifuged at 27,000 x *g* for 30 min. The soluble fraction was incubated with a 5 mL slurry of Ni-NTA beads (Qiagen; Mississauga, ON), rinsed in binding buffer (5 mM imidazole, 0.5 M NaCl and 20 mM Tris-HCl, pH 8.0), and allowed to mix by end-over-end rotation overnight at 4°C. After washing with binding buffer and wash buffer (60 mM imidazole, 0.5 M NaCl, and 20 mM Tris-HCl, pH 8.0), the purified protein was eluted in elution buffer (100 mM imidazole, 0.5 M NaCl, and 20 mM Tris-HCl, pH 8, 20% glycerol). Purified Sbm protein was concentrated and stored at -80^{o}C. Purified YgfD was concentrated, exchanged into storage buffer (50 mM HEPES, pH 8.0, containing 300 mM KCl, 2.5 mM $MgCl_2$ and 5% glycerol), and stored at -80°C. Protein concentrations were determined using the Bradford protein assay (Bio-Rad; Mississauga, ON) with bovine serum albumin as a standard according to the manufacturer's directions.

Antibody production

The full-length, N-terminal His-tagged Sbm and YgfD were used for the generation of polyclonal antibodies made in rabbit (SACRI Hybridoma Facility, University of

Calgary). An enzyme-linked immunosorbant assay (ELISA) was performed using procedures described by Garkavtsev (Garkavtsev et al., 1997) to ensure antibody reactivity to the antigen. Immune and pre-immune sera were tested by Western blot and visualized using the ECL detection system (Amersham/GE Healthcare; Baie d'Urfe, QC). Antibodies were affinity purified using purified proteins bound to HiTrap NHS-activated HP columns, following manufacturer's protocols (Amersham/GE Healthcare).

Immunoprecipitation

Immunoprecipitation experiments were performed using affinity purified antibodies that were immobilized using the Profound Co-immunoprecipitation kit (Pierce; Rockford, IL), according to manufacturer's instructions. Briefly, antibodies were immobilized to aldehyde-activated agarose beads by cross-linking in the presence of 5 M cyanoborohydride. Immobilized antibodies were incubated over-night with 300 µl *E. coli* total cell lysate at 4°C with rotation. This complex was washed with 400 µl PBS and centrifuged for 1 min at 5000 x *g* three times. Protein was eluted using 100 µl low pH buffer (pH 2.8) and pH neutralized by addition of 10 µl 1 M Tris, pH 9.5. Protein was then mixed with 30 µl 2X SDS buffer and the solution was heated for 2 min at 95^{o}C. Proteins in the supernatant were resolved by SDS-PAGE on a 10% polyacrylamide gel and visualized by staining with Coomassie brilliant blue R-250 (EMD; Gibbstown, NJ) or used for immunoblotting.

Immunobloting procedures

Proteins from SDS-PAGE were transferred to nitrocellulose membrane by capillary action. The membranes were blocked with 5% skim milk in PBS overnight at 4°C with shaking. Membranes were then incubated with primary antibody (anti-YgfD at 1:2000, anti-Sbm at 1:2000 in Tris-buffered saline plus 1% Tween-20, TBST) for 1 h, washed 3 x with TBST and incubated with secondary antibody (1:2500 Goat anti-Rabbit IgG HRP, Biorad, in TBST) for 45 min. Immune complexes were detected using ECL Reagent (Amersham/GE Healthcare) according to manufacturer's recommendations and exposed to Hyperfilm (Amersham/GE Healthcare).

Size exclusion chromatography

Gel filtration was accomplished by fast protein liquid chromatography (FPLC) using a Superdex 200 HR 10/30 column (AKTA Purifier, Amersham/GE Healthcare) monitored by following the change in OD_{280}. A 500 µg solution of YgfD or Sbm in sample buffer (10 mM Tris-HCl, pH 8.0, 10 mM KCl, 50 mM $MgCl_2$, 3 mM GTP and 5 mM AdoCbl) was used in each experiment. GTP and AdoCbl were used in the sample buffer in an effort to stabilize YgfD. For the experiment where YgfD and Sbm were run together, they were first pre-incubated in the dark for 15 min. The column was calibrated using proteins of known molecular weight, including bovine milk α-lactalbumin (14.2 kDa), bovine erythrocytes carbonic anhydrase (29 kDa), chick egg albumin (45 kDa), BSA (66 kDa – monomer, 132 kDa – dimer), and Jack bean urease (272 kDa – trimer, 545 kDa – hexamer) (Sigma) as standards. These proteins were also used as a protein milieu for the gel filtration of YgfD and Sbm mixtures.

PAGE analysis of complex formation

To analyze complex formation between YgfD and Sbm, 10 µg of apo-Sbm or holo-Sbm (prepared by incubating Sbm with 50 µM AdoCbl and 0.05 mM methylmalonyl-CoA at 20°C in storage buffer) was incubated with 15 µg of YgfD, either alone or pre-incubated with (i) 5 mM GTP, (ii) 5 mM GDP or (iii) 5 mM GMPPNP at 20°C for 10 min. The mixtures were then separated by PAGE under non-denaturing conditions in a 4-15% gradient gel (Bio-Rad) for 12 h at room temperature.

GTPase Assay

GTPase activity was determined by using the ATPase/GTPase ELIPA Biochem Kit (Cytoskeleton; Denver, CO), according to the manufacturer's instructions. For reactions, 15 µl of YgfD (750 ng) in storage buffer was added to 135 µl reaction mix (25 nmol MESG, 0.135 units PNP, 12 mM PIPES and 5 mM $MgCl_2$) containing various concentrations of GTP (0-1000 µM). Reactions were carried out in 96 well plates (Corning; Corning, NY) in duplicate, read by a PowerWave X (Bio-Tek Instruments; Winooski, VT) at 360 nm and plotted using KaleidaGraph (V3.6, Synergy Software; Reading, PA).

Results

YgfD and Sbm characterization

Although Sbm was shown to express a functional methylmalonyl CoA mutase *in vitro,* it was not thought to be expressed *in vivo* because of its placement in a presumed promoterless operon (145). We evaluated the endogenous expression of Sbm and YgfD in *E. coli* using polyclonal antibodies generated in rabbit against recombinant YgfD and Sbm. These antibodies were used to probe cell lysates from two wild type strains of *E. coli*, DH5α and MGC1876, as well as the *ygfD* knock-out strain MGC1876Δ*ygfD* (Fig. 5.2A). In both wild-type strains, proteins of the appropriate size, ~78 kDa for Sbm and ~37 kDa for YgfD, were detected on immunoblots (Fig. 5.2A). For MGC1876Δ*ygfD*, the appropriately sized-band was detected for Sbm but not YgfD, as expected (Fig. 5.2A). Therefore, we conclude that the Sbm operon is functional in *E. coli*.

Given its identification as a G3E P-loop GTPase, we expected that YgfD could also function as a GTPase. Assay of GTPase activity confirmed GTP hydrolysis (Fig. 5.2B), however, the protein proved to be extremely unstable during isolation and purification and was observed to precipitate in pure and semi-pure extracts. Therefore, we were able to demonstrate hydrolysis but could not obtain reliable kinetic data.

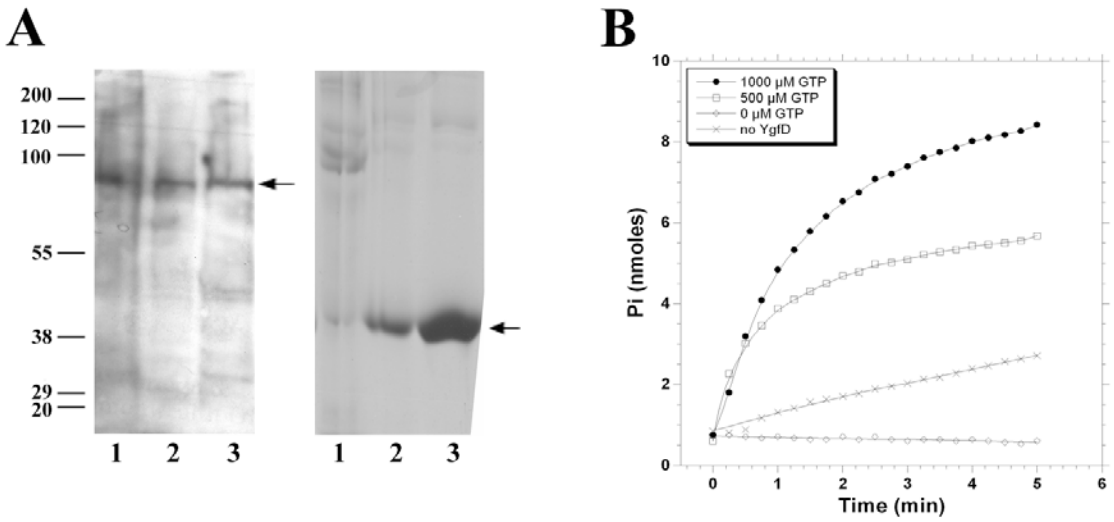

Figure 5.2. Sbm and YgfD protein expression and GTPase activity of YgfD.

A. Western blot analysis of whole cell lysates from *E. coli* MGC1876Δ*ygfD*. (lane 1), DH5α (lane 2), and MGC1876 (lane 3), probed with anti-Sbm (left panel) and anti-YgfD (right panel). **B.** GTPase activity of YgfD. Measured by the production of inorganic phosphate (Pi) from GTP, monitored at A_{360}.

YgfD and Sbm physically interact in vivo

Based on the observation that MeaB physically interacts with MCM in *Methylobacterium extorquens in vitro* (79), we evaluated whether YgfD and Sbm might interact *in vivo*. For this experiment, we made use of immobilized anti-YgfD to capture protein from a lysate of wild type *E. coli* grown in LB (Fig. 5.3A). Western blot analysis of the protein released from the immobilized antibody revealed the presence of both YgfD and Sbm (Fig. 5.3A, lanes 3, 4). A more elaborate experiment in which both anti-YgfD and anti-Sbm were used as the immobilized antibody followed by Western blot analysis using antibodies against the two proteins to identify the immunoprecipitated species is shown in Fig. 3B. Using strains BL21 and MGC1876, immunocapture by either anti-YgfD or anti-Sbm recovered both YgfD and Sbm proteins (Fig. 5.3B, lanes 1,2,4,5). In contrast, in MGC1876Δ*ygfD*, anti-Sbm but not anti-YgfD identified Sbm in the knockout strain lacking YgfD (Fig. 5.3B, lanes 3,6). These experiments confirm that YgfD and Sbm physically interact *in vivo* and that detection of Sbm following immunocapture using anti-YgfD is dependent on the presence of YgfD protein. They also imply that YgfD is not essential for either the viability of these cells or the expression of Sbm, as neither was affected by knockout of the YgfD protein.

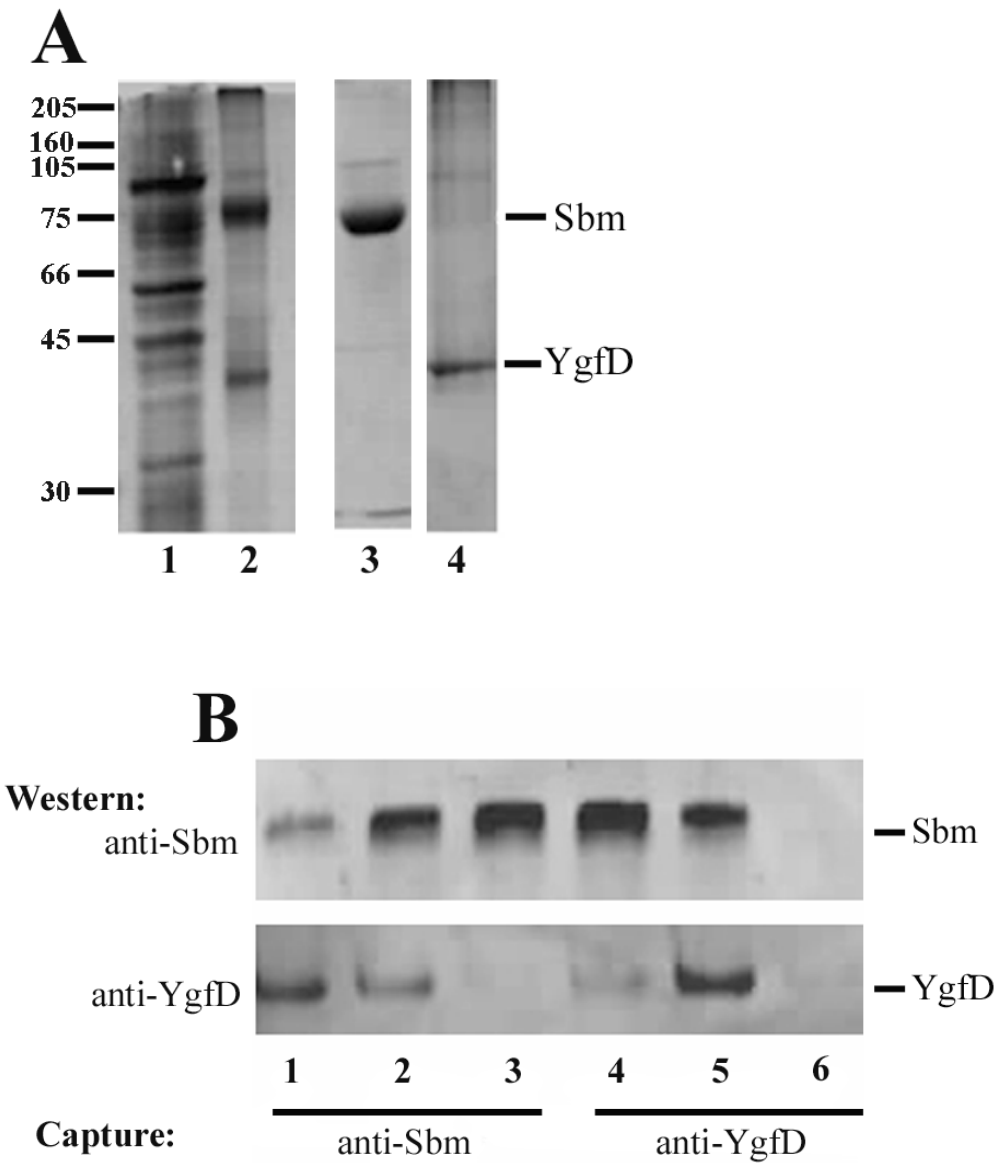

Figure 5.3. Interaction of YgfD and Sbm *in vivo*.

A. Proteins from MGC1876 crude cell lysate (lane 1) or immunoprecipitated from crude cell lysate with anti-YgfD (lanes 2-4) were analyzed by Coomassie blue staining (lanes 1 and 2) or Western blot analysis, probed with anti-Sbm (lane 3) or anti-YgfD (lane 4). Note anti-YgfD captures a complex of YgfD and Sbm (lane 2). **B.** Immunocapture of YgfD and Sbm using immobilized anti-Sbm (lanes 1-3) or anti-YgfD antibodies (lanes 4-6) followed by SDS-PAGE and Western blot analysis using anti-Sbm (upper) or anti-YgfD (lower). Lanes 1, 4, strain BL21; lanes 2, 5, MG1876; lanes 3, 6, MGC1876Δ*ygfD*.

Interaction of YgfD and Sbm in vitro

To investigate the nature of the interaction between YgfD and Sbm, we examined cofactor requirements for interaction *in vitro*. Recombinant YgfD and Sbm containing N-terminal His tags were expressed in *E. coli* and purified by nickel affinity chromatography, as described previously (145). Both proteins were obtained in high yield (10-15 mg/L) and migrated with molecular masses of ~40 kDa for YgfD and ~80 kDa for Sbm, as monitored by SDS-PAGE (Fig. 5.4A). When apo-Sbm was separated on a native gel, it migrated both as a monomer and as a dimer (Fig. 5.4B). This result was supported by size-exclusion chromatography, which also showed peaks corresponding to an Sbm monomer and dimer (Fig. 5.4C panel 2). This was not surprising as most methylmalonyl-CoA mutases form dimers, whether encoded by two genes (heterodimeric) (79, 151) or a single gene (homodimeric) (152). In contrast, while clearly visible as a band on an SDS gel (Fig. 4A), YgfD by itself could not be visualized on a native gel (Fig. 4B), a behavior that was also observed with MeaB (Padovani et al., 2006). However, native YgfD could be detected by size exclusion chromatography and eluted as a monomer (Fig. 5.4C panel 3), although it was very unstable and had to be run in the presence of molecular weight standards to minimize precipitation. Therefore, all subsequent gel exclusion chromatography experiments were run in the presence of molecular weight standards. When YgfD and Sbm were mixed and incubated in the absence of cofactor and nucleotide substrate, novel high molecular weight species indicative of complex formation could not be detected on a native gel. However, when YgfD was pre-incubated with the non-hydrolysable GTP analog (GMPPNP) and then

incubated with Sbm, two new migrating species were observed with molecular masses greater than the 232 kDa molecular weight marker (Fig. 5.4B, Complex 1 and Complex 2). Maximal complex formation occurred when the YgfD:GMPPNP mix was at a molar ratio of 4:1 with Sbm. Such a high ratio may have been required to drive complex formation owing to the instability of YgfD. Complex formation was not affected by whether or not B_{12} was bound to Sbm, and the complex was not observed when YgfD was pre-incubated with GTP or GDP as the nucleotide (Fig. 5.4D). By size exclusion chromatography, the YgfD:Sbm complex could be detected in the presence of GTP and AdoCbl, revealing that under these milder conditions, complex formation between the two proteins could be observed in the absence of GMPPNP. Under these conditions, the complex migrated with a size corresponding to ~258 kDa, suggestive of a stoichiometry of 2 YgfD + 2 Sbm (Fig. 5.4C panel 4). However, the accuracy of molecular weight determinations in this range is limited and by this method, shape dependent, so our estimate is only approximate.

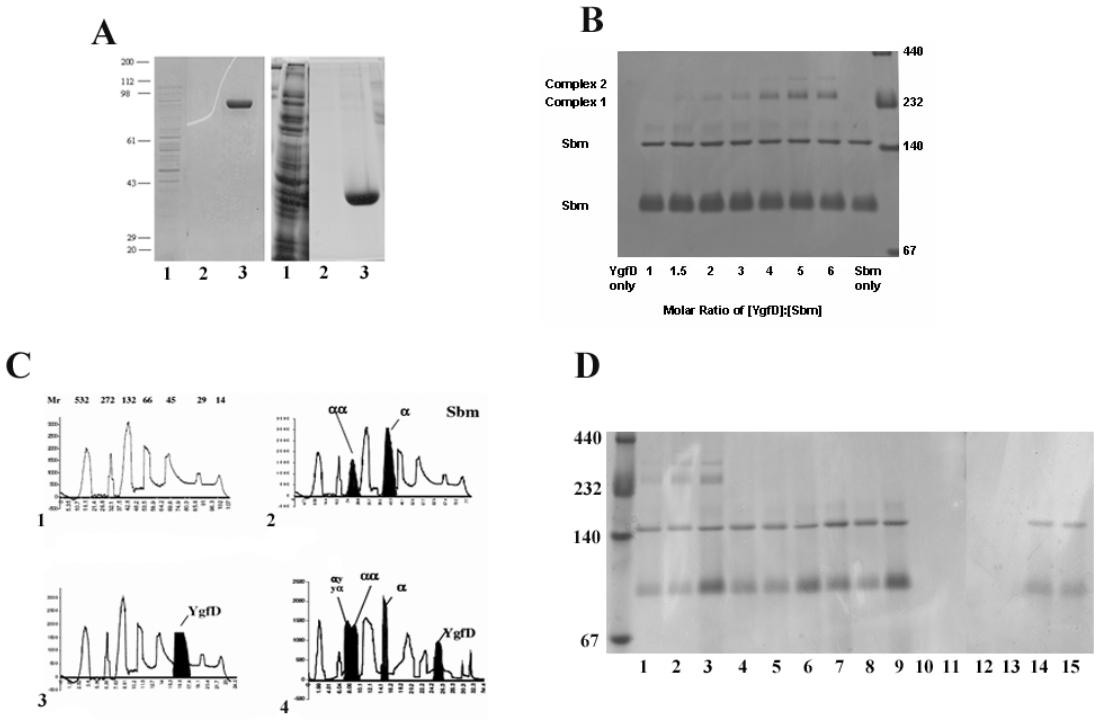

Figure 5.4. Interaction of YgfD and Sbm *in vitro*.

A. Expression and purification of His-tagged Sbm (left panel) and YgfD (right panel) run on 12% SDS-PAGE and stained by Coomassie blue. For both: lane 1, total cell lysate; lane 2, final wash fraction before elution; lane 3, eluate containing purified protein. B. Native 4-20% polyacrylamide gel containing Sbm apoenzyme incubated with increasing molar equivalents of YgfD pre-incubated with GMPPNP. Sbm ran at ~80 kDa monomer and ~160 kDa dimer (Sbm only lane), while YgfD (~40 kDa) was run off this gel but not seen previously (YgfD only lane). Note appearance of species (Complex 1 and Complex 2) with masses in excess of the 232 kDa MW standard at increasing YgfD ratio (maximal band shift obtained at 4:1 YgfD:Sbm incubation mix). C. Purified Sbm, YgfD, or an equal mixture of the two, were analyzed by gel filtration. Proteins were run in the presence of MW standards (bovine milk α-lactalbumin (14.2 kDa), bovine erythrocytes carbonic anhydrase (29 kDa), chick egg albumin (45 kDa), BSA (66 kDa – monomer, 132 kDa – dimer), and Jack Bean urease (272 kDa – trimer, 545 kDa – hexamer)) to prevent precipitation and loss of proteins during sieving. Panel 1, MW standards with molecular masses in kDa indicated above each peak; Panel 2, Sbm plus MW standards, with Sbm monomer ("α") and dimer ("αα") peaks filled in black; Panel 3, YgfD plus MW standards with YgfD peak in black; Panel 4, YgfD plus Sbm with each protein and putative complex ("ααγγ") filled in black. Peaks in black were determined by comparison with peaks in Panel 1. The x- and y-axis refer to time (min) and elution profile at OD_{280}, respectively, for all charts. D. Native 4-20% polyacrylamide gel containing different combinations of YgfD and Sbm with or without prior incubation to cofactor/coenzyme demonstrating that only YgfD pre-incubated with GMPPNP results in complex formation with Sbm. Lane 1, YgfD:GMPPNP & Sbm:AdoCbl; Lane 2, YgfD:GMPPNP & Sbm:HOCbl; Lane 3, YgfD:GMPPNP & Sbm; Lane 4, YgfD & Sbm:AdoCbl; Lane 5, YgfD & Sbm:HOCbl; Lane 6, YgfD & Sbm; Lane 7, Sbm:AdoCbl; Lane 8, Sbm:HOCbl; Lane 9, Sbm; Lane 10, YgfD:GMPPNP; Lane 11, YgfD; Lane 12, YgfD:GTP; Lane 13, YgfD:GDP; Lane 14, YgfD:GTP & Sbm; Lane 15, YgfD:GDP & Sbm.

Discussion

We report the expression of Sbm and YgfD, contiguous members of an *E. coli* operon comprised of *sbm-ygfD-ygfG-ygfH*. Past attempts to demonstrate enzyme activity associated with Sbm had failed (145, 153), leading to the gene name "sleeping beauty mutase." Although Haller *et al*. (145) successfully expressed all four proteins *in vitro*, they were able to assign functions to only three of them, predicting a cycle for the conversion of succinyl-CoA to propionyl-CoA. The function of YgfD could not be assessed. In this study, we confirmed the expression of native Sbm and YgfD in *E. coli* and demonstrated that the two proteins form a complex *in vitro* and *in vivo*. We showed further that YgfD has GTPase activity and that binding a non-hydrolyzable GTP analog stabilizes the association *in vitro*.

Identified as a member of the G3E family of P-loop GTPases (148), YgfD shares 48% sequence identity with MeaB, the orthologous protein from *M. extorquens*, and 46% with MMAA, its counterpart in human cells. While MeaB has previously been shown to interact with MCM *in vitro*, this was not demonstrated *in vivo* (79, 81). Our finding that YgfD and Sbm physically interact *in vivo* was made by co-immunoprecipitation of the two proteins using antibodies to either YgfD or Sbm as the capture reagent, a result that was confirmed with the use of a *ygfD* knockout strain. Further, we showed *in vitro* that recombinant YgfD and Sbm form a stable complex that can be separated on a non-denaturing gel or by size exclusion chromatography. The interaction depended on pre-incubation of YgfD with non-hydrolyzable GTP for detection by electrophoresis. A

YgfD-Sbm complex could also be detected on the sieving column in the presence of GTP and AdoCbl, although the conditions for interaction were not further evaluated in this medium owing to the extreme lability of the proteins. Our results are consistent with a 2YgfD:2Sbm structure by molecular sieving, in contrast to MeaB:MCM which behaves as a heterodimer. While we found that Sbm was detected as a mixture of monomer and dimer, YgfD was only seen as a monomer in contrast to MeaB in which a dimer was observed (81).

The *sbm* operon does not appear to be essential for cell growth, at least under the culture conditions used in this study. Further, Haller *et al.* were unable find evidence for an effect of hydroxocobalamin on cell growth under either aerobic or anaerobic conditions with succinate or propionate as the carbon source (145). Likewise, when the *ygfD* gene was disrupted, we did not observe any effect on cell viability.

While we have characterized the interaction between Sbm and YgfD, the significance of this interaction remains incompletely understood. The stabilization of the complex using a non-hydrolyzable form of GTP suggests that GTP is required for complex formation *in vivo*. Yet, co-immunoprecipitation of the complex was obtained from extracts of cells grown in standard LB medium. As well, while YgfD and Sbm are expressed endogenously, previous studies failed to demonstrate a functional pathway (145, 153). Since recombinant Sbm has been shown to be functional when overexpressed in *E. coli* in medium containing vitamin B_{12} (153), one can only speculate that under standard growth

conditions, expression of Sbm, while detectable, must be too low to produce a functional pathway.

CHAPTER 6: *IN VIVO* BUT NOT *IN VITRO* INTERACTION OF MMAA AND MUT

Introduction

In humans, methylmalonyl-CoA mutase (Mut, MCM) is a mitochondrial protein which catalyzes the enzymatic conversion of $_{L}$-methylmalonyl-CoA to succinyl-CoA, an important step in the metabolism of four amino acids (threonine, methionine, valine and isoleucine), odd-chain fatty acids and cholesterol (114, 154). To do so, Mut requires adenosylcobalamin (AdoCbl) as cofactor and any block in the ability of the cell to produce or in the ability of Mut to utilize this cofactor results in an inborn error.

The Mut protein is encoded by the *MUT* gene (155) and nearly 200 mutations have thus far been described (93, 156). Common mutations of Mut include c. 655A>T (p. N219Y), c. 1106G>A (p. R369H), c. 2080C>T (p.R694W), c. 322C>T (p.R108C) (Hispanic patients) and c.2150G>T (p.G717V) (Black patients) (94). Defects in Mut are split into mut^{-} and mut^{0} based on the presence or absence of residual enzyme activity or detectable [^{14}C]-propionate metabolism in cultured cells (95). mut^{0} mutations result in no detectible Mut activity, whereas mut^{-} mutations have a low residual activity that can usually be stimulated with high concentrations of hydroxocobalamin (OHCbl) (157, 158). mut^{0} patients have a higher frequency of morbidity, mortality and neurologic complications than mut^{-} patients (75, 76, 159).

Other disorders, designated *cblA, B, C, D* and *F*, have been shown to interfere with Mut function, as these metabolic enzymes are required for the intracellular production of AdoCbl. Of these, two proteins, LMBRD1 (*cblF*) and MMACHCH (*cblC*), are responsible for entry of cobalamin into the cell and early cellular cobalamin processing, respectively (43, 47). Defects in these enzymes also result in deficiency of methionine synthase (MS), the other cobalamin dependent enzyme in humans. One protein, MMADHC (*cblD*), has been predicted to shuttle cobalamin to the cytosol or mitochondrial pathway and can result in deficiency of Mut, MS or both (42). The remaining disorders, *cblA* and *cblB*, result in deficiency only of Mut and represent the mitochondrial enzymes MMAA and MMAB, respectively (77, 83, 84). MMAB has been shown to encode ATP:cob(I)alamin adenosyltransferase and is the enzyme responsible for physically adding the adenosyl group to cobalamin, resulting in the production of AdoCbl (83, 84). MMAA, while integral to Mut function and AdoCbl production as witnessed by an absence of both with mutations in this enzyme, does not yet conclusively have a function associated with it.

Studies conducted in bacteria on orthologs of Mut and MMAA have been integral to our understanding of their structure and function thus far. MCM from *P. shermanii* has been crystallized and described in detail, allowing easier understanding of the structure of human Mut (PDB: 3BIC), since the α-subunit of *P. shermanii* MCM is 60% identical (75% similar) to the human enzyme (96). Each subunit of *P. shermanii* MCM contains an N-terminal $(\beta\alpha)_8$ TIM barrel (residues 88-422 in MCM, residues 86-373 in Mut) housing the substrate binding site, a C-terminal $(\beta\alpha)_5$ AdoCbl binding domain (residues

578-750 in MCM; residues 606-727 in Mut) with a groove for binding the dimethybenzimidazole (DMB) side chain of AdoCbl as well as residues to stabilize the lower face of the corrin ring, and a linker region (residues 423-577 in MCM; residues 374-605 in Mut) between them that houses the upper face of the corrin ring and the 5'-deoxyadenosyl group of AdoCbl (97-99). Likewise, MeaB, the *Methylobacterium extorquens* homolog of MMAA, has also been crystallized (160). MeaB forms a homodimer, with the C-terminal ~70 amino acids critical for dimer formation. Additionally, each subunit contains a G domain typical of the G3E family of P-loop GTPases with which it belongs (148), consisting of a 7 parallel-stranded β-sheet that houses the GTPase active site. Finally, the N-terminus of MeaB contains ~ 50 amino acids whose function are not readily apparent, but were predicted by Hubbard *et al.* to be important for the interaction of MeaB with methylmalonyl-CoA mutase, which in *M. extorquens* consists of McmA and McmB (hereafter mutually referred to as Mcm). Indeed, previously Korotkova *et al.* (79) as well as Padovani *et al.* (81) demonstrated the *in vitro* physical interaction of MeaB with *M. extorquens* Mcm, by native gel as well as isothermal calorimetry. Additionally, they showed that this binding was altered depending on the state of Mcm, holo- vs. apoenzyme, as well as by the state of MeaB, unbound or bound to GDP or GTP (79, 81). Later, we showed that YgfD and Sbm, *E. coli* homologs of MMAA and Mut, respectively, also were able to physically interact both *in vitro* and *in vivo* (80). However, for this interaction to be seen by native gel, YgfD was required to be bound to a non-hydrolyzable form of GTP (80).

These results suggest that the human proteins MMAA and Mut might also interact, possibly in a manner modulated by ligand binding. Here we investigated their possible interaction *in vitro* using purified recombinant protein as well as *in vivo* using pull-downs followed by immunoblotting. We demonstrate the purification of recombinant MMAA and Mut protein and the ability of MMAA to bind GDP as well as hydrolysable and non-hydrolysable forms of GTP, but not ATP. We also demonstrate the ability of Mut to bind AdoCbl. We show, by native gel electrophoresis, MMAA and Mut do not interact *in vitro*, including in the presence of GDP, non-hydrolysable GTP, AdoCbl or OHCbl. A result further corroborated by a lack of interaction seen by size-exclusion chromatography. However, *in vivo*, we show the ability to detect Mut after pull-down with over-expressed MMAA-flag, a result that wasn't observed with the pull-down of an over-expressed control protein (TdP1) bound to flag. These data suggest that *in vivo*, MMAA and Mut interact, but the conditions of this interaction are not readily apparent *in vitro*.

Materials and Methods

Materials

Adenosylcobalamin (AdoCbl), hydroxocobalamin (OHCbl), AMP, ADP, ATP, ATPγS, GMP, GDP, GTP, GTPγS and GMPPNP were purchased from Sigma-Aldrich (Oakville, ON). Anti-flag generated in rabbit was obtained from Sigma-Aldrich. anti-Mut has been previously described (Froese MGM 2008). Protein-A and Protein-G sepharose were from GE Healthcare (Baie d'Urfe, QC). All other chemicals were reagent grade.

Plasmid Generation

pNIC-Mut-CTHF (C-terminal his- and flag-tag) was a generous gift from Udo Opperman (SGC, Oxford) whose protein sequence is available (PDB: 3BIC). pNIC28-Bsa4-MMAA (N-terminal his-tag) was constructed using the forward primer TACTTCCAATCCATGgaaggactttctgataaagag and the reverse primer TATCCACCTTTACTGTTAgtctctgcttttaaaagc, where capitalized letters represent LIC cloning sites, to generate MMAA cDNA minus the first 310 nucleotides, which was subsequently cloned into pNIC28-Bsa4 (GenBank accession EF198106). The corresponding MMAA protein had an N-terminal truncation of the first 75 amino acids of full-length MMAA protein. pFLAG-CMV-2 was from Sigma. pTDP1-flag was a generous gift from S. Lees-Miller (University of Calgary) and has been previously published (161). C-terminally flag-tagged MMAA in pCMV-Entry (pMMAA-flag) was purchased from OriGENE (Rockville, MD). Mut in pCMV6-XL5 was purchased from OriGENE. A C-terminal His-tag was added to pCMV6-XL5-Mut by first performing PCR using the primers mut-A (ATG TGC TGC TAG CGG AGA TGG [an NheI site is underlined]) and mut-B (TTA ATG GTG ATG GTG ATG GTG TAC AGA TTG CTG CTT CTT TT [the added 6x His is underlined]) to give PCR fragment mutAB, as well as mut-C (GTA CAC CAT CAC CAT CAC CAT TAA TAT CCT CTT TTT GTT TT [the added 6x His is underlined]) and mut-D (ATG ACC GCG GCC GCA ATC TAG AGT [a SacII site is underlined]) to give PCR fragment mutCD. Then, mutAB and mutCD were used as template DNA with the primers mut-A and mut-D for an additional PCR reaction to give the PCR fragment mutAD. Finally, both the mutAD and the original pCMV6-

XL5-Mut vector were cut with SacII and NheI restriction enzymes (NEB; Ipswich, MA), column purified (Qiagen; Mississauga, ON) and ligated using T4 DNA ligase (Invitrogen; Burlington, ON) to give pCMV6-XL5-Mut with a C-terminal 6x His-tag (pMut-His).

Protein Expression and Purification

pNIC28-Bsa4-MMAA and pNIC-Mut-CTHF were transformed into BL21(DE3)-pRARE cells. For expression, both were grown overnight in 50 mL Terrific Broth (Novagen; Madison, WI) at 37°C with shaking at 180 rpm. Cells were then reinoculated in 1:100 Terrific Broth and grown at 37°C until an OD_{600} of 0.8-1.2., upon which, for Mut, the temperature was decreased to 18°C and 1 mM IPTG was added, and for MMAA, the temperature was kept at 37°C and 0.5 mM IPTG was added. Cells were grown over-night (16 hours), pelleted by centrifugation and resuspended in binding buffer (50 mM HEPES, pH 7.5; 0.5 M NaCl; 5% glycerol and 20 mM imidazole). Resuspended cells were broken by 5 passes at 15,000 psi in a homogenzer (EmusiFlex C3, Avestin; Ottawa, ON) and insoluble material was removed by centrifugation at 27,000 x*g* for 45 minutes. The supernatant was then incubated with Ni-NTA resin (Qiagen) over-night at 4°C with rotation. Protein was purified from the resin by washing with 10 column volumes (CV) of binding buffer, 10 CV wash buffer (50 mM HEPES, pH 7.5; 0.5 M NaCl; 5% glycerol and 40 mM imidazole) and eluted with 2 CV each of elution buffer (50 mM HEPES, pH 7.5; 0.5 M NaCl; 5% glycerol) containing 60 mM imidazole, 80 mM imidazole, 100 mM imidazole, 150 mM imidazole and 250 mM imidazole. MMAA was further purified by size exclusion chromatography (Superdex S75, GE Healthcare), while Mut was further

purified by ion exchange chromatography (MonoQ, GE Heathcare) in Tris pH, 8.0 with a NaCl gradient of 0.1-0.5 M. Both proteins were switched into gel filtration (GF) buffer (50 mM HEPES, pH 7.5; 0.5 M NaCl and 5% glycerol) by buffer exchange (HiPrep 26/10 Desalting column, GE Healthcare). Purified protein was stored at - 80°C. The yield for each protein was ~20 mg/L culture.

Differential Scanning Fluorimetry

DSF was performed and analyzed as described in Niesen *et al.* (132) with minor modifications. Purified MMAA or Mut proteins were diluted to 0.1 mg/ml in GF buffer with 1:1000 Sypro Orange (Sigma-Aldrich) and incubated with the ligand described. All conditions were run in triplicate. The proteins were subjected to a ramp of 1°C/min in a thermocycler (C1000 Thermocycler, CFX96 Real-time system, Bio-rad; Mississauga, ON) at a temperature gradient of 25 to 95°C. All graphs were normalized so that minimum fluorescence was set to 0 and maximum fluorescence set to 1. This was done because OHCbl and AdoCbl showed fluorescence quenching at higher concentrations. However, quenching did not affect T_m's as a control protein (GST) showed no T_m shift with any cobalamin used. Final graphs were generated using Kaleidagraph 4.0 (Synergy Software; Reading, PA).

Cell culture and nucleofection

HepG2 cells (ATCC: HB-8065) were cultured in DMEM (Invitrogen) supplemented with 10% serum (5% fetal bovine serum, 5% bovine calf serum) and antibiotics-antimycotics.

10 µg of plasmid DNA, either pMMAA-flag or pMut-His, was nucleofected into cells as per manufacturer's protocol (Amaxa Biosystems; Gaithersburg, MD).

Immunoprecipitation procedures

Nucleofected HepG2 cells were lysed by incubation in lysis buffer (1% NP-40; 0.5% deoxycholine; 150 mM NaCl; 50 mM Tris, pH 7.5) with sonication by 2x 10 second bursts by a Misonix XL-2000 sonicator (Mandel Scientific; Guelph, ON) at 4°C. After sonication, cell fragments were centrifuged at 10,000 x*g* for 10 minutes at 4°C. For IP with anti-flag antibody, anti-flag was added to supernatant and incubated for 20 minutes at 4°C with rotation. Protein-G-agarose (Qiagen) was then added to the mixture and the solution incubated over-night at 4°C with rotation. Anti-Mut antibody was pre-conjugated to protein-G-agarose by dimethyl pimelimidate (DMP), as previously described (162). Anti-Mut-protein-G-agarose was incubated with supernatant overnight at 4°C with rotation. For each, the mixture was centrifuged at 1500 x*g* for 2 minutes at room temperature (RT) and washed 3x with lysis buffer and 1x with high salt buffer (lysis buffer with 500 mM NaCl) by incubation in 1 mL of buffer with rotation at RT for 5 minutes, followed by centrifugation at 1500 x*g* at RT for 2 minutes and then aspirating off supernatant. Finally, antibody-bound protein was resuspended in 2X sample buffer (0.09 M Tris, pH 6.8; 20% glycerol; 2% SDS; 0.02% bromophenol blue; 0.1 M DTT) and heated at 95°C for 20 minutes to release the protein and added to SDS-PAGE for analysis or immunoblotting.

Immunoblotting procedures

Immunoblotting procedures were done as described previously (163), except that anti-flag was used as a primary antibody at 1:2000 dilution.

Size-exclusion chromatography

Gel filtration was accomplished by fast protein liquid chromatography using a Superose 6 10/30 GL column (GE Healthcare) monitored by following the change in OD_{280}. A 100 µl solution of either 88 µg Mut, 175 µg MMAA or both, in GF buffer was used in each experiment. For the experiment where both proteins were run together, MMAA and Mut were first pre-incubated together for 10 minutes at RT. The column was calibrated with standards of known molecular weight, including blue dextran 2000, thyroglobulin (660 kDa), ferritin (440 kDa), aldolase (158 kDa), conalbumin (75 kDa) and ovalbumin (44 kDa), which were used to calculate the size of Mut and MMAA using the equation $K_{av}= V_e-V_o/V_c-V_o$ where V_o = column void volume, V_e = elution volume and V_c = geometric column volume, as per manufacturer's instructions (GE Healthcare).

Native PAGE analysis of pure proteins

For native PAGE, 50 µg MMAA and 25 µg Mut were analyzed on a 4-20% gradient gel (Bio-Rad), alone, together and/or in the presence of 5 mM GDP, 5 mM GMPPNP, 50 µM AdoCbl and/or 50 µM OHCbl as described in the text. Additionally, proteins were incubated in the same conditions with 10 mM $MgCl_2$, with no discernable effect. Proteins were initially pre-incubated in GF buffer with each other and/or their cofactor in a total volume of 20 µl for 10 minutes in the dark. Reactions were centrifuged at 10,000

x*g* for 10 minutes to pellet any precipitate, and then loaded onto the gel. PAGE under non-denaturing conditions was run at 5 mA for 5 hours at room temperature in the dark, followed by staining with Coomassie Brilliant Blue R-250 (EMD; Gibbstown, NJ). Standards used were Urease (272 kDa and 545 kDa) and BSA (132 kDa and 66 kDa) (Bio-Rad). For 2nd dimension SDS-PAGE, protein was run on 4-20% native gel as described above, the entire lane cut out with a razor, then loaded horizontally on a single lane 7.5% acrylamide gel. SDS-PAGE was run at 15 mA for 90 minutes, followed by staining with Coomassie Brilliant Blue R-250. Standards used were low range molecular weight standards (Bio-Rad).

Results

Purification and ligand binding of MMAA and Mut

We expressed and purified MMAA and Mut by Ni-NTA affinity chromatography as described in the Materials and Methods. Both proteins were > 90% pure as analyzed by SDS-PAGE (Fig. 6.1A). To characterize whether these proteins were folded properly and to determine their preferred substrates, we analyzed their change in stability upon ligand binding by differential scanning fluorimetry (DSF). We found that MMAA had increased stabilization upon incubation with GDP, GTP and the non-hydrolyzable GTP analogs GTPγS and GMPPNP (Fig. 6.1B). However, MMAA showed no increase in stability upon incubation with GMP, AMP, ADP, ATP or ATPγS (Fig. 6.1B). Since increased stability by this method is proportional to binding affinity (164), we inferred from this result that the preferred substrates of MMAA are GDP and GTP. By the same

method, we found that Mut underwent a concentration specific increase in stability upon binding to AdoCbl (Fig. 6.1C), confirming its ability to bind this cofactor.

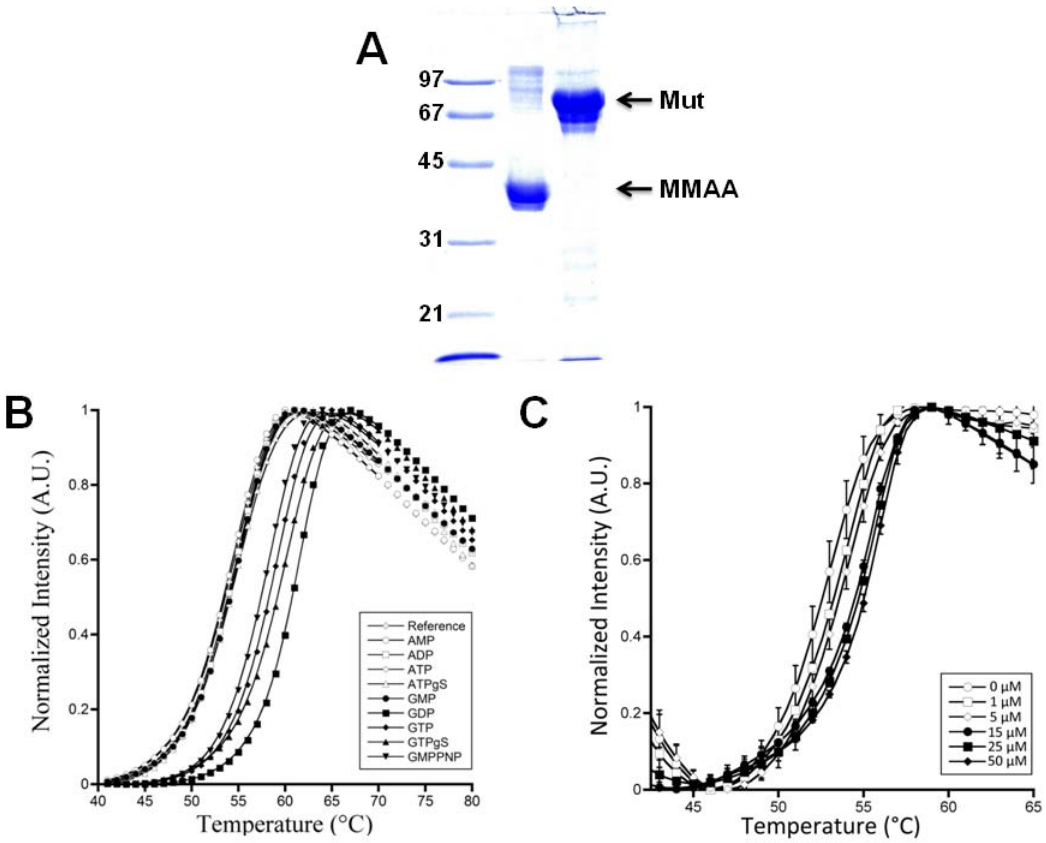

Figure 6.1. Purification and ligand binding test of MMAA and Mut.

A. SDS-PAGE of purified MMAA and Mut. Gel stained with Coomassie Brilliant Blue. Expected sizes: MMAA = 41.1 kDa, Mut = 84.7 kDa **B.** DSF of MMAA with 1 mM adenine and guanosine nucleotides. A shift to the right from the reference spectrum in this assay is indicative of ligand binding. ATPgS is ATPγS, GTPgS is GTPγS, and GMPPNP is non-hydrolyzable GTP. **C.** DSF of Mut with increasing concentrations of AdoCbl.

Ligand effect in native gel investigations of MMAA and Mut

To investigate a possible *in vitro* interaction between MMAA and Mut, we used non-denaturing (native) PAGE. First, we incubated each protein with their expected ligands to determine whether these had an effect on their PAGE separation characteristics (Fig. 6.2A). MMAA was analyzed alone (lane 1) or in the presence of GMPPNP (lane 2) or GDP (lane 3), while Mut was analyzed alone (lane 4) or in the presence of AdoCbl (lane 5) or OHCbl (lane 6). Additionally, MMAA and Mut were incubated together and analyzed (lane 7). Regardless of the presence or absence of ligand, the majority of MMAA was found as aggregate at the top of the gel with a minor band at ~200 kDa (lanes 1-3). Likewise, regardless of the presence or absence of ligand, Mut had a major band at ~300 kDa (lanes 4-6). When pre-incubated together, the Mut band at ~300 kDa became less intense, the MMAA band at ~200 kDa became slightly more intense, but no new 'interaction' bands became evident (lane 7).

To determine if ligand binding might be required for interaction, we analyzed MMAA and Mut pre-incubated together in the presence of GDP, GMPPNP, OHCbl or AdoCbl, singly or in combinations, as described in the figure legend (Fig. 2B). We found no difference in the number of bands or band intensity with any combination of ligands (Fig. 6.2B lanes 1-9).

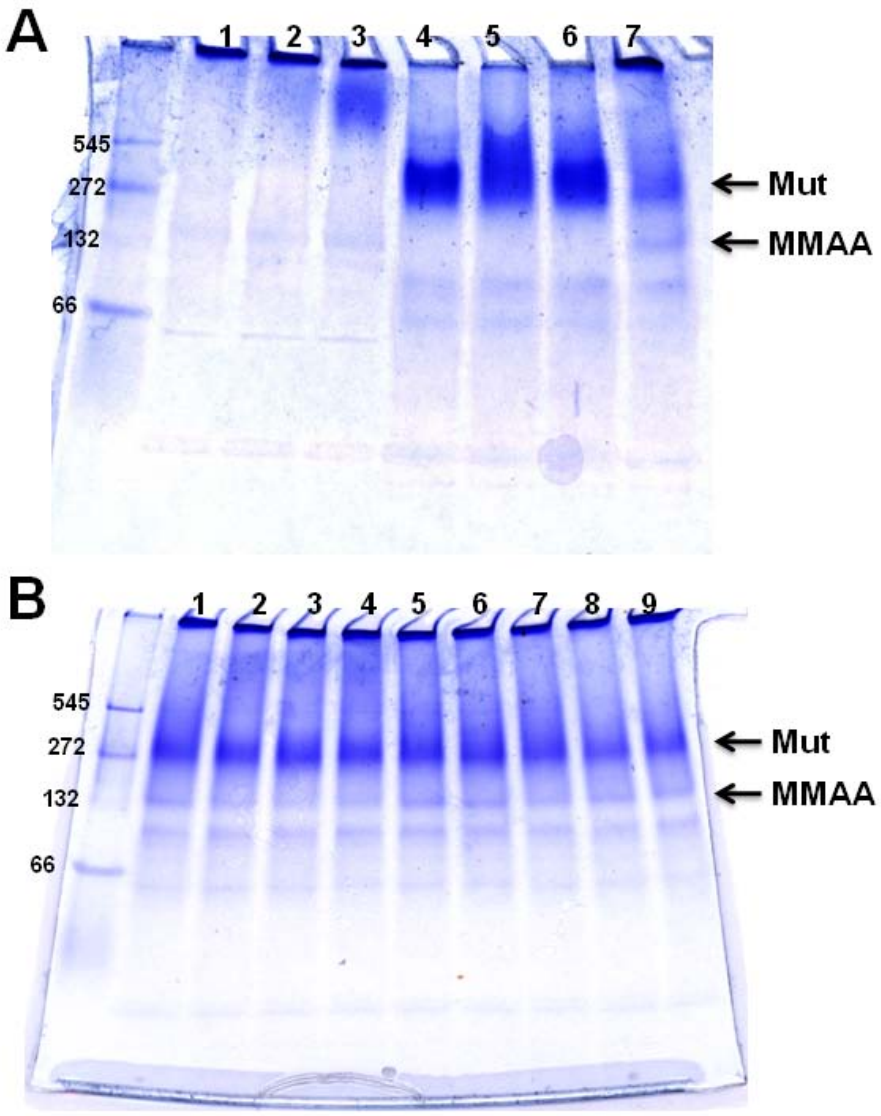

Figure 6.2. Native 4-20% PAGE of Mut and MMAA.

A. Incubation of Mut and MMAA with relevant small molecules. Lane 1, MMAA; lane 2, MMAA:GMPPNP; lane 3, MMAA-GDP; lane 4, Mut; lane 5, Mut:AdoCbl; lane 6, Mut:OHCbl; lane 7, Mut and MMAA. **B.** Incubation of Mut and MMAA together with small molecules. Lane 1, Mut and MMAA; lane 2, Mut and MMAA:GDP; lane 3, Mut:AdoCbl and MMAA:GDP; lane 4, Mut:OHCbl and MMAA:GDP; lane 5, Mut and MMAA:GMPPNP; lane 6 Mut:AdoCbl and MMAA:GMPPNP; lane 7, Mut:OHCbl and MMAA:GMPPNP; lane 8, Mut:AdoCbl and MMAA; lane 9, Mut:OHCbl and MMAA. For A and B, concentrations: Mut = 12 µM, MMAA = 48 µM, GDP = 5 mM, GMPPNP = 5 mM, AdoCbl = 50 µM, OHCbl = 50 µM.

Molar ratio and analysis by two dimensional electrophoresis

To determine whether the molar ratio between MMAA and Mut might be important for a possible interaction, we incubated MMAA and Mut in increasing molar ratio and analyzed them by native PAGE (Fig. 6.3A). With increasing MMAA, the Mut specific band at ~300 kDa decreased in intensity while the Coomassie Blue stained material at the top of the gel increased in intensity, suggesting aggregation or precipitation at the top of the gel (Fig. 6.3A). To investigate this further, we selected lanes containing only Mut (Fig. 3B, top panel), only MMAA (Fig. 6.3B, bottom panel) or a mixture (6:1 MMAA:Mut) of both proteins (Fig. 6.3B, middle panel). The lanes were excised from the gel and placed horizontally at the top of a 7.5% SDS-PAG for electrophoresis under denaturing conditions. From the top panel it can be observed that, when run alone, the majority of Mut in the native gel occurs in the intense ~300 kDa band, but upon incubation with MMAA (middle panel), most of the Mut protein precipitated at the top of the gel, as indicated by a left-ward shift of the Mut band on the SDS-PAGE gel in the middle panel compared to the upper panel (Fig. 6.3B). From the bottom panel we can see that most of MMAA is found at top of the gel, with a minor amount of protein found in a band at ~200 kDa. Upon incubation with Mut (middle panel), the pattern of MMAA protein does not seem to change. These data did not indicate that MMAA and Mut interact but rather that the majority of MMAA is found aggregated and that Mut is not normally found aggregated, but upon incubation with MMAA, does aggregate and becomes trapped at the top of the gel. Since the native first dimension electrophoresis can resolve soluble species in the mega-Da range, we conclude that mixing Mut and MMAA

fails to produce interacting, larger species than the high MW forms produced when run alone.

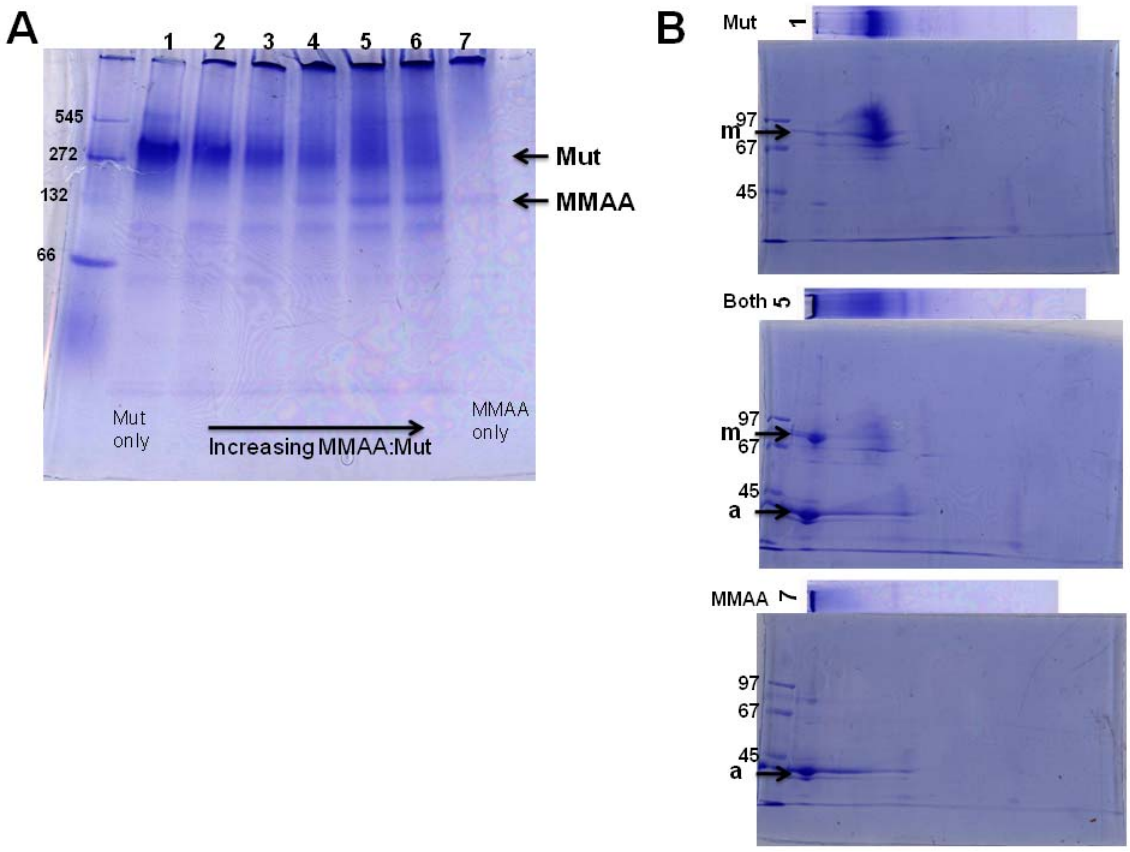

Figure 6.3. Increasing molar ratio of MMAA to MutA and 2nd dimension SDS-PAGE analysis of bands.

A. Increasing molar ratio of MMAA to MutA. Lane 1, 12 µM Mut; lane 2, 12 µM Mut and 12 µM MMAA; lane 3, 12 µM Mut and 24 µM MMAA; lane 4, 12 µM Mut and 48 µM MMAA; lane 5, 12 µM Mut and 72 µM MMAA; lane 6, 12 µM Mut and 96 µM MMAA; lane 7, 48 µM MMAA. **B.** 2nd dimension SDS-PAGE analysis of bands. Upper panel: Mut only (same as lane 1 from panel A), Middle pane: Mut and MMAA (same as lane 5 from panel A), Lower panel: MMAA only (same as lane 7 from panel A). "m" points to the band for Mut and "a" points to the band for MMAA.

Size-exclusion chromatography of MMAA and Mut.

Since in the native gel the majority of MMAA was found at the top of the gel as a large aggregate or precipitate, we used size-exclusion chromatography as an alternative method to analyse the possible interaction of MMAA and Mut. With this method, we found that MMAA protein alone was found as a major peak at ~183 kDa (Fig. 6.4, upper panel), that Mut protein alone was found as a major peak at ~ 307 kDa (Fig. 6.4, bottom panel), and that together MMAA and Mut ran as two major peaks in almost the exact same position as the proteins alone, at ~181 kDa and ~296 kDa, respectively (Fig. 6.4, middle panel). These results indicated that MMAA and Mut did not interact by this method. Given the similarity of the MW of the soluble proteins between the gel and sieving procedures, we conclude that the aggregated species at the top of the elecrophoresis gel were indeed precipitates and not an indication of high MW species.

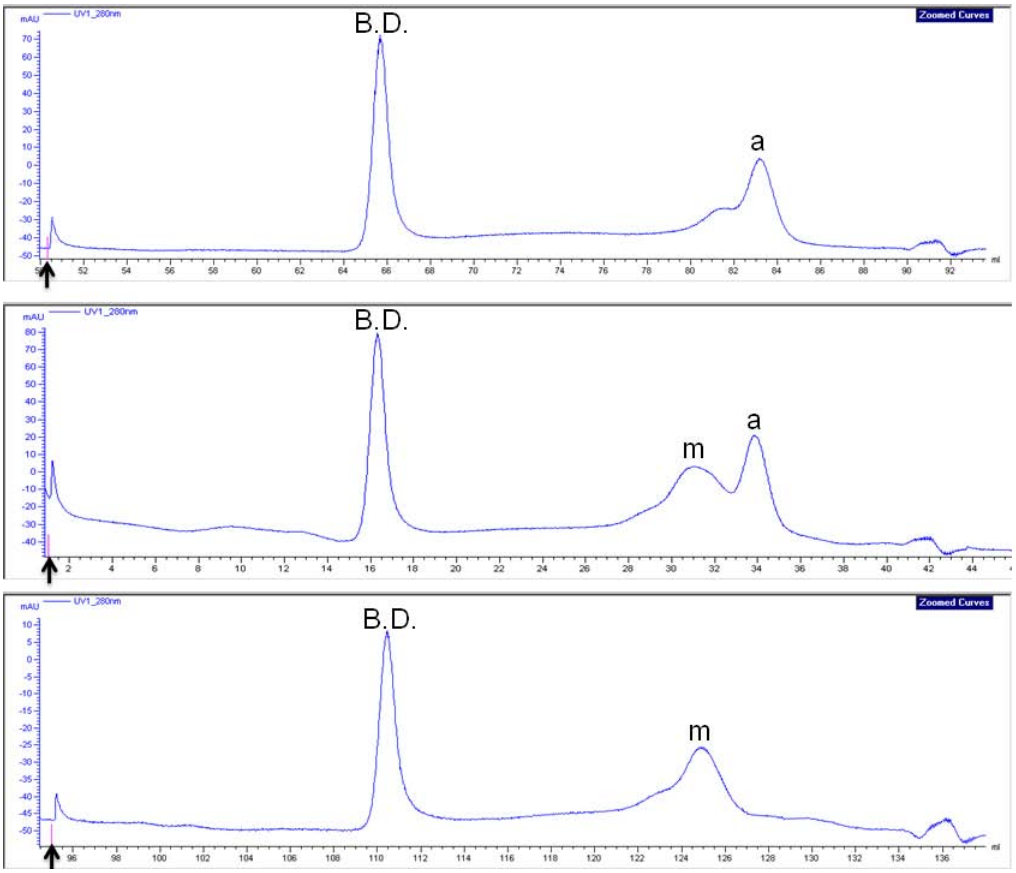

Figure 6.4. Gel filtration of Mut and MMAA.

Upper panel. MMAA alone. "a" peak corresponds to 183 kDa. Middle panel, MMAA and Mut. "m" corresponds to 296 kDa and "a" to 181 kDa. Bottom panel, Mut alone. "m" peak corresponds to 307 kDa. For all panels, arrow points to injection time, B.D. is blue dextran which corresponds to the void volume of the column.

MMAA and Mut physically interact in vivo

Since we failed to obtain evidence for interaction between Mut and MMAA *in vitro*, we turned to cell culture experiments to determine if interaction could be observed *in vivo*, i.e. in the intracellular environment. We transfected HepG2 cells with pMMAA-flag with or without co-transfection with pMut-His. After 48 hours incubation, the cells were extracted and proteins were immunoprecipated with anti-flag, followed by Western blot detection with anti-flag and anti-Mut (Fig. 6.5A). We found that co-transfections with pMMAA-flag and pMut-His or transfection with pMMAA-flag alone, pull-down with anti-flag yielded both MMAA (via anti-flag) and Mut (via anti-Mut) by Western blot analysis (Fig. 6.5A, lanes 2 and 3). Cells that were transfected only with pFlag-CMV-2 gave no bands in the MMAA or Mut positions following pull-down with anti-flag, indicating absence of any ambiguity due to background bands (Fig. 6.5A, lane 1). In a second experiment, we included immunoprecipitation with anti-Mut, in addition to anti-flag, followed by detection for Mut and Flag. We also ran a transfection with pTdP1-flag instead of pMMAA-flag as an additional control (Fig. 6.5B). We found that following transfection of pMMAA-flag and pMut-His, we were once again able to detect both MMAA and Mut by Western blot analysis (Fig. 6.5B, lane 1). However, following pull-down by anti-Mut, we were only able to detect Mut and not MMAA (Fig. 6.5B, lane 2). Importantly, following transfection with pTdP1-flag and pull-down by anti-flag, we were able to detect TdP1 but not Mut, indicating that the ability to detect Mut after pull-down with flag is specific to the MMAA protein (Fig. 6.5B, lane 3).

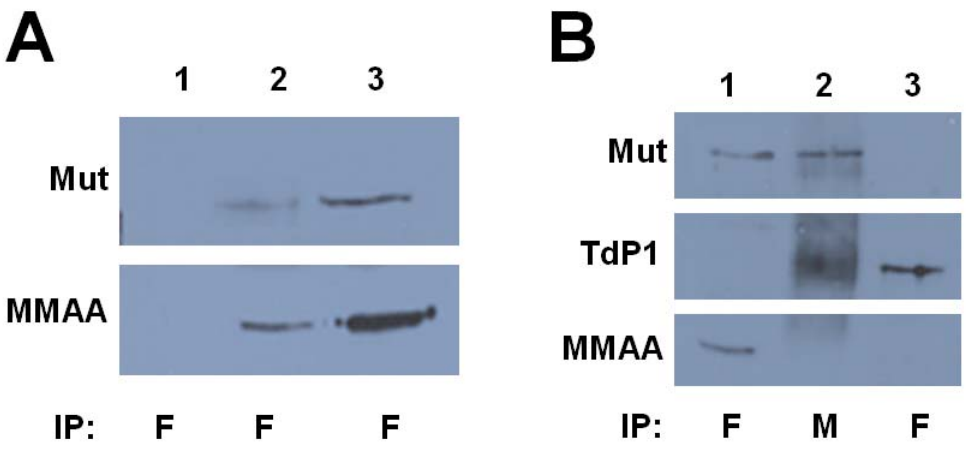

Figure 6.5. *In vivo* interaction of MMAA and Mut in human HepG2 cells.

A. HepG2 cells were transfected with pFlag-CMV-2 (lane 1), pMMAA-flag and pMut-His (lane 2) or pMMAA-flag (lane 3), pulled-down with anti-flag and probed for anti-flag or anti-Mut. Shown is detected Mut protein (upper panel) comprised of endogenous Mut as well as Mut-His and MMAA protein (lower panel) comprised of MMAA-flag. **B.** HepG2 cells were transfected with pMMAA-flag and pMut-His (lanes 1 and 2) or pTdP1-flag (lane 3). Then they were pulled down with anti-flag (lanes 1 and 3) or anti-Mut (lane 2). Shown is detected Mut protein (upper panel) by detection of Mut, TdP1 protein (middle panel) by detection of flag, and MMAA protein (bottom panel) by detection of flag. Band detected with TdP1 in lane 2 was consistent with a smear throughout that lane rather than a discrete band. For A and B, IP indicates whether protein was pulled-down with anti-flag (F) or anti-Mut (M).

Discussion

The aim of this study was to determine if human Mut and MMAA proteins physically interact by analogy with the protein interactions demonstrated for bacterial orthologs of these proteins. Using *in vitro* and *in vivo* methods, we found evidence of interaction in cells expressing recombinant Mut and MMAA *in vivo* but did not demonstrate interaction under *in vitro* conditions. The failure to show *in vitro* interaction was not due to misfolded recombinant MMAA or Mut, since both proteins were shown to bind their expected substrates. Indeed, using ligand-mediated stabilization of the proteins, we demonstrated that MMAA showed specificity towards binding GDP and GTP but showed no binding of ATP. This result is consistent with the inclusion of MMAA in the G3E family of P-loop GTPases, (148) a family that demonstrates the [NT]KxD motif which is responsible for the specificity of guanine over other bases (165). We also demonstrated the concentration specific increase in thermostability of Mut upon binding to AdoCbl using DSF, demonstrating the ability of this recombinant protein to bind its cofactor.

The bacterial orthologs of MMAA and Mut, MeaB and Mcm in *M. extorquens* and YgfD and Sbm in *E. coli*, have previously been shown to interact *in vitro* by native gel electrophoresis (79-81). Incubation of MeaB and Mcm in the absence of any ligand resulted in the formation of higher MW species (79). Additionally, pre-incubation of MeaB with GTP or GDP slightly stimulated formation of the complex. This same interaction was further characterized by Padovani *et al.* (81) who showed that MeaB bound to GMPPNP, a non-hydrolyzable form of GTP, induced complex formation with

Mcm in a ratio that saturated at 1 MeaB homodimer to 1 heterodimer of Mcm (1:1 ratio). When we investigated the interaction between YgfD and Sbm in *E. coli*, we were also able to visualize a high MW complex by native gel electrophoresis (80). However, unlike the previous proteins, the complex was only seen in the presence of GMPPNP. Additionally, complex formation saturated at a 4:1 ratio of YgfD to Sbm, although this may have been related to YgfD instability. Unlike our experience with the *E. coli* proteins, we failed to observe interaction of Mut and MMAA *in vitro* despite demonstrating it *in vivo*. Several explanations are possible: 1) These proteins truly do not interact. While this must be an acknowledged possibility, it seems unlikely in light of the fact that multiple homologs have shown interaction as well as our *in vivo* results on these specific proteins. 2) Since our MMAA protein was truncated N-terminally by 75 amino acids, perhaps we are missing the amino acids required for interaction. After crystallization of MeaB, Hubbard *et al.* (160) proposed that the N-terminal ~50 amino acids, which form 3 α-helices, might be responsible for the interaction with Mcm. This is unlikely to explain the failed interaction *in vitro*. First, a predicted 37 amino acids likely corresponds to the mitochondrial targeting sequence (SignalP 3.0; (166)). Further, alignment of the N-terminus of MeaB and MMAA suggests that the first methionine of MeaB does not align with MMAA until residue 79 (160). Therefore, the full sequence corresponding to the 50 amino acids required for the N-terminal 3 α-helices proposed to be required for interaction is present on the human protein. 3) The interaction requires other proteins or conditions not replicated by our experiments or the complex is fragile. This is the most likely possibility given our *in vivo* result. As well, the ease of interaction differred significantly in the *M. extorquens* and *E. coli* systems. In the former, MeaB and

Mcm could interact in the absence of added factors, while in the latter, YgfD and Sbm required the presence of the nonhydrolyzable analog GMPPNP to confirm interaction. Perhaps there are more stringent requirements for interaction of MMAA and Mut, which could be fulfilled *in vivo* but not *in vitro*. Indeed, Padovani *et al.* (91) have shown that MeaD, a homolog of MMAB, the ATP:Cob(I)alamin adenosyltransferase, directly transfers AdoCbl to Mcm in a manner dependent on association of Mcm and MeaD. Perhaps all three proteins are involved in the interaction in human cells and that MMAB is required to be present for the interaction of the other two.

By size-exclusion chromatography we saw no indication of interaction between MMAA and Mut. Interestingly, we found that both proteins ran at the same approximate molecular weights as they did in native gel electrophoresis, underscoring the oligomeric nature of the proteins in both cases. MMAA was found at ~ 200 kDa on the native gel and ran at ~180 kDa on the sieving column. Mut had a major band at ~300 kDa on the native gel and also ran at ~300 kDa on the sieving column. While the calculated sizes for the native gel are gross approximations, the sieving column approximations are much tighter. These data suggest that MMAA may run as a tetramer or pentamer while Mut occurs as a tetramer. Neither result was expected, as the orthologs of MMAA in *M. extorquens and E. coli* behave as a monomer (YgfD; (80)) or dimer (MeaB; (81, 160)). Mut isolated from human liver was found as a dimer with a molecular weight of ~ 150 kDa (101), and from sheep as a dimer with a molecular weight of 165 kDa (167). These differences cannot be reconciled and require additional investigation.

In vivo, we were able to demonstrate interaction between MMAA and Mut by overexpressing MMAA-flag, pulling down with anti-flag and probing for MMAA-flag and Mut. Ideally we would have conducted this experiment without overexpression. Unfortunately a lack of a specific anti-MMAA antibody made that impossible. However, since overexpression of Flag only, as well as TdP1-flag, did not result in the pull-down of Mut, we are confident in the specificity of MMAA as the protein that allowed detection of Mut. That the reverse experiment, i.e. pull-down with anti-Mut and detection with flag, did not result in the detection of MMAA-flag is not surprising. While we have hypothesized interaction between MMAA and Mut, it does not preclude an equilibrium between interacting and free proteins. If MMAA-Mut interaction is a regulated process, there may well be an excess of free Mut, even in the presence of overexpressed MMAA. Antibody to Mut may only see the majority species. Alternatively, potent epitopes on Mut may well be blocked by interaction with MMAA, especially since both are expected to target to surface features on Mut. Here, multiple antibodies, targeted to different domains on the protein, might be required.

The *cblA* complementation group was originally described in cobalamin deficient cell lines that could not produce AdoCbl in intact cells, but showed normal AdoCbl synthesis in broken cell extracts (78). From this, the *cblA* protein was thought to either function in the mitochondrial transport of cobalamin or in the reduction of cob(II)alamin to cob(I)alamin, both of which would be necessary in intact cells but bypassed in a cell extract assay (78, 168). Cloning of the gene responsible for *cblA*, *MMAA*, revealed that this protein did not have reductase-like domains, leaving only the role of mitochondrial

transport left (77). However, work done with the bacterial homologs MeaB and YgfD have since revealed interaction with Mut and a potential role in protection of AdoCbl bound to Mut, giving no indication of a role in transport (80-82). These results have left the original result, the inability of MMAA deficient cells to accumulate AdoCbl, unresolved. Our demonstration of the *in vivo* interaction between MMAA and Mut, with a predicted involvement of MMAB, may provide an explanation for such a block. Since MMAA and Mut, in addition to MMAB and Mut (in *M. extorquens*), interact, all three proteins may be required to form a complex *in vivo* for the production and utilization of AdoCbl. The requirement of all three proteins for proper function would explain the inability of MMAA deficient cells to produce AdoCbl, as well as our inability to generate a complex between MMAA and Mut without MMAB *in vitro*. This hypothesis is fully compatible with a hypothesis recently put forward by Banerjee and colleagues, which suggests that in order to make full use of the minutely available intracellular cobalamin and to protect cells from reactive cobalamin species, cobalamin is sequestered and chaperoned by proteins that themselves also interact with other proteins in the pathway (27). Any further research into the function of MMAA may need to include both Mut and MMAB, and investigations into this possibility are ongoing.

SUMMARY, CONJECTURE AND FUTURE DIRECTIONS: THE B_{12} CHAPERONE HYPOTHESIS

While cobalamin is an essential intracellular cofactor, we do not yet fully understand how it reaches its target enzymes. Two major challenges to intracellular cobalamin processing suggest it that may be sequestered throughout its intracellular travels. First, cobalamin is found at a very low concentration intracellularly, from as high as 0.6 µM in the liver to as low as 0.03 µM in the brain (125). This contrasts with other cofactors such as vitmain B_6, which has a 14-fold higher liver concentration (169). Second, it is a very reactive molecule. Alkyl-Cbls, including both cofactor forms, are extremely photolabile with an easily cleavable Co-C bond (170). Additionally, cob(I)alamin, the form required for the adenosylation or methylation of cobalamin to produce the cofactor forms, has been described as a supernucleophile, one of the most reactive nucleophiles known in biology (8). Therefore, with both these challenges in mind, it is very important for the cell to efficiently deliver cobalamin to its target enzymes while keeping it sequestered from adventitious reactions. Recently, a theory proposing that cobalamin is bound by chaperones throughout its cellular travels has been championed by Ruma Banerjee (27, 171). This theory posits that cobalamin is bound to protein from the moment it enters the cell until the moment it reaches its final destination enzymes. With the recent description of all of the proteins responsible for the human cobalamin complementation groups, this has become a testable hypothesis and early evidence suggests that this may be the case.

Cobalamin enters the cell via the LMBRD1 protein, corresponding to *cblF*, which is almost assuredly a lysosomal efflux protein (43). There is evidence that MMACHC may interact with LMBRD1 to assist in the import of cobalamin. This evidence comes in the form of the putative structural folding homology that the C-terminus of MMACHC has with TonB, a bacterial protein that provides the energy for cobalamin import in some Gram-negative bacteria by physically interacting with the cobalamin outer-membrane transport protein (47, 172). By analogy with the bacterial system, MMACHC would provide energy to LMBRD1 to facilitate release of cobalamin from the lysosome into the cytosol. While experimental evidence of this interaction is thus far lacking, it is a tantalizing explanation for some MMACHC C-terminal truncation mutations which unexpectedly cause severe disease while earlier mutations may cause only moderate disease (47). Following import into the cytosol, it is likely that MMACHC would directly bind the released cobalamin, since MMACHC has already been shown to bind many different types of cobalamin, including OHCbl and CNCbl, the predominant cobalamin forms obtained from food and supplements, respectively (48, 49, 131). It may be at this point that the cobalamin bound to MMACHC, either as OHCbl or CNCbl, is reduced to cob(II)alamin. The reduction of OHCbl to cob(II)alamin is simple and indeed the two are expected to exist in equilibrium in the cell. The reductive decyanation of CNCbl to cob(II)alamin is more difficult but has been shown to proceed either via a reductase enzyme, e.g. MSR, or from natural reducing agents in the cell, namely NADPH and FAD, with CNCbl bound to MMACHC (48, 131). The advantage to the cell of producing cob(II)alamin mainly lies in its easier ability to transition to the base-off form, compared to OHCbl or CNCbl, an important factor since both MS and MMAB, the

cytosolic and mitochondrial downstream targets, respectively, use cobalamin in the base-off form (173, 174). Following the chaperone hypothesis, MMACHC would next either pass off cob(II)alamin to MMADHC, or alternatively, be directed by MMADHC to its target enzymes. MMADHC is considered to be the sorting enzyme of the cobalamin pathway in that it is expected to direct intracellular cobalamin either towards MS or Mut, since mutations in the *MMADHC* gene can cause defects in either or both pathways (42). Evidence for MMADHC binding of cobalamin comes from the presence of the canonical DxHxxG cobalamin binding domain in the MMADHC protein, but cobalamin binding is yet to be tested biochemically. No evidence yet exists for physical interaction of MMACHC and MMADHC protein. Proceeding along the cytosolic pathway, MMACHC/MMADHC is expected to hand-off cobalamin in the base-off cob(II)alamin form to MS, upon which it would be reductively activated by MSR in a reaction described previously (see intro). For the mitochondrial pathway, it is still not known how cobalamin enters the mitochondria, but MMADHC has a mitochondrial leader sequence and we have confirmed mitochondrial expression (unpublished observations), and therefore it may function as the carrier. Once in the mitochondria, cobalamin would be handed to MMAB, the enzyme responsible for the adenosylation of cobalamin. Since MMAB requires cobalamin to be in the base-off cob(II)alamin form, prior reduction to this form may facilitate transmission from MMACHC/MMADHC to MMAB. For its adenosylation, cobalamin must be reduced to the highly unstable cob(I)alamin form. Like cellular decyanation, mitochondrial reduction of cob(II)alamin may proceed via a direct interaction with a reductase as shown by Leal *et al.* (74), or by reducing agents in the cell (unpublished observations), but either way reduction almost certainly happens while

bound to MMAB. After adenosylation, MMAB most likely directly passes the AdoCbl to Mut via physical interaction. Indeed, using the *M. extorquens* homologs for MMAB and Mut, MeaD and Mcm, respectively, Padovani *et al.* showed in a series of papers that MeaD produces AdoCbl in two of its three active sites, then upon binding ATP in the third site, it ejects one of the preformed AdoCbls directly to Mcm via association (91, 92). Additionally, MMAA physically interacts with Mut, as witnessed by bacterial orthologs as well as human studies (79, 80)(Chapter 6) perhaps for protection from oxidation of the AdoCbl attached to Mut (82). Indeed, all three proteins may come together as one large complex, thus keeping cobalamin sequestered, directly transferred and protected, from the production of cob(I)alamin through to the utilization of AdoCbl.

This chaperone hypothesis is a general explanation of cobalamin sequestration and processing throughout the cell. There is already good evidence in support of it, but there is also room for many key experiments. Integral to the evaluation of this hypothesis will be biochemical evidence of many of the interactions only hypothesized thus far, including MMACHC with LMBRD1 and MMACHC with MMADHC. Antibodies specific to all three proteins would allow testing of interaction by co-immunoprecipitation experiments, analogous to our work with MMAA and Mut, or even by electron microscopy. Additionally, interaction could be probed using *in vitro* assays with recombinant proteins, however, as we demonstrated with MMAA and Mut, the specific conditions required for their interaction must first be met. Alternatively, cobalamin analogs might be used to “fish” for these proteins, particularly MMACHC and MMADHC. Indeed, a collection of cobalamin analogs have already been generated and

substitutions on the *e*-propionamide group of cobalamin, including the addition of a biotin group, were compatible with uptake by a murine lymphoma cell line but inhibited cell growth (175). Importantly, some of these analogs could be competed out with CNCbl, suggesting that they were being processed through the normal cobalamin metabolic pathway. Incubating cell lines with the biotin substituted cobalamin analog and pulling down with streptavidin may be a novel way to isolate these proteins, alone or as a complex.

MMADHC is considered to be the intracellular cobalamin sorting protein based on genetic evidence, but there is currently no biochemical evidence to demonstrate how it accomplishes this function. Accordingly, important unknowns concerning MMADHC include: why N-terminal truncations of the protein result in a block only of the mitochondrial cobalamin pathway, whether MMADHC is able to bind cobalamin, what interactions MMADHC has with elements of the cytosolic and mitochondrial pathway and how exactly it sorts cobalamin to these two pathways. That N-terminal truncation mutations in MMADHC do not cause a block in both pathways when the same mutations in the middle of the protein do, suggests that, in the case of N-terminal mutations, some protein must be still made. It could be that two different protein versions are normally made by alternative splicing, one with a mitochondrial leader sequence that works in conjunction with the mitochondrial pathway and one without that that functions with the cytosolic pathway. Investigations into alternative splicing might answer this question. Alternatively, generating antibodies to different epitopes of MMADHC and probing by immunofluorescence or by Western blot analysis after cellular fractionation might

determine cellular localization of each part of MMADHC and possibly see both versions in some compartments. Determining MMADHC cobalamin binding may be as simple as testing recombinant protein as previously described for MMACHC, or alternatively, it may be found by the *in vivo* cobalamin analog experiment. Failing either of those, running MMADHC through a B_{12} column, analogous to the one used by Yamada *et al.* (73) for MS purification, may also determine if this protein binds cobalamin. The most difficult experiment may be to determine how MMADHC sorts cobalamin to the two different cellular compartments. One hypothesis is that MMADHC may bind to the outside of the mitochondria and sort cobalamin from there, or alternatively, it may form two different isoforms each responsible for a different pathway, as previously discussed. To test between these two hypotheses, the simplest way may be to isolate mitochondria and probe for MMADHC in intact versus broken mitochondria, where outside localized MMADHC would be found in intact mitochondria whereas inside localized MMADHC would be found only in the broken mitochondria.

Many questions remain about the mitochondrial cobalamin pathway. Conspicuously absent are explanations for how cobalamin enters the mitochondria, how cobalamin is reduced to cob(I)alamin in the mitochondrion and what role MMAA plays in its association with Mut. Investigations into MMADHC may provide an answer for mitochondrial entry, but it is also possible that cobalamin enters the mitochondria unbound through a multi-use transporter. If so, it may take genetic studies in a less complex model organism, such as *Dictyostelium* or *C. elegans*, which may not use the transporter for other molecules, to narrow down which transporter is utilized by

cobalamin. Using random mutagenesis followed by testing for ^{14}C-propionate incorporation could conceivably isolate the transporter necessary for cobalamin mitochondrial localization as well as the reductase required to produce cob(I)alamin. This would most likely involve a very large screen and assurance that the organism metabolizes cobalamin the same way humans do. Investigations into the association of MMAA with Mut and possibly MMAB *in vivo* could conceivably be done in the same manner as I did in Chapter 6, but with the addition of more specific antibodies, including antibodies to specific epitopes of each protein, for higher specificity. Additionally, testing the same interaction *in vitro*, but with all three proteins and using an increased number of conditions may determine the requirements necessary for interaction. It is possible that doing a small ligand screen for each protein in order to isolate all possible cofactors may be necessary to generate all parts necessary. This could be done using DSF, as DSF is very amenable to high-throughput screening (176). The most likely function of MMAA is to protect cob(II)alamin from oxidation, a function Padovani demonstrated with MeaB and Mcm (82). It is also possible that MMAA might regulate the specificity of Mut binding to AdoCbl over OHCbl, since OHCbl binding inactivates Mut. Both possible functions could be tested using recombinant MMAA and Mut by measuring the oxidation of cob(II)alamin to cob(III)alamin on functioning Mut in the presence or absence of MMAA, in both aerobic and anaerobic conditions. It is also possible that MMAB would be required for this assay, and incubation with all three proteins, OHCbl and a reducing system might be very enlightening in terms of how these three proteins function together. Additionally, running the assay in the presence or

absence of GTP to delineate the possible effect of MMAA GTPase activity could help us understand how this putative complex functions.

Finally, generating protein crystal structures is an important way to understand protein folding and ligand binding and can also help deduce protein function that might not be apparent from amino acid sequence alone. Currently, the only human cobalamin proteins to have been crystallized are MS, MCM and MMAB. Crystallization of MMAA, MMACHC and MMADHC in particular would aid our understanding of intracellular cobalamin processing. Additionally, crystallization of a complex of any of the proteins, including MMAA and Mut, might give further clues as to how these proteins functionally interact. Finally, protein crystallization allows the identification of how specific mutations, most notably patient mutations, affect protein folding and function, and may help us better understand how to create a stable protein or protein complex and therefore better treat vitamin B_{12} diseases.

Overall, answering the many questions left in cobalamin metabolism will take many thoughtful and insightful experiments and will keep the exploration of human vitamin B_{12} metabolism exciting for years to come.

REFERENCES

Reference List

1. Smith, E. L. (1948) *Nature* **161**, 638.
2. Rickes, E. L., Brink, N. G., Koniuszy, F. R., Wood, T. R., & Folkers, K. (1948) *Science* **107**, 396-397.
3. Minot, G. R. & Murphy, W. P. (1926) *Yale J. Biol. Med.* **74**, 341-353.
4. Rosenberg, L. E., Lilljeqvist, A., & Hsia, Y. E. (1968) *Science* **162**, 805-807.
5. Hodgkin, D. C., Kamper, J., Mackay, M., Pickworth, J., Trueblood, K. N., & White, J. G. (1956) *Nature* **178**, 64-66.
6. Krautler, B. (2005) *Biochem. Soc. Trans.* **33**, 806-810.
7. Stich, T. A., Yamanishi, M., Banerjee, R., & Brunold, T. C. (2005) *J. Am. Chem. Soc.* **127**, 7660-7661.
8. Schrauzer, G. N., Deutsch, E., & Windgassen, R. J. (1968) *J. Am. Chem. Soc.* **90**, 2441-2442.
9. Lexa, D. & Saveant, J. M. (1983) *Acc. Chem. Res.* **16**, 235-243.
10. Ludwig, M. L. & Matthews, R. G. (1997) *Annu. Rev. Biochem.* **66**, 269-313.
11. Eschenmoser, A. (1988) *Angwe. Chem. Int. Ed. Engl.* **27**, 5-39.
12. Benner, S. A., Ellington, A. D., & Tauer, A. (1989) *Proc. Natl. Acad. Sci. U. S. A* **86**, 7054-7058.
13. Roth, J. R., Lawrence, J. G., & Bobik, T. A. (1996) *Annu. Rev. Microbiol.* **50**, 137-181.
14. Brown, K. L. (2005) *Chem. Rev.* **105**, 2075-2149.
15. Banerjee, R. & Ragsdale, S. W. (2003) *Annu. Rev. Biochem.* **72:209-47.**, 209-247.
16. Zhang, Y., Rodionov, D. A., Gelfand, M. S., & Gladyshev, V. N. (2009) *BMC. Genomics* **10**, 78.
17. Rosenblatt, D. S. & Fenton, W. A. (2001) in *The Metabolic and Molecular Bases of Inherited Diseases*, eds. Scriver, C. R., Beaudet, A. L., Valle, D., Sly, W. S.,

Childs, B., Kinzler, K. W., & Vogelstein, B. (McGraw-Hill, New York), pp. 3897-3933.

18. Davey, G. K., Spencer, E. A., Appleby, P. N., Allen, N. E., Knox, K. H., & Key, T. J. (2003) *Public Health Nutr.* **6**, 259-269.

19. Pfeiffer, C. M., Johnson, C. L., Jain, R. B., Yetley, E. A., Picciano, M. F., Rader, J. I., Fisher, K. D., Mulinare, J., & Osterloh, J. D. (2007) *Am. J. Clin. Nutr.* **86**, 718-727.

20. Pfeiffer, C. M., Caudill, S. P., Gunter, E. W., Osterloh, J., & Sampson, E. J. (2005) *Am. J. Clin. Nutr.* **82**, 442-450.

21. Allen, L. H. (2009) *Am. J. Clin. Nutr.* **89**, 693S-696S.

22. Metz, J. (2008) *Food Nutr. Bull.* **29**, S74-S85.

23. Brown, C. A., McKinney, K. Q., Kaufman, J. S., Gravel, R. A., & Rozen, R. (2000) *J. Cardiovasc. Risk* **7**, 197-200.

24. Choi, S. W. (1999) *Nutr. Rev.* **57**, 250-253.

25. Ma, J., Stampfer, M. J., Christensen, B., Giovannucci, E., Hunter, D. J., Chen, J., Willett, W. C., Selhub, J., Hennekens, C. H., Gravel, R. *et al.* (1999) *Cancer Epidemiol. Biomarkers Prev.* **8**, 825-829.

26. Fowler, B. (1998) *Eur. J. Pediatr.* **157 Suppl 2**, S60-S66.

27. Banerjee, R. (2006) *ACS Chem. Biol.* **1**, 149-159.

28. Moestrup, S. K., Kozyraki, R., Kristiansen, M., Kaysen, J. H., Rasmussen, H. H., Brault, D., Pontillon, F., Goda, F. O., Christensen, E. I., Hammond, T. G. *et al.* (1998) *J. Biol. Chem.* **273**, 5235-5242.

29. Fyfe, J. C., Madsen, M., Hojrup, P., Christensen, E. I., Tanner, S. M., de la, C. A., He, Q., & Moestrup, S. K. (2004) *Blood* **103**, 1573-1579.

30. Whitehead, V. M. (2006) *Br. J. Haematol.* **134**, 125-136.

31. Morkbak, A. L., Hvas, A. M., Lloyd-Wright, Z., Sanders, T. A., Bleie, O., Refsum, H., Nygaard, O. K., & Nexo, E. (2006) *Clin. Chem.* **52**, 1104-1111.

32. Kolhouse, J. F. & Allen, R. H. (1977) *Proc. Natl. Acad. Sci. U. S. A* **74**, 921-925.

33. Finkler, A. E. & Hall, C. A. (1967) *Arch. Biochem. Biophys.* **120**, 79-85.

34. Hall, C. A. & Finkler, A. E. (1963) *Biochim. Biophys. Acta* **78**, 234-236.

35. Sennett, C., Rosenberg, L. E., & Mellman, I. S. (1981) *Annu. Rev. Biochem.* **50**, 1053-1086.

36. Allen, R. H. (1975) *Prog. Hematol.* **9**, 57-84.

37. Fedosov, S. N., Berglund, L., Fedosova, N. U., Nexo, E., & Petersen, T. E. (2002) *J. Biol. Chem.* **277**, 9989-9996.

38. Youngdahl-Turner, P., Mellman, I. S., Allen, R. H., & Rosenberg, L. E. (1979) *Exp. Cell Res.* **118**, 127-134.

39. Youngdahl-Turner, P., Rosenberg, L. E., & Allen, R. H. (1978) *J. Clin. Invest* **61**, 133-141.

40. Quadros, E. V., Nakayama, Y., & Sequeira, J. M. (2009) *Blood* **113**, 186-192.

41. Gravel, R. A., Mahoney, M. J., Ruddle, F. H., & Rosenberg, L. E. (1975) *Proc. Natl. Acad. Sci. U. S. A* **72**, 3181-3185.

42. Coelho, D., Suormala, T., Stucki, M., Lerner-Ellis, J. P., Rosenblatt, D. S., Newbold, R. F., Baumgartner, M. R., & Fowler, B. (2008) *N. Engl. J. Med.* **358**, 1454-1464.

43. Rutsch, F., Gailus, S., Miousse, I. R., Suormala, T., Sagne, C., Toliat, M. R., Nurnberg, G., Wittkampf, T., Buers, I., Sharifi, A. *et al.* (2009) *Nat. Genet.* **41**, 234-239.

44. Rosenblatt, D. S., Hosack, A., Matiaszuk, N. V., Cooper, B. A., & Laframboise, R. (1985) *Science* **228**, 1319-1321.

45. Lerner-Ellis, J. P., Anastasio, N., Liu, J., Coelho, D., Suormala, T., Stucki, M., Loewy, A. D., Gurd, S., Grundberg, E., Morel, C. F. *et al.* (2009) *Hum. Mutat.*

46. Rosenblatt, D. S., Aspler, A. L., Shevell, M. I., Pletcher, B. A., Fenton, W. A., & Seashore, M. R. (1997) *J. Inherit. Metab Dis.* **20**, 528-538.

47. Lerner-Ellis, J. P., Tirone, J. C., Pawelek, P. D., Dore, C., Atkinson, J. L., Watkins, D., Morel, C. F., Fujiwara, T. M., Moras, E., Hosack, A. R. *et al.* (2006) *Nat. Genet.* **38**, 93-100.

48. Kim, J., Gherasim, C., & Banerjee, R. (2008) *Proc. Natl. Acad. Sci. U. S. A* **105**, 14551-14554.

49. Hannibal, L., Kim, J., Brasch, N. E., Wang, S., Rosenblatt, D. S., Banerjee, R., & Jacobsen, D. W. (2009) *Mol. Genet. Metab*.

50. Mellman, I., Willard, H. F., Youngdahl-Turner, P., & Rosenberg, L. E. (1979) *J. Biol. Chem.* **254**, 11847-11853.

51. Willard, H. F., Mellman, I. S., & Rosenberg, L. E. (1978) *Am. J. Hum. Genet.* **30**, 1-13.

52. Suormala, T., Baumgartner, M. R., Coelho, D., Zavadakova, P., Kozich, V., Koch, H. G., Berghauser, M., Wraith, J. E., Burlina, A., Sewell, A. *et al.* (2004) *J. Biol. Chem.* **279**, 42742-42749.

53. Watkins, D., Matiaszuk, N., & Rosenblatt, D. S. (2000) *J. Med. Genet.* **37**, 510-513.

54. Li, Y. N., Gulati, S., Baker, P. J., Brody, L. C., Banerjee, R., & Kruger, W. D. (1996) *Hum. Mol. Genet.* **5**, 1851-1858.

55. Leclerc, D., Campeau, E., Goyette, P., Adjalla, C. E., Christensen, B., Ross, M., Eydoux, P., Rosenblatt, D. S., Rozen, R., & Gravel, R. A. (1996) *Hum. Mol. Genet.* **5**, 1867-1874.

56. Chen, L. H., Liu, M. L., Hwang, H. Y., Chen, L. S., Korenberg, J., & Shane, B. (1997) *J. Biol. Chem.* **272**, 3628-3634.

57. Matthews, R. G. (1984) in *Folates and Pterins*, eds. Blakely, R. L. & Bencovic, S. J. (J. Wiley & Sons, Inc., New York), pp. 497-553.

58. Taylor, R. T. (1983) in *B12*, ed. Dolphin, D. (John Wiley & Sons, Inc., New York), pp. 307-355.

59. Matthews, R. G. (1999) in *Chemistry and Biochemistry of B12*, ed. Banerjee, R. (John Wiley & Sons, New York), pp. 681-706.

60. Matthews, R. G. & Ludwig, M. L. (2001) in *Homocysteine in health and disease*, eds. Carmel, R. & Jacobsen, D. W. (Cambridge University Press, Cambridge), pp. 100-112.

61. Watkins, D., Ru, M., Hwang, H. Y., Kim, C. D., Murray, A., Philip, N. S., Kim, W., Legakis, H., Wai, T., Hilton, J. F. *et al.* (2002) *Am. J. Hum. Genet.* **71**, 143-153.

62. Watkins, D. & Rosenblatt, D. S. (1989) *Am. J. Med. Genet.* **34**, 427-434.

63. Harding, C. O., Arnold, G., Barness, L. A., Wolff, J. A., & Rosenblatt, D. S. (1997) *Am. J. Med. Genet.* **71**, 384-390.

64. Chen, L. H., Liu, M. L., Hwang, H. Y., Chen, L. S., Korenberg, J., & Shane, B. (1997) *J. Biol. Chem.* **272**, 3628-3634.

65. Goulding, C. W., Postigo, D., & Matthews, R. G. (1997) *Biochemistry* **36**, 8082-8091.

66. Banerjee, R. V., Johnston, N. L., Sobeski, J. K., Datta, P., & Matthews, R. G. (1989) *J. Biol. Chem.* **264**, 13888-13895.

67. Dixon, M. M., Huang, S., Matthews, R. G., & Ludwig, M. (1996) *Structure.* **4**, 1263-1275.

68. Leclerc, D., Wilson, A., Dumas, R., Gafuik, C., Song, D., Watkins, D., Heng, H. H., Rommens, J. M., Scherer, S. W., Rosenblatt, D. S. *et al.* (1998) *Proc. Natl. Acad. Sci. U. S. A* **95**, 3059-3064.

69. Drummond, J. T., Huang, S., Blumenthal, R. M., & Matthews, R. G. (1993) *Biochemistry* **32**, 9290-9295.

70. Loughlin, R. E., Elford, H. L., & Buchanan, J. M. (1964) *J. Biol. Chem.* **239**, 2888-2895.

71. Taylor, R. T. & Weissbach, H. (1973) in *The Enzymes*, ed. Boyer, P. D. (Academic, New York), pp. 121-165.

72. Olteanu, H. & Banerjee, R. (2001) *J. Biol. Chem.* **276**, 35558-35563.

73. Yamada, K., Gravel, R. A., Toraya, T., & Matthews, R. G. (2006) *Proc. Natl. Acad. Sci. U. S. A.* **%20;103**, 9476-9481.

74. Leal, N. A., Olteanu, H., Banerjee, R., & Bobik, T. A. (2004) *J. Biol. Chem.* **279**, 47536-47542.

75. Matsui, S. M., Mahoney, M. J., & Rosenberg, L. E. (1983) *N. Engl. J. Med.* **308**, 857-861.

76. Horster, F., Baumgartner, M. R., Viardot, C., Suormala, T., Burgard, P., Fowler, B., Hoffmann, G. F., Garbade, S. F., Kolker, S., & Baumgartner, E. R. (2007) *Pediatr. Res.* **62**, 225-230.

77. Dobson, C. M., Wai, T., Leclerc, D., Wilson, A., Wu, X., Dore, C., Hudson, T., Rosenblatt, D. S., & Gravel, R. A. (2002) *Proc. Natl. Acad. Sci. U. S. A* **99**, 15554-15559.

78. Mahoney, M. J., Hart, A. C., Steen, V. D., & Rosenberg, L. E. (1975) *Proc. Natl. Acad. Sci. U. S. A* **72**, 2799-2803.

79. Korotkova, N. & Lidstrom, M. E. (2004) *J. Biol. Chem.* **279**, 13652-13658.

80. Froese, D. S., Dobson, C. M., White, A. P., Wu, X., Padovani, D., Banerjee, R., Haller, T., Gerlt, J. A., Surette, M. G., & Gravel, R. A. (2009) *Microbiol. Res.* **164**, 1-8.

81. Padovani, D., Labunska, T., & Banerjee, R. (2006) *J. Biol. Chem.* **281**, 17838-17844.

82. Padovani, D. & Banerjee, R. (2006) *Biochemistry* **45**, 9300-9306.

83. Dobson, C. M., Wai, T., Kadir, H., Narang, M., Lerner-Ellis, J., Hudson, T. J., Rosenblatt, D. S., & Gravel, R. A. (2002) *Hum. Mol. Genet.* **11**, 3361-3369.

84. Leal, N. A., Park, S. D., Kima, P. E., & Bobik, T. A. (2003) *J. Biol. Chem.* **278**, 9227-9234.

85. Lerner-Ellis, J. P., Gradinger, A. B., Watkins, D., Tirone, J. C., Villeneuve, A., Dobson, C. M., Montpetit, A., Lepage, P., Gravel, R. A., & Rosenblatt, D. S. (2006) *Mol. Genet. Metab* **87**, 219-225.

86. Schubert, H. L. & Hill, C. P. (2006) *Biochemistry* **45**, 15188-15196.

87. Zhang, J., Dobson, C. M., Wu, X., Lerner-Ellis, J., Rosenblatt, D. S., & Gravel, R. A. (2006) *Mol. Genet. Metab* **87**, 315-322.

88. Buan, N. R. & Escalante-Semerena, J. C. (2006) *J. Biol. Chem.* **281**, 16971-16977.

89. Johnson, C. L., Buszko, M. L., & Bobik, T. A. (2004) *J. Bacteriol.* **186**, 7881-7887.

90. Johnson, C. L., Pechonick, E., Park, S. D., Havemann, G. D., Leal, N. A., & Bobik, T. A. (2001) *J. Bacteriol.* **183**, 1577-1584.

91. Padovani, D., Labunska, T., Palfey, B. A., Ballou, D. P., & Banerjee, R. (2008) *Nat. Chem. Biol.* **4**, 194-196.

92. Padovani, D. & Banerjee, R. (2009) *Biochemistry* **48**, 5350-5357.

93. Lempp, T. J., Suormala, T., Siegenthaler, R., Baumgartner, E. R., Fowler, B., Steinmann, B., & Baumgartner, M. R. (2007) *Mol. Genet. Metab* **90**, 284-290.

94. Fowler, B., Leonard, J. V., & Baumgartner, M. R. (2008) *J. Inherit. Metab Dis.* **31**, 350-360.

95. Willard, H. F. & Rosenberg, L. E. (1980) *J. Clin. Invest* **65**, 690-698.

96. Thoma, N. H. & Leadlay, P. F. (1996) *Protein Sci.* **5**, 1922-1927.

97. Mancia, F., Keep, N. H., Nakagawa, A., Leadlay, P. F., McSweeney, S., Rasmussen, B., Bosecke, P., Diat, O., & Evans, P. R. (1996) *Structure.* **4**, 339-350.

98. Mancia, F. & Evans, P. R. (1998) *Structure.* **6**, 711-720.

99. Thoma, N. H., Meier, T. W., Evans, P. R., & Leadlay, P. F. (1998) *Biochemistry* **37**, 14386-14393.

100. Kolhouse, J. F., Utley, C., & Allen, R. H. (1980) *J. Biol. Chem.* **255**, 2708-2712.

101. Fenton, W. A., Hack, A. M., Willard, H. F., Gertler, A., & Rosenberg, L. E. (1982) *Arch. Biochem. Biophys.* **214**, 815-823.

102. Leclerc, D., Odievre, M., Wu, Q., Wilson, A., Huizenga, J. J., Rozen, R., Scherer, S. W., & Gravel, R. A. (1999) *Gene* **240**, 75-88.

103. Narang, M. A., Dumas, R., Ayer, L. M., & Gravel, R. A. (2004) *Hum. Mol. Genet.* **13**, 15-23.

104. Wilson, A., Leclerc, D., Rosenblatt, D. S., & Gravel, R. A. (1999) *Hum. Mol. Genet.* **8**, 2009-2016.

105. Wolthers, K. R. & Scrutton, N. S. (2007) *Biochemistry* **46**, 6696-6709.

106. Chenna, R., Sugawara, H., Koike, T., Lopez, R., Gibson, T. J., Higgins, D. G., & Thompson, J. D. (2003) *Nucleic Acids Res.* **31**, 3497-3500.

107. Nicholas, K. B., Nicholas, H. B. J., & Deerfield, D. W. II. (1997) p. 14.

108. Knowles, R. G. & Moncada, S. (1994) *Biochem. J.* **298 (Pt 2)**, 249-258.

109. Miller, W. L., Huang, N., Fluck, C. E., & Pandey, A. V. (2004) *Lancet* **364**, 1663.

110. Chen, Z. & Banerjee, R. (1998) *J. Biol. Chem.* **273**, 26248-26255.

111. Paine, M. J., Garner, A. P., Powell, D., Sibbald, J., Sales, M., Pratt, N., Smith, T., Tew, D. G., & Wolf, C. R. (2000) *J. Biol. Chem.* **275**, 1471-1478.

112. Kwasnicka-Crawford, D. A. & Vincent, S. R. (2005) *Biochem. Biophys. Res. Commun.* **336**, 565-571.

113. Olteanu, H. & Banerjee, R. (2003) *J. Biol. Chem.* **278**, 38310-38314.

114. Rosenblatt, D. S. & Fenton, W. A. (2001) in *The Metabolic and Molecular Bases of Inherited Disease*, eds. Scriver, C. R., Beaudet, A. L., Valle, D., & Sly, W. S. (McGraw-Hill, New York), pp. 3897-3933.

115. Ben-Omran, T. I., Wong, H., Blaser, S., & Feigenbaum, A. (2007) *Am. J. Med. Genet. A* **143A**, 979-984.

116. Rossi, A., Cerone, R., Biancheri, R., Gatti, R., Schiaffino, M. C., Fonda, C., Zammarchi, E., & Tortori-Donati, P. (2001) *AJNR Am. J. Neuroradiol.* **22**, 554-563.

117. Thauvin-Robinet, C., Roze, E., Couvreur, G., Horellou, M. H., Sedel, F., Grabli, D., Bruneteau, G., Tonneti, C., Masurel-Paulet, A., Perennou, D. *et al.* (2008) *J. Neurol. Neurosurg. Psychiatry* **79**, 725-728.

118. Morel, C. F., Lerner-Ellis, J. P., & Rosenblatt, D. S. (2006) *Mol. Genet. Metab* **88**, 315-321.

119. Nogueira, C., Aiello, C., Cerone, R., Martins, E., Caruso, U., Moroni, I., Rizzo, C., Diogo, L., Leao, E., Kok, F. *et al.* (2008) *Mol. Genet. Metab* **93**, 475-480.

120. Andersson, H. C. & Shapira, E. (1998) *J. Pediatr.* **132**, 121-124.

121. Picaud, S. S., Muniz, J. R., Kramm, A., Pilka, E. S., Kochan, G., Oppermann, U., & Yue, W. W. (2009) *Proteins* **76**, 507-511.

122. Chowdhury, S. & Banerjee, R. (1999) *Biochemistry* **38**, 15287-15294.

123. Lakowicz, J. R. (2008) *Principles of Fluorescence Spectroscopy* (Springer Press.

124. Sampedro, J. G., Ruiz-Granados, Y. G., Najera, H., Tellez-Valencia, A., & Uribe, S. (2007) *Biochemistry* **46**, 5616-5622.

125. Hsu, J. M., Kawin, B., Minor, P., & Mitchell, J. A. (1966) pp. 1264-1265.

126. Vlasie, M., Chowdhury, S., & Banerjee, R. (2002) *J. Biol. Chem.* **277**, 18523-18527.

127. Zheng, D. & Lu, T. (1997) *J. Electroanal. Chem.* 61-65.

128. Go, Y. M. & Jones, D. P. (2008) *Biochim. Biophys. Acta* **1780**, 1273-1290.

129. Mellman, I. S., Youngdahl-Turner, P., Willard, H. F., & Rosenberg, L. E. (1977) *Proc. Natl. Acad. Sci. U. S. A* **74**, 916-920.

130. Qureshi, A. A., Rosenblatt, D. S., & Cooper, B. A. (1994) *Crit Rev. Oncol. Hematol.* **17**, 133-151.

131. Froese, D. S., Zhang, J., Healy, S., & Gravel, R. A. (2009) *Mol Genet Metab*.

132. Niesen, F. H., Berglund, H., & Vedadi, M. (2007) *Nat. Protoc.* **2**, 2212-2221.

133. Epps, D. E., Sarver, R. W., Rogers, J. M., Herberg, J. T., & Tomich, P. K. (2001) *Anal. Biochem.* **292**, 40-50.

134. Pantoliano, M. W., Petrella, E. C., Kwasnoski, J. D., Lobanov, V. S., Myslik, J., Graf, E., Carver, T., Asel, E., Springer, B. A., Lane, P. *et al.* (2001) *J. Biomol. Screen.* **6**, 429-440.

135. Hopper, E. D., Pittman, A. M., Fitzgerald, M. C., & Tucker, C. L. (2008) *J. Biol. Chem.* **283**, 30493-30502.

136. Lo, M. C., Aulabaugh, A., Jin, G., Cowling, R., Bard, J., Malamas, M., & Ellestad, G. (2004) *Anal. Biochem.* **332**, 153-159.

137. Poklar, N., Lah, J., Salobir, M., Macek, P., & Vesnaver, G. (1997) *Biochemistry* **36**, 14345-14352.

138. Pantoliano, M. W., Petrella, E. C., Kwasnoski, J. D., Lobanov, V. S., Myslik, J., Graf, E., Carver, T., Asel, E., Springer, B. A., Lane, P. *et al.* (2001) *J. Biomol. Screen.* **6**, 429-440.

139. Vedadi, M., Niesen, F. H., lali-Hassani, A., Fedorov, O. Y., Finerty, P. J., Jr., Wasney, G. A., Yeung, R., Arrowsmith, C., Ball, L. J., Berglund, H. *et al.* (2006) *Proc. Natl. Acad. Sci. U. S. A* **103**, 15835-15840.

140. Bodamer, O. A., Rosenblatt, D. S., Appel, S. H., & Beaudet, A. L. (2001) *Neurology* **56**, 1113.

141. Baggett, B., Roy, R., Momen, S., Morgan, S., Tisi, L., Morse, D., & Gillies, R. J. (2004) *Mol Imaging* **3**, 324-332.

142. Foster, M. A., Tejerina, G., Guest, J. R., & WOODS, D. D. (1964) *Biochem. J.* **92**, 476-488.

143. Guest, J. R., Friedman, S., FOSTER, M. A., Tejerina, G., & WOODS, D. D. (1964) *Biochem. J.* **92**, 497-504.

144. Foster, M. A., Jones, K. M., & Woods, D. D. (1961) *Biochem. J.* **80**, 519-531.

145. Haller, T., Buckel, T., Retey, J., & Gerlt, J. A. (2000) *Biochemistry* **39**, 4622-4629.

146. Roy, I. & Leadlay, P. F. (1992) *J. Bacteriol.* **174**, 5763-5764.

147. Bobik, T. A. & Rasche, M. E. (2001) *J. Biol. Chem.* **276**, 37194-37198.

148. Leipe, D. D., Wolf, Y. I., Koonin, E. V., & Aravind, L. (2002) *J Mol Biol* **317**, 41-72.

149. White, A. P., Collinson, S. K., Burian, J., Clouthier, S. C., Banser, P. A., & Kay, W. W. (1999) *Vaccine* **17**, 2150-2161.

150. White, A. P., len-Vercoe, E., Jones, B. W., DeVinney, R., Kay, W. W., & Surette, M. G. (2007) *Can. J. Microbiol.* **53**, 56-62.

151. Marsh, E. N., Harding, S. E., & Leadlay, P. F. (1989) *Biochem. J.* **260**, 353-358.

152. Miyamoto, E., Watanabe, F., Charles, T. C., Yamaji, R., Inui, H., & Nakano, Y. (2003) *Arch. Microbiol.* **180**, 151-154.

153. Dayem, L. C., Carney, J. R., Santi, D. V., Pfeifer, B. A., Khosla, C., & Kealey, J. T. (2002) *Biochemistry* **41**, 5193-5201.

154. Frenkel, E. P. & Kitchens, R. L. (1975) *Br. J. Haematol.* **31**, 501-513.

155. Ledley, F. D., Lumetta, M., Nguyen, P. N., Kolhouse, J. F., & Allen, R. H. (1988) *Proc. Natl. Acad. Sci. U. S. A* **85**, 3518-3521.

156. Worgan, L. C., Niles, K., Tirone, J. C., Hofmann, A., Verner, A., Sammak, A., Kucic, T., Lepage, P., & Rosenblatt, D. S. (2006) *Hum. Mutat.* **27**, 31-43.

157. Willard, H. F. & Rosenberg, L. E. (1977) *Biochem. Biophys. Res. Commun.* **78**, 927-934.

158. Willard, H. F. & Rosenberg, L. E. (1979) *Biochem. Genet.* **17**, 57-75.

159. Shevell, M. I., Matiaszuk, N., Ledley, F. D., & Rosenblatt, D. S. (1993) *Am. J. Med. Genet.* **45**, 619-624.

160. Hubbard, P. A., Padovani, D., Labunska, T., Mahlstedt, S. A., Banerjee, R., & Drennan, C. L. (2007) *J. Biol. Chem.* **282**, 31308-31316.

161. Zhou, T., Lee, J. W., Tatavarthi, H., Lupski, J. R., Valerie, K., & Povirk, L. F. (2005) *Nucleic Acids Res.* **33**, 289-297.

162. Harlow, E. a. L. D. (1999) *Using Antibodies: A Laboratory Manual , Cold Spring Harbour Laboratory Press, NY.*

163. Froese, D. S., Wu, X., Zhang, J., Dumas, R., Schoel, W. M., Amrein, M., & Gravel, R. A. (2008) *Mol. Genet. Metab* **94**, 68-77.

164. Bullock, A. N., Debreczeni, J. E., Fedorov, O. Y., Nelson, A., Marsden, B. D., & Knapp, S. (2005) *J. Med. Chem.* **48**, 7604-7614.

165. Bourne, H. R., Sanders, D. A., & McCormick, F. (1991) *Nature* **349**, 117-127.

166. Bendtsen, J. D., Nielsen, H., von, H. G., & Brunak, S. (2004) *J. Mol Biol.* **340**, 783-795.

167. Cannata, J. J., Focesi, A., Jr., Mazumder, R., Warner, R. C., & Ochoa, S. (1965) *J. Biol. Chem.* **240**, 3249-3257.

168. Fenton, W. A. & Rosenberg, L. E. (1978) *Annu Rev Genet* **12**, 223-248.

169. Ballantyne, R. M. & McHenry, E. W. (1949) *Cancer Res.* **9**, 689-691.

170. Waddington, M. D. & and Finke, R. G. (1993) *J Am Chem Soc* **115**, 4629-4640.

171. Yamanishi, M., Vlasie, M., & Banerjee, R. (2005) *Trends Biochem. Sci.* **30**, 304-308.

172. Braun, V. (1995) *FEMS Microbiol. Rev.* **16**, 295-307.

173. Drennan, C. L., Matthews, R. G., & Ludwig, M. L. (1994) *Curr. Opin. Struct. Biol.* **4**, 919-929.

174. Yamanishi, M., Labunska, T., & Banerjee, R. (2005) *J. Am. Chem. Soc.* **127**, 526-527.

175. McLean, G. R., Pathare, P. M., Wilbur, D. S., Morgan, A. C., Woodhouse, C. S., Schrader, J. W., & Ziltener, H. J. (1997) *Cancer Res.* **57**, 4015-4022.

176. Senisterra, G. A., Markin, E., Yamazaki, K., Hui, R., Vedadi, M., & Awrey, D. E. (2006) *J. Biomol. Screen.* **11**, 940-948.